

## Fluorovinylsulfones and -Sulfonates as Potent Covalent Reversible Inhibitors of the Trypanosomal Cysteine Protease Rhodesain: Structure–Activity Relationship, Inhibition Mechanism, Metabolism, and In Vivo Studies

Sascha Jung,<sup>†‡</sup> Natalie Fuchs,<sup>†‡</sup> Patrick Johe, Annika Wagner, Erika Diehl, Tri Yuliani, Collin Zimmer, Fabian Barthels, Robert A. Zimmermann, Philipp Klein, Waldemar Waigel, Jessica Meyr, Till Opatz, Stefan Tenzer, Ute Distler, Hans-Joachim Räder, Christian Kersten, Bernd Engels, Ute A. Hellmich, Jochen Klein, and Tanja Schirmeister\*



Cite This: *J. Med. Chem.* 2021, 64, 12322–12358



Read Online

ACCESS |



Metrics & More

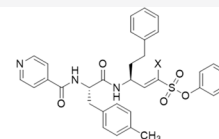
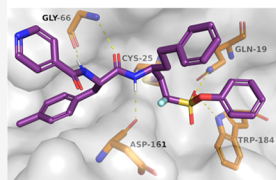


Article Recommendations



Supporting Information

**ABSTRACT:** Rhodesain is a major cysteine protease of *Trypanosoma brucei rhodesiense*, a pathogen causing Human African Trypanosomiasis, and a validated drug target. Recently, we reported the development of  $\alpha$ -halovinylsulfones as a new class of covalent reversible cysteine protease inhibitors. Here,  $\alpha$ -fluorovinylsulfones/-sulfonates were optimized for rhodesain based on molecular modeling approaches. **2d**, the most potent and selective inhibitor in the series, shows a single-digit nanomolar affinity and high selectivity toward mammalian cathepsins B and L. Enzymatic dilution assays and MS experiments indicate that **2d** is a slow-tight binder ( $K_i = 3$  nM). Furthermore, the nonfluorinated **2d-(H)** shows favorable metabolism and biodistribution by accumulation in mice brain tissue after intraperitoneal and oral administration. The highest antitrypanosomal activity was observed for inhibitors with an N-terminal 2,3-dihydrobenzo[*b*][1,4]dioxine group and a 4-Me-Phe residue in P2 (**2e/4e**) with nanomolar EC<sub>50</sub> values (0.14/0.80  $\mu$ M). The different mechanisms of reversible and irreversible inhibitors were explained using QM/MM calculations and MD simulations.



<b>2d</b> (X = F) slowly reversible	<b>2d-(H)</b> (X = H) irreversible
$K_i(\text{Rho}) = 3$ nM	$K_i(\text{Rho}) = 0.45$ nM
$K_i(\text{CatL}) = 78$ nM	$K_i(\text{CatL}) = 8.2$ nM
$K_i(\text{CatB}) > 11$ $\mu$ M	$K_i(\text{CatB}) = 348$ nM

## INTRODUCTION

Human African Trypanosomiasis (HAT, sleeping sickness) is a severe disease classified as a neglected tropical disease (NTD).<sup>1</sup> HAT is caused by the protozoan parasite *Trypanosoma brucei* (*T. brucei*), which is transmitted to humans via the bite of the Tsetse fly.<sup>2</sup> Sleeping sickness is fatal if left untreated. Pentamidine and suramin are used to treat the early, hemolymphatic stage of the disease, while eflornithine and melarsoprol and the combination therapy nifurtimox-eflornithine target the late, neurological stage of the disease.<sup>3</sup> Recently, the nitroimidazole fexinidazole was introduced as the first oral treatment of both, stage-1 and stage-2 *T. b. gambiense* HAT.<sup>4</sup> However, most available drugs show severe toxicity, poor bioavailability, and need long-time administration due to their lack of efficiency.<sup>5</sup> Therefore, there is an urgent need to develop new therapies against this disease and, in addition, *T. brucei* can serve as a valuable model organism for other pathogenic kinetoplastid diseases. The cysteine protease rhodesain (*TbCatL*) is essential for the development of the parasite and for the progression of the disease.<sup>6,7</sup> Inhibition of the parasitic cysteine protease activity has been validated as a

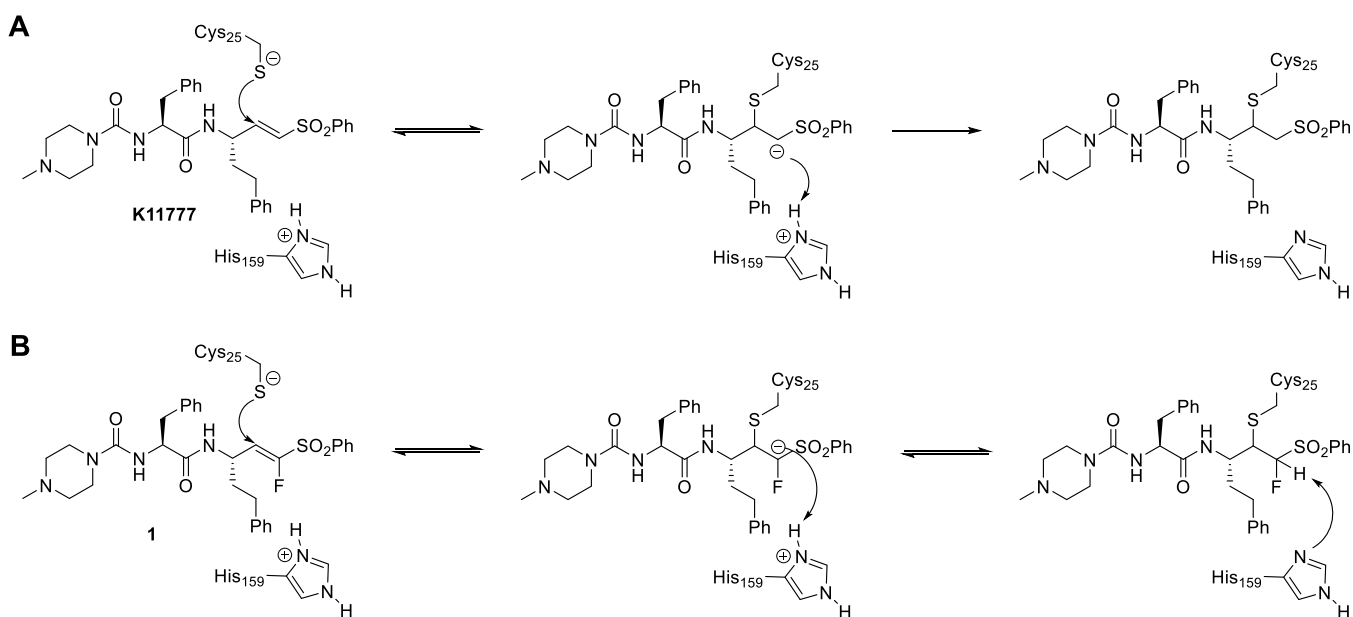
drug target in vitro and in vivo.<sup>8</sup> Consequently, rhodesain represents a promising target for the development of safer drugs against HAT.

Rhodesain belongs to the papain family of cysteine proteases and shares high structural similarity with the human cathepsins, especially cathepsin L (CatL; sequence identity 44.7%, similarity 59.1%, C <sub>$\alpha$</sub> -RMSD 1.35 Å).<sup>9,10</sup> A prominent inhibitor of papain-family cysteine proteases is K11777, a peptide-based vinyl-sulfone that mimics the autoinhibition of prorrhodesain and that reacts in a Michael-type addition with the active-site cysteine (Figure 1).<sup>10,11</sup> The arising carbanion is protonated, resulting in the irreversible formation of the covalent enzyme–inhibitor complex. Substitution of the hydrogen at the  $\alpha$ -position of the

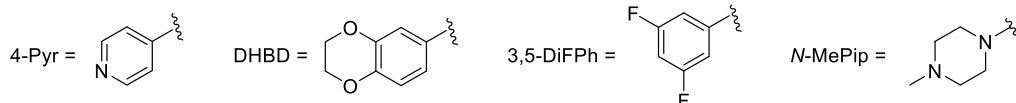
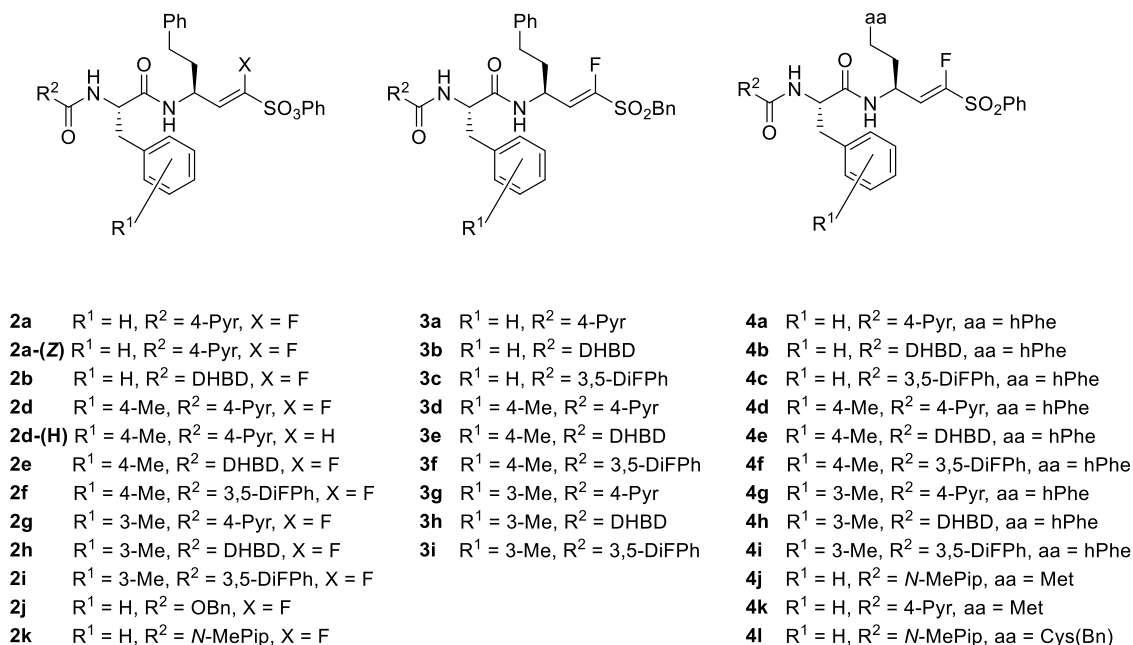
Received: June 3, 2021

Published: August 11, 2021





**Figure 1.** Structures and inhibition mechanisms of irreversible (**K11777**; A) and covalent reversible (**1**; B) peptide-based vinylsulfones.

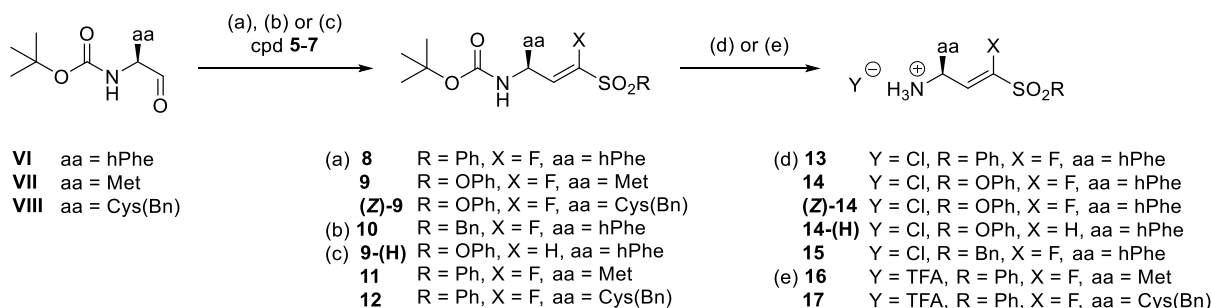


**Figure 2.** Structures of compounds **2a–4l**.

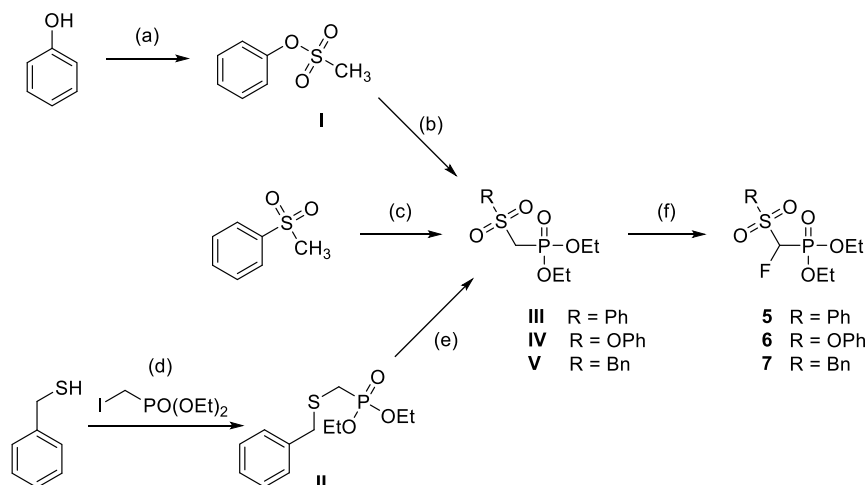
double bond by fluorine (compound **1**) generates an  $\alpha$ -fluorovinylsulfone, which can undergo a reversible Michael-type addition with thiols (Figure 1).<sup>12</sup>

The development of covalent inhibitors has seen a resurgence in academia as well as in the industry during the past decade.<sup>13</sup> There is much debate on the advantages and disadvantages of covalent inhibition, especially concerning reversible covalent inhibition mechanisms.<sup>14</sup> On the one hand, covalent reversible inhibitors alleviate some of the concerns arising from covalent

irreversible protein modifications, such as toxicity emerging from off-target effects,<sup>15</sup> idiosyncratic toxicity,<sup>16</sup> and haptization,<sup>17</sup> but maintain benefits such as enhanced potency and prolonged residence times.<sup>18,19</sup> In recent studies with reversible fluorinated vinylsulfones and their irreversible counterparts, it was shown that the electrophilic group, the so-called warhead, and not the binding of the peptidic recognition unit limits the kinetics of inhibition of the protease and that the fluorinated vinylsulfone warhead reduces the rate constant of binding.<sup>20,21</sup>

Scheme 1. Synthesis of Building Blocks 13–17<sup>a</sup>

<sup>a</sup>Reagents and conditions: aa = amino acid side chain; (a) NaH, THF, 0 °C, 1 h, 22–43%; (b) KHMDS, THF, –78 °C for 20 min, 1 h at rt, 47%; (c) LHMDS, THF, –78 °C for 30 min, 12 h at rt, 54–75%; (d) 4 M HCl in dioxane, rt, 30 min, quant.; and (e) TFA, DCM, 0 °C, 1 h, quant.

Scheme 2. Preparation of Phosphonates 5–7<sup>a</sup>

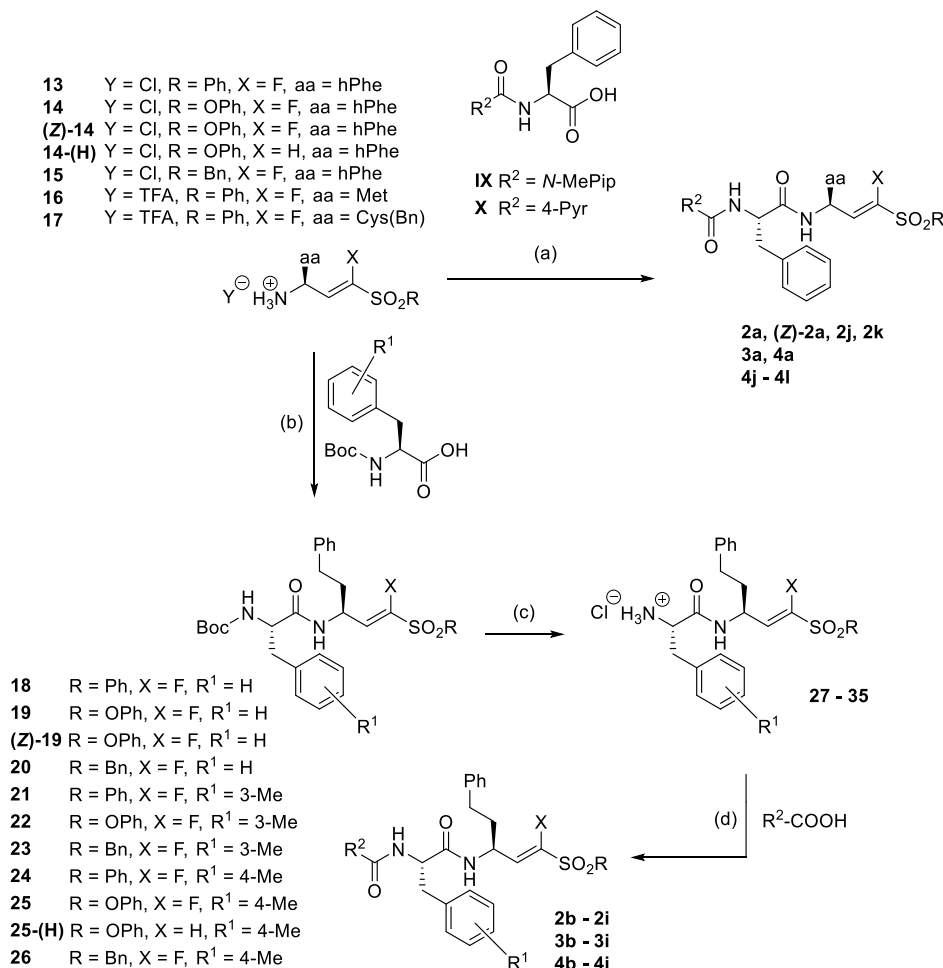
<sup>a</sup>Reagents and conditions: (a) Ms-Cl, TEA, EtOAc, 0 °C to rt, 30 min, 92%; (b) diethyl chlorophosphite (DECP), KHMDS, THF, –78 to –60 °C, 1 h, 74%; (c) DECP, *n*-BuLi, THF, 0 °C, 1 h, 52%; (d) NaH, THF, 0 °C to rt, 4 h, 84%; (e) *m*CPBA, DCM, 0 °C to rt, 12 h, 99%; and (f) Selectfluor, KHMDS, THF/DMF, –78 °C to rt, 3 h, 48–62%.

Based on the previously reported structure of the covalent reversible inhibitor **1**,<sup>12</sup> in the present study we performed structure–activity relationship (SAR) studies to optimize inhibition potency for rhodesain and selectivity against human cathepsins B and L using molecular docking approaches. Additionally, quantum chemical-based computations were performed to get further information about the differences in the inhibition mechanisms of **K11777** and its fluorinated counterpart **1**. These studies were performed because in our previous study, the computed reaction energies for X = F and X = H in the  $\alpha$ -position of the warhead (Figure 1) did not differ significantly. Thus, the transition from irreversible to reversible inhibition by exchange of hydrogen by fluorine could not be explained conclusively. The covalent behavior of the compounds was experimentally evaluated with MS studies, and reversibility was demonstrated with enzymatic dilution and dialysis assays.

Furthermore, the ADME parameters of compound **1** and the optimized inhibitor **2d-(H)** were investigated via in vitro metabolism studies and in vivo mouse studies in order to determine their organ distribution and their accumulation in brain tissue, thus evaluating their potential as candidates for the treatment of stage-2 HAT.

## RESULTS AND DISCUSSION

**Design of Inhibitors.** Structural variations of the fluorinated vinylsulfone **1** (Figure 1B) were inspired by peptide-based inhibitors of rhodesain, which contain structural elements at the P3, P2, and P1' positions<sup>21</sup> that are known to either enhance potency against rhodesain and/or increase selectivity against CatL and CatB.<sup>22–25</sup> For the P3 position, introduction of aromatic and heteroaromatic systems was reported to favor inhibition of rhodesain over CatL and CatB.<sup>22–24</sup> Introduction of an additional methyl group to the 3- or 4-position of the phenylalanine aromatic ring at the P2 position can improve potency and selectivity for rhodesain.<sup>22</sup> Additionally, the extension of the phenyl ring at the warhead into the S1' pocket via linker atoms increases potency for rhodesain.<sup>25</sup> Based on these observations, a virtual library of 511 modified compounds was generated. These compounds were docked at rhodesain (crystal structure of rhodesain bound to **K11777**, protein databank (PDB) 2p7u<sup>11</sup>) using FlexX<sup>26</sup> and DOCKTITE,<sup>27</sup> as reported previously (Table S1).<sup>12</sup> The noncovalent enzyme–inhibitor complex was generated with FlexX, and the scores reflect whether the designed compounds have an improved noncovalent affinity compared to the starting vinylsulfone **1**. Only compounds with a comparable or higher score were selected for synthesis. In addition, the covalent complex was modeled with DOCKTITE.<sup>27</sup> In this case, the scores (Table S1)

Scheme 3. Synthesis of Compounds 2a–4l from Building Blocks 13–17<sup>a</sup>

may be interpreted in terms of stability of the protein-bound state.

Based on the results obtained from docking, a series of compounds (2a–4i) were selected for synthesis and subsequent evaluation of SAR (Figure 2). For all selected compounds, scores obtained from both docking approaches were generally higher when compared to starting compound 1 (Table S1). Depending on the substitution pattern of the warhead at the P1' position, compounds can be subdivided into aromatic fluorovinylsulfones (phenyl substituent at P1', cpds 4a–4i), aliphatic fluorovinylsulfones (benzyl group at P1', cpds 3a–3i), and fluorovinylsulfonates (phenol ester at P1', cpds 2a–2k).

Based on noncovalent docking (Table S1), compounds (4j–4l) with methionine and *S*-benzylcysteine at P1 were suggested to show a comparable (yet slightly lower) affinity to the respective molecules with a homophenylalanine residue. Therefore, these compounds were included in the present study and investigated for their potency.

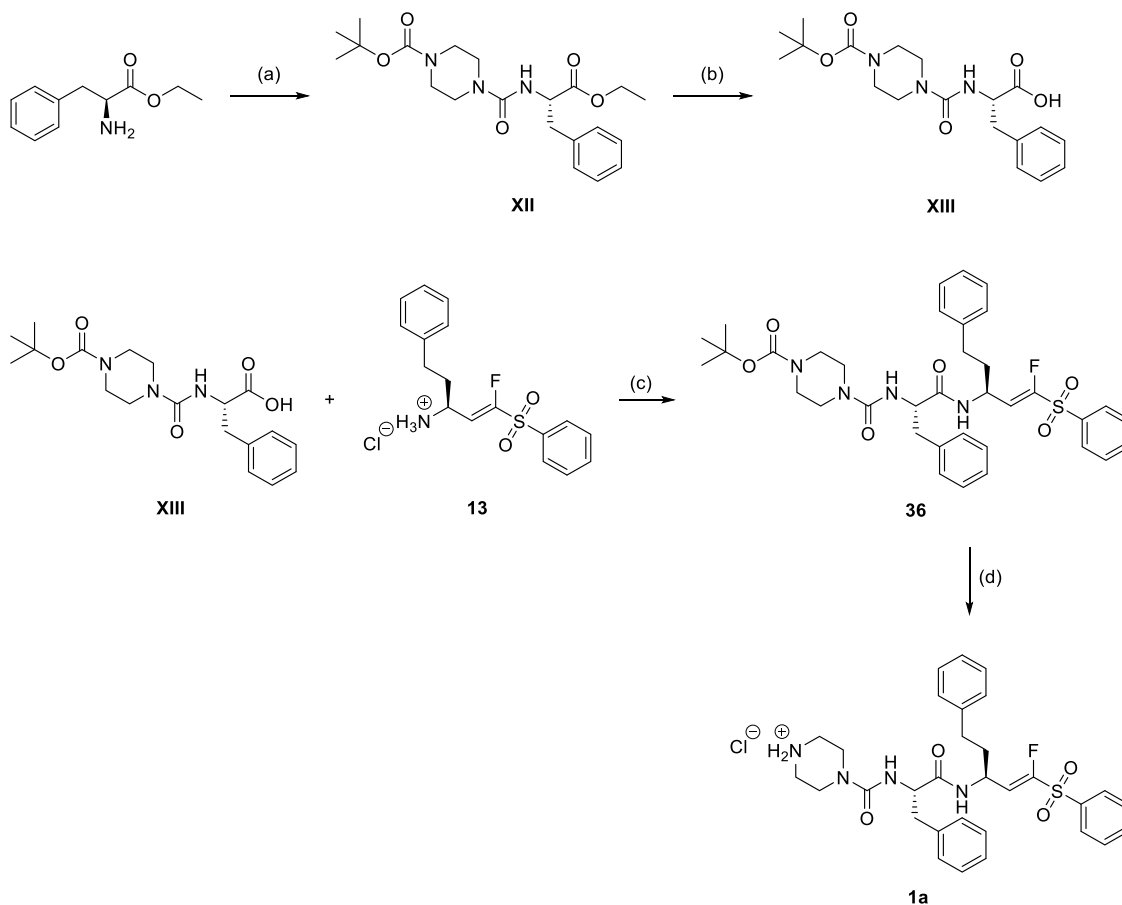
**Chemistry.** Compounds 2a–4l (Figure 2) were synthesized using Horner–Wadsworth–Emmons (HWE) chemistry as the key step (Scheme 1). The required boc-protected aminoaldehydes (VI–VIII) were prepared using Weinreb chemistry. The appropriate phosphonates (5–7) were synthesized in three different ways (Scheme 2). The preparation of phosphonate 5 has been published previously.<sup>12</sup> Phosphonates 6 and 7 were

obtained by fluorination of the respective nonhalogenated precursors (IV, V) with Selectfluor in the presence of KHMDS. The nonhalogenated precursors (III–V) were synthesized according to literature procedures.<sup>28</sup>

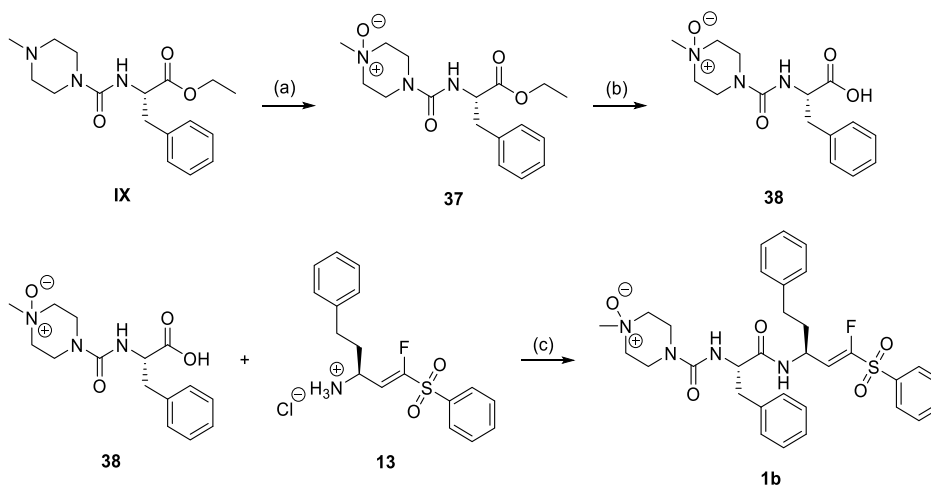
HWE olefination of the aldehydes (VI–VII) with the respective phosphonates (5–7) provided the corresponding boc-protected vinylsulfones (8–12) as mixtures of (*E*)/(*Z*)-isomers (Scheme 1), whereby the (*E*)-isomer was generally favored under the employed conditions. Overall yields ranged from 59 to 75%. The (*E*)-isomers were isolated by column chromatography in acceptable yields (41–63%) and used for the next steps. In the case of vinylsulfonate 9, the (*Z*)-isomer was also isolated ((*Z*)-9, yield 22%). In the next step, the boc-group was removed using standard protocols, either 4 M HCl in dioxane or TFA in DCM, giving the amine building blocks 13–17 in quantitative yields (Scheme 2). These building blocks were subjected to peptide chemistry based on the boc strategy with TBTU/HOBt as the coupling reagent (Scheme 3). The desired compounds (2a–4l) were obtained after one or two coupling and deprotection steps.

The metabolites of compounds 1 and 2d-(H), namely 1a, 1b, and 2l, were synthesized using similar procedures to that described above. For the *N*-demethylated metabolite 1a (Scheme 4), vinylsulfone 13 was coupled with XIII. After removal of the boc group, 1a was obtained with a yield of 93%.



Scheme 4. Synthesis of the *N*-Demethylated Metabolite 1a<sup>a</sup>

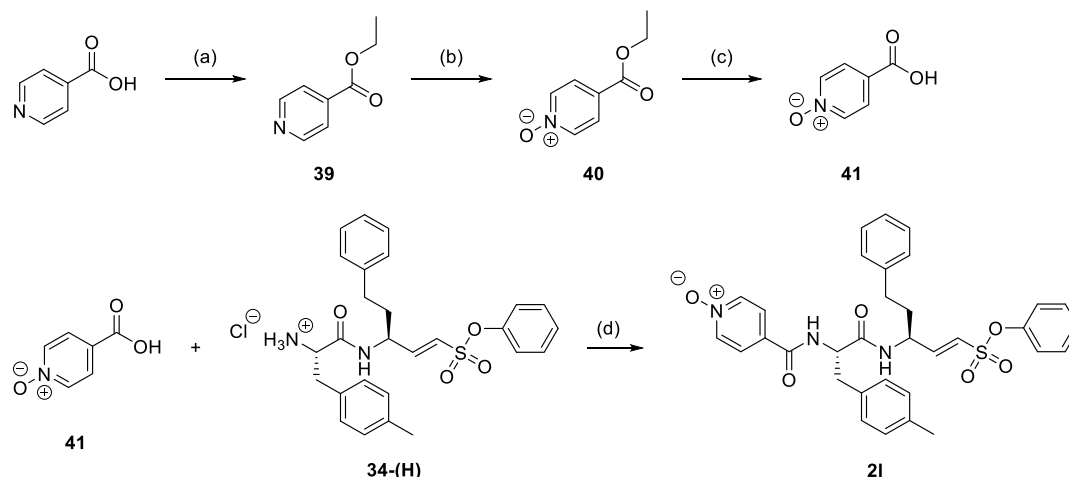
<sup>a</sup>Reagents and conditions: (a) (1) triphosgene, DCM, 0 °C, 1 h, 85%. (2) 1-Boc piperazine, THF, rt, 18 h, 50%, (b) LiOH, THF, 0 °C to rt, 3 h, 74%, (c) HOBt, TBTU, DIEA, DCM, 0 °C to rt, 12 h, 45%, and (d) 4 M HCl in dioxane, rt, 1 h, 93%.

Scheme 5. Synthesis of the *N*-Oxidized Metabolite 1b<sup>a</sup>

<sup>a</sup>Reagents and conditions: (a) *m*CPBA, DCM, 0 °C, 16 h, 52%; (b) LiOH, THF, 0 °C to rt, 3 h, 53%; and (c) HOBt, TBTU, DIEA, DCM/DMF, 0 °C to rt, 24 h, 23%.

In Scheme 5, the preparation of the metabolite 1b, the *N*-oxide of compound 1, is described. The synthesis started with compound IX, which was oxidized with *m*CPBA,<sup>29</sup> resulting in ester 37, which was hydrolyzed with LiOH. Compound 38 was then coupled with vinylsulfone 13, yielding compound 1b.

The *N*-oxidized metabolite 2l of compound 2d-(H) was prepared as shown in Scheme 6. Isonicotinic acid was esterified and then oxidized with *m*CPBA.<sup>29</sup> The resulting compound 40 was hydrolyzed to 41 and then coupled with 34-(H), yielding the *N*-oxide 2l.

Scheme 6. Synthesis of the N-Oxidized Metabolite 2l of Compound 2d-(H)<sup>a</sup>

<sup>a</sup>Reagents and conditions: (a) ethanol, H<sub>2</sub>SO<sub>4</sub>, reflux, 24 h, 73%; (b) *m*CPBA, DCM, 0 °C, 16 h, 29%; (c) LiOH, THF, 0 °C to rt, 3 h, 90%; and (d) HOBt, TBTU, DIEA, DCM, 0 °C to rt, 24 h, 13%.

Table 1. Inhibition Data for Compounds 2a–2k<sup>a</sup>

Cpd	substitution		rhodesain		CatL		CatB	
	R <sup>1</sup>	R <sup>2</sup>	K <sub>i</sub> /μM <sup>b</sup>	K <sub>i</sub> <sup>*</sup> /μM <sup>b</sup>	K <sub>i</sub> /μM <sup>c</sup>	K <sub>i</sub> <sup>*</sup> /μM <sup>c</sup>	SI <sup>d</sup>	K <sub>i</sub> /μM
2a	H	4-Pyr	0.098 <sup>g</sup>	0.015 <sup>g</sup>	0.258 <sup>g</sup>	0.060 <sup>g</sup>	4	1.7
(Z)-2a	H	4-Pyr	0.525 <sup>e,g</sup>		n.d.		n.d.	n.d.
2b	H	DHBD	0.045 <sup>g</sup>	0.009 <sup>g</sup>	n.d.	n.d.	n.d.	n.d.
2d	4-Me	4-Pyr	0.024 <sup>g</sup>	0.003 <sup>g</sup>	0.313 <sup>g</sup>	0.078 <sup>g</sup>	26	38% <sup>f</sup>
2e	4-Me	DHBD	0.098 <sup>g</sup>	0.007 <sup>g</sup>	0.348 <sup>g</sup>	0.039 <sup>g</sup>	6	14% <sup>f</sup>
2f	4-Me	3,5-F <sub>2</sub> Ph	0.034 <sup>g</sup>	0.005 <sup>g</sup>	n.d.	n.d.	n.d.	n.d.
2g	3-Me	4-Pyr	0.094 <sup>g</sup>	0.007 <sup>g</sup>	0.266 <sup>g</sup>	0.030 <sup>g</sup>	4	50% <sup>f</sup>
2h	3-Me	DHBD	0.059 <sup>g</sup>	0.010 <sup>g</sup>	n.d.	n.d.	n.d.	n.d.
2i	3-Me	3,5-F <sub>2</sub> Ph	0.152 <sup>g</sup>	0.021 <sup>g</sup>	n.d.	n.d.	n.d.	n.d.
2j	H	OBn	0.158 <sup>e,g</sup>		n.d.		n.d.	n.d.
2k	H	N-MePip	0.108 <sup>e</sup>		n.d.		n.d.	n.d.

<sup>a</sup>K<sub>i</sub><sup>\*</sup> denotes the dissociation constant of the high-affinity complex in the case of biphasic, time-dependent inhibition. <sup>b</sup>Calculated with method 1 (see the text). <sup>c</sup>Calculated with method 2 (Dixon equation). <sup>d</sup>SI = K<sub>i</sub><sup>\*</sup>(CatL)/K<sub>i</sub><sup>\*</sup>(rhodesain). <sup>e</sup>Calculated from IC<sub>50</sub> value with the Cheng–Prusoff equation. <sup>f</sup>% inhibition at 11 μM inhibitor concentration (single measurement). <sup>g</sup>Mean value of three independent assays; standard deviations less than 10%.

**Enzyme Assays.** Inhibition of rhodesain was tested with the fluorogenic substrate Cbz-Phe-Arg-AMC as described previously.<sup>12,30</sup> For the three series of compounds, the results from the fluorometric enzyme assays with rhodesain and the related mammalian enzymes cathepsin L and B are summarized in Tables 1–3.

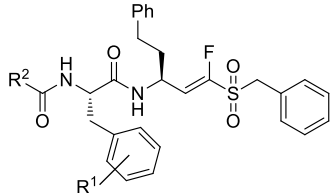
For benzyl and phenyl fluorovinylsulfones (cpds 3a–3i, 4a–4l), the progress curves for inhibition of rhodesain were found to be linear in all cases, indicating a fast reversible inhibition (exemplarily shown for compound 3d in Figure 3A and for 4a in Figure 3B). In order to confirm the competitive behavior of these compounds, IC<sub>50</sub> values were measured at seven different substrate concentrations. IC<sub>50</sub> values were found to increase linearly with ascending substrate concentration, showing competitive inhibition (Figure 3C,D). This was assumed to be

the case for all compounds of the series. Consequently, IC<sub>50</sub> values were converted to K<sub>i</sub> values using the Cheng–Prusoff relationship (Tables 2 and 3).<sup>32</sup>

Reversibility was confirmed by dilution assays, that is, the enzyme was incubated with an excess of inhibitor (10-fold the IC<sub>50</sub> concentration) to ensure full inhibition. Then, the mixture was diluted 100-fold to yield an inhibitor concentration of 0.1-fold the IC<sub>50</sub> concentration. In the case of reversible inhibition, the enzyme activity should recover, whereas in the case of irreversible inhibition, it should not. For both compounds (3d, 4a), enzyme activity recovers after dilution, whereas for the irreversible inhibitor K11777 used as a control, enzyme activity does not recover (Figure 4A).

For vinylsulfonates (2a–2k), the progress curves for inhibition of rhodesain were not linear for most of the

Table 2. Inhibition Data for Compounds 3a–3i

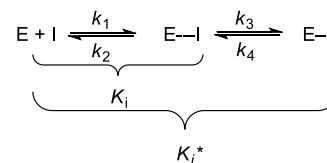


cpd	substitution		rhodesain	CatL		CatB
	R <sup>1</sup>	R <sup>2</sup>	K <sub>i</sub> /μM	K <sub>i</sub> /μM	SI <sup>a</sup>	K <sub>i</sub> /μM
3a	H	4-Pyr	0.053 <sup>d</sup>	0.226 <sup>d</sup>	4	44% <sup>b</sup>
3b	H	DHBD	0.046 <sup>d</sup>	n.d.	n.d.	n.d.
3c	H	3,5-F <sub>2</sub> Ph	0.124 <sup>d</sup>	n.d.	n.d.	n.d.
3d	4-Me	4-Pyr	0.015 <sup>d</sup>	0.181 <sup>d</sup>	12	35% <sup>b</sup>
3e	4-Me	DHBD	0.014 <sup>d</sup>	0.076 <sup>d</sup>	6	8% <sup>b</sup>
3f	4-Me	3,5-F <sub>2</sub> Ph	0.029 <sup>d</sup>	n.d.	n.d.	n.d.
3g	3-Me	4-Pyr	0.061 <sup>d</sup>	0.122 <sup>d</sup>	2	1.7 <sup>c</sup>
3h	3-Me	DHBD	0.092 <sup>d</sup>	n.d.	n.d.	n.d.
3i	3-Me	3,5-F <sub>2</sub> Ph	0.380 <sup>d</sup>	n.d.	n.d.	n.d.

<sup>a</sup>K<sub>i</sub>(CatL)/K<sub>i</sub>(rhodesain). <sup>b</sup>% inhibition at 11 μM (single measurement). <sup>c</sup>Single measurement. <sup>d</sup>Mean value of three independent assays; standard deviations less than 10%.

compounds (2a–2i), but showed time-dependency (exemplified for 2d in Figure 5A). Inhibition by all vinylsulfonates was found to be competitive with respect to the substrate (Figure 5B). Time-dependent inhibition is typical for irreversible inhibitors but may also be observed for covalent reversible inhibition. In the case of irreversible inhibition, the progress curves reach a plateau value with the terminal enzyme activity, that is, the steady-state velocity of substrate turnover in the presence of the inhibitor,  $v_s = 0$ . For covalent reversible inhibition, time-dependent progress curves reflect a biphasic behavior with the terminal enzyme activity in the presence of the inhibitor  $v_s \neq 0$ , but with  $v_s < v_i$  ( $v_i$  = the initial enzyme activity in

the presence of the inhibitor). To distinguish between these two scenarios, dilution assays were performed (see above), exemplarily shown for inhibitor 2d (Figure 4A). The results clearly indicate that vinylsulfonate 2d is a reversible inhibitor, but dissociates significantly slower compared to compounds 4a and 3d, indicating a tight covalent reversible inhibition according to the following inhibition mechanism, with  $K_i = k_2/k_1$  as the dissociation constant of the initial noncovalent enzyme–inhibitor (E⋯I) complex and  $K_i^*$  as the dissociation constant of the final covalent, high-affinity complex (E–I)<sup>33</sup>



For these inhibitors, the initial ( $v_i$ ) and steady-state ( $v_s$ ) velocities in the presence of the inhibitor as well as the pseudo-first order rate constants  $k_{\text{obs}}$  were determined for the different inhibitor concentrations by fitting the progress curves (shown for cpd 2d in Figure 5A) to the slow-binding equation (off = offset)<sup>33</sup>

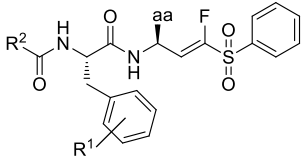
$$[P] = v_s \times t + \frac{v_i - v_s}{k_{\text{obs}}} [1 - \exp(-k_{\text{obs}} \times t)] + \text{off}$$

The  $k_{\text{obs}}$  values were replotted against the inhibitor concentrations [I] (Figure 5C) with the equation<sup>33</sup>

$$k_{\text{obs}} = k_4 + \left( \frac{k_3 \times [I]}{K_i^{\text{app}} + [I]} \right)$$

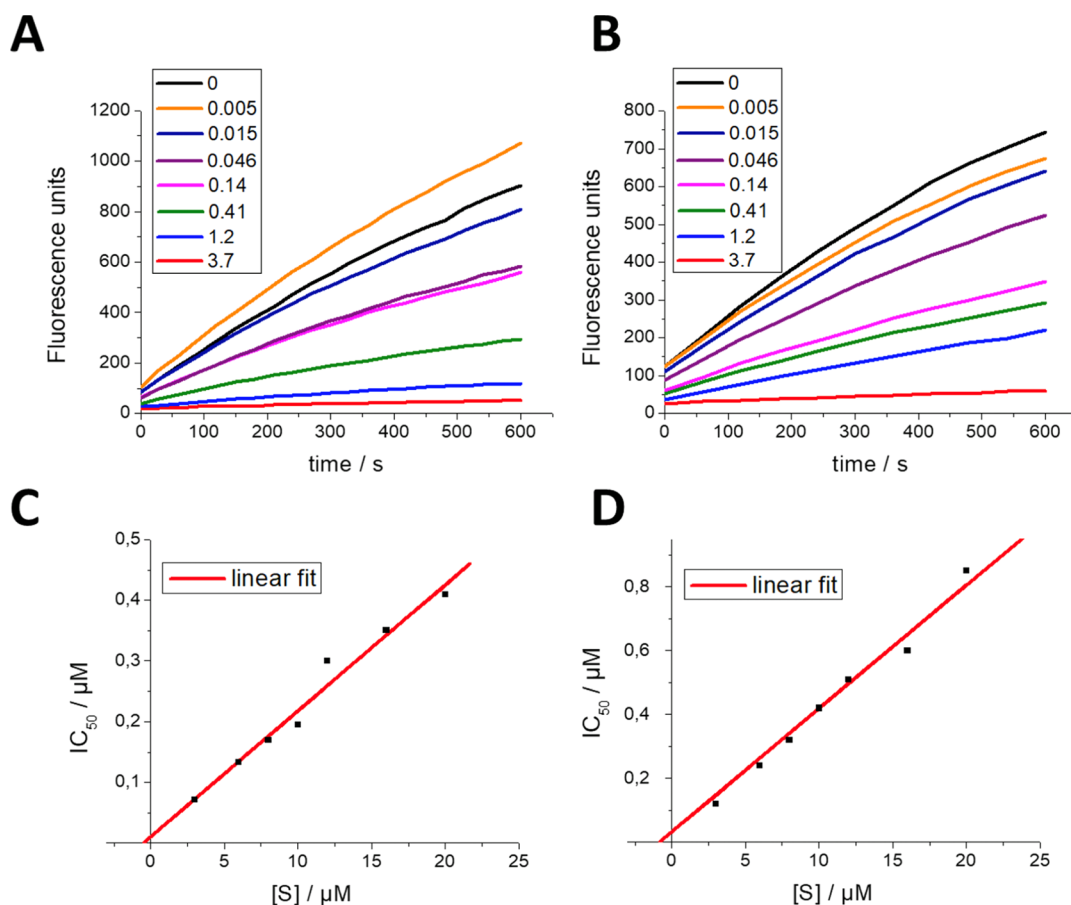
to yield the apparent dissociation constant  $K_i^{\text{app}}$  of the initial enzyme–inhibitor complex, as well as the rate constants  $k_3$  and  $k_4$  of the second inhibition step (Method 1). Because the compounds display competitive inhibition with respect to the substrate (Figure 5B), the  $K_i^{\text{app}}$  value was converted to  $K_i$  for the

Table 3. Inhibition Data for Compounds 4a–4l



cpd	substitution			rhodesain	CatL		CatB
	R <sup>1</sup>	R <sup>2</sup>	aa	K <sub>i</sub> /μM	K <sub>i</sub> /μM	SI <sup>a</sup>	K <sub>i</sub> /μM
1	H	N-MePip	hPhe	0.190 <sup>c,e</sup>	0.023 <sup>e</sup>	0.1	0.47 <sup>d</sup>
4a	H	4-Pyr	hPhe	0.032 <sup>c,e</sup>	0.110 <sup>e</sup>	3	3.13 <sup>d</sup>
4b	H	DHBD	hPhe	0.012 <sup>e</sup>	0.033 <sup>e</sup>	3	4.81 <sup>d</sup>
4c	H	3,5-F <sub>2</sub> Ph	hPhe	0.035 <sup>e</sup>	n.d.	n.d.	n.d.
4d	4-Me	4-Pyr	hPhe	0.008 <sup>e</sup>	0.115 <sup>e</sup>	14	2.08 <sup>d</sup>
4e	4-Me	DHBD	hPhe	0.005 <sup>e</sup>	0.023 <sup>e</sup>	5	34% <sup>b</sup>
4f	4-Me	3,5-F <sub>2</sub> Ph	hPhe	0.010 <sup>e</sup>	n.d.	n.d.	n.d.
4g	3-Me	4-Pyr	hPhe	0.025 <sup>e</sup>	0.049 <sup>e</sup>	2	0.35 <sup>d</sup>
4h	3-Me	DHBD	hPhe	0.035 <sup>e</sup>	n.d.	n.d.	n.d.
4i	3-Me	3,5-F <sub>2</sub> Ph	hPhe	0.329 <sup>e</sup>	n.d.	n.d.	n.d.
4j	H	N-MePip	Met	0.360 <sup>e</sup>	0.173 <sup>e</sup>	0.5	1.20 <sup>d</sup>
4k	H	4-Pyr	Met	0.056 <sup>e</sup>	0.577 <sup>e</sup>	10	6.17 <sup>d</sup>
4l	H	N-MePip	Cys(Bn)	0.630 <sup>e</sup>	0.628 <sup>e</sup>	1	8.62 <sup>d</sup>

<sup>a</sup>K<sub>i</sub>(CatL)/K<sub>i</sub>(rhodesain). <sup>b</sup>% inhibition at 11 μM. <sup>c</sup>Ref 12; n.d.: not determined. <sup>d</sup>Single measurement. <sup>e</sup>Mean value of three independent assays; standard deviations less than 10%.



**Figure 3.** (A) Example for progress curves for inhibition of rhodesain by compound **3d**. Inhibitor concentrations in μM. (B) Example for progress curves for inhibition of rhodesain by compound **4a**. Inhibitor concentrations in μM. (C) Dependence of inhibition potency (IC<sub>50</sub> values) on substrate concentration for inhibition of rhodesain by compound **3d**. Increasing IC<sub>50</sub> values at ascending substrate concentrations show competitive inhibition. The  $K_i$  value is obtained as the intercept of the regression line with the y-axis ( $K_i = 25$  nM). (D) Dependence of inhibition potency (IC<sub>50</sub> values) on the substrate concentration for inhibition of rhodesain by compound **4a**. Increasing IC<sub>50</sub> values at ascending substrate concentrations prove competitive inhibition. The  $K_i$  value is obtained as the intercept of the regression line with the y-axis ( $K_i = 47$  nM).

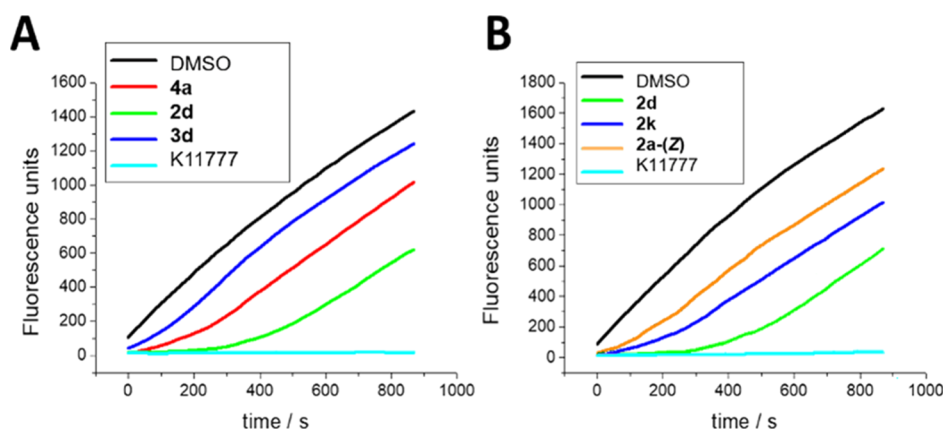


**Figure 4.** (A) Dilution assays show reversible inhibition of rhodesain (see the text). For all compounds, enzyme activity did recover after dilution, except for the irreversible vinylsulfone **K11777** (control). Compound **3d** showed faster reversibility than compound **4a**. Vinylsulfonate **2d** can be considered a tight-binding, slowly reversible inhibitor. (B) Dilution assays of several compounds of the series of vinylsulfonates. In the case of compound **2d**, which showed two-step inhibition in the enzyme assay, enzymatic activity recovers slower compared to vinylsulfonates **2k** and **2a-(Z)**, which did not show biphasic behavior. The irreversible inhibitor **K11777** was used as a control.

initial inhibitor complex with the Cheng–Prusoff equation.<sup>32</sup>

The  $K_i^*$  value as the dissociation constant of the final complex

was calculated from

$$K_i^* = \frac{K_i}{1 + \left(\frac{k_3}{k_4}\right)}$$

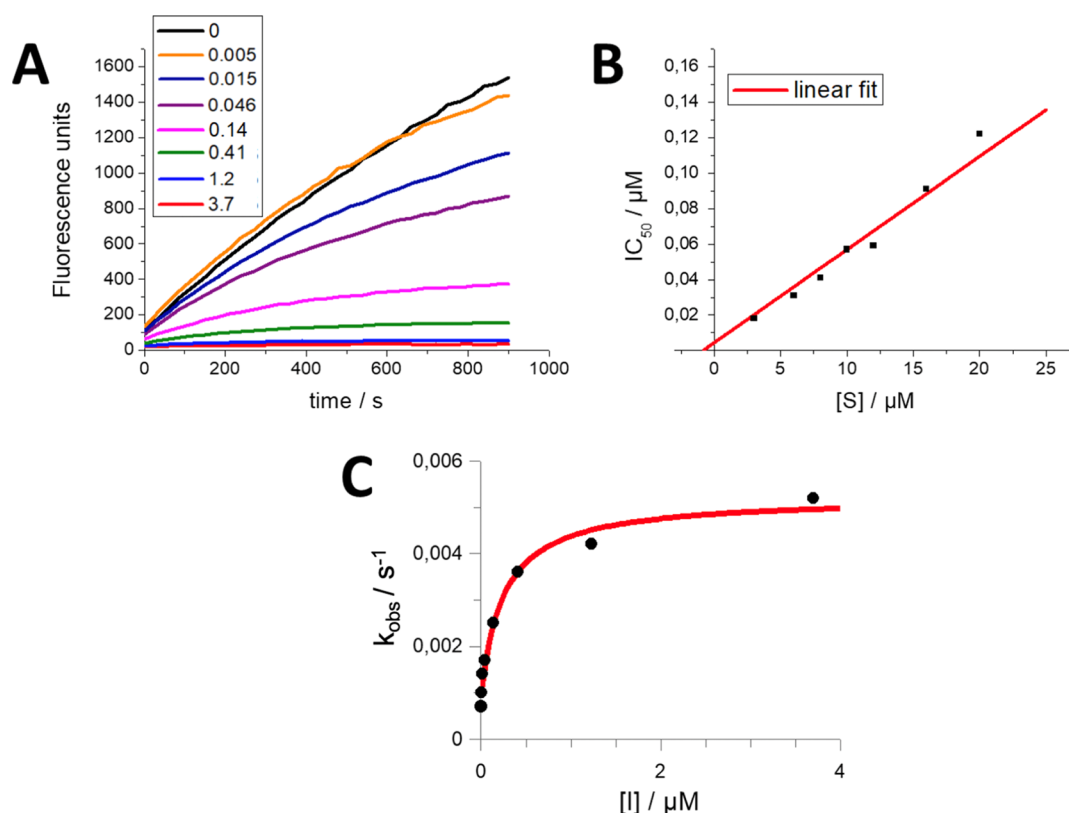


**Figure 5.** (A) Example for progress curves for inhibition of rhodesain by compound **2d**. Curve shape indicates time-dependent inhibition. Inhibitor concentrations in  $\mu\text{M}$ . (B) Dependence of inhibition potency ( $\text{IC}_{50}$  values) from the substrate concentration for inhibition of rhodesain by compound **2d**. Increasing  $\text{IC}_{50}$  values at ascending substrate concentrations show competitive inhibition. The  $K_i$  value is obtained as the intercept of the regression line with the  $y$ -axis ( $K_i = 19 \text{ nM}$ ). (C) Plot of the rate constants  $k_{\text{obs}}$  for the progress curves of compound **2d** from Figure 5A as a function of the inhibitor concentration.  $k_4$  is obtained from the intercept of the regression curve with the  $y$ -axis. The maximum value of  $k_{\text{obs}}$  at infinite inhibitor concentration provides the sum of  $k_3$  and  $k_4$ . The concentration of inhibitor yielding a half-maximal value of  $k_{\text{obs}}$  is equal to  $K_i^{\text{app}}$ .

Both dissociation constants,  $K_i$  and  $K_i^*$ , were also calculated by fitting the initial ( $v_i$ ) and steady-state ( $v_s$ ) velocities, respectively, against the inhibitor concentrations using the Dixon equation (Method 2)<sup>31</sup>

$$\frac{v_{i,s}}{v_0} = \frac{[I]}{1 + \left(\frac{[I]}{K_i^{(*)\text{app}}}\right)}$$

$K_i^{\text{app}}$  was obtained from fitting  $v_i$  against  $[I]$  and  $K_i^{(*)\text{app}}$  from fitting  $v_s$  against  $[I]$  ( $v_0$  is the substrate turnover velocity in the absence of the inhibitor), and both constants were converted into  $K_i$  and  $K_i^*$  with the Cheng–Prusoff equation.<sup>32</sup>

A comparison of the dissociation constants for inhibition of rhodesain by inhibitors **2a–2i** obtained by both methods is shown in Table 4.

The data show that both methods yield similar dissociation constants for the initial low-affinity as well as for the final high-affinity complex proving that both methods are reliable. For all compounds, the rate constant of dissociation of the final complex ( $k_4$ ) was found to be slower than the rate constant of association ( $k_3$ ), indicating tight binding of these inhibitors. Interestingly, vinylsulfonates (**Z**)-**2a**, **2k**, and **2j** did not show time dependency of inhibition, but linear progress curves similar to the benzyl and phenyl vinylsulfones. Dilution assays for these three vinylsulfonates [(**Z**)-**2a**, **2k**, and **2j**] indicated a significantly faster recovery of the enzyme activity compared to the time-dependent inhibitor **2d** [shown for compound (**Z**)-**2a** and **2k** in Figure 4B].

**Table 4. Inhibition Data and Kinetic Parameters  $k_3$  and  $k_4$  for Time-Dependent Inhibition of Rhodensain by Compounds **2a–2i****

Cpd	method 1 (slow-binding equation) <sup>a</sup>				method 2 (Dixon equation) <sup>b</sup>	
	$K_i/\mu\text{M}$	$K_i^*/\mu\text{M}$	$k_3/\text{s}^{-1}$	$k_4/\text{s}^{-1}$	$K_i/\mu\text{M}$	$K_i^*/\mu\text{M}$
<b>2a</b>	0.098	0.015	0.055	0.010	0.110	0.008
<b>2b</b>	0.045	0.009	0.045	0.011	0.060	0.005
<b>2d</b>	0.024	0.003	0.075	0.010	0.022	0.002
<b>2e</b>	0.098	0.007	0.065	0.005	0.124	0.002
<b>2f</b>	0.034	0.005	0.049	0.009	0.052	0.004
<b>2g</b>	0.094	0.007	0.062	0.005	0.089	0.004
<b>2h</b>	0.059	0.010	0.074	0.015	0.068	0.006
<b>2i</b>	0.152	0.021	0.055	0.010	0.155	0.024

<sup>a</sup>Calculated with slow-binding equation (see the text). <sup>b</sup>Calculated with the Dixon equation (see the text).<sup>31</sup> Mean values of three independent assays, standard deviations less than 10%.

To further quantify the degree of reversibility for the different warheads, compounds **2d**, **3d**, and **4d** with identical recognition units were subjected to a dialysis experiment.<sup>12</sup> Here, rhodensain was incubated with an excess of inhibitor (10-fold the  $\text{IC}_{50}$  concentration) to ensure full inhibition. Then, the mixture was dialyzed against a continuous flow of enzyme buffer using a 3.5 kDa cut-off dialysis tubing.<sup>34</sup> Samples were taken after 10, 30, 60, and 120 min and analyzed for their residual enzyme activity with the standard fluorometric assay. The results are presented as the



fractional activity of uninhibited rhodesain, which was subjected to dialysis in the same experiment (Figure 6). Compound 3d

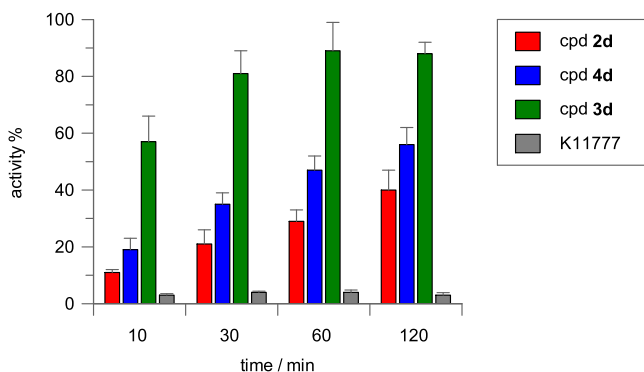


**Figure 6.** Dialysis experiment for compounds 2d, 3d, 4d, and K11777. Rhodesain was incubated with the inhibitors at a concentration of 10-fold the respective  $IC_{50}$  value. The mixture was dialyzed against a continuous flow of buffer. Samples were taken after 10, 30, 60, and 120 min and the substrate was added to measure the residual enzyme activity. K11777 was used as an irreversible control.

showed the fastest reversibility (89% recovery after 1 h), which is in accordance with findings from the dilution assay. Compound 4d dissociated significantly slower (47% recovery after 1 h). Vinylsulfonate 2d displayed the slowest reversibility (29% after 1 h), which supports the tight-binding nature of the inhibition with the formation of a very stable high-affinity complex. K11777 was used as an irreversible control, showing no recovery of the enzymatic activity.

The most potent compounds of each series were also tested against the human enzymes CatL and CatB. For the tested vinylsulfonates (2a, 2d, 2e, and 2g), a biphasic behavior was also observed for inhibition of CatL. In these cases,  $K_i$  and  $K_i^*$  values were calculated with the Dixon equation (Table 2).<sup>31</sup> For inhibition of CatB, no biphasic behavior was observed for these compounds (2a, 2d, 2e, and 2g). This can be explained with the low affinity of the compounds for CatB. Notably, compounds 2d, 2e, and 2g showed only very weak inhibition at concentrations of up to 11  $\mu$ M.

**Discussion of SAR.** Comparison of the  $K_i$  values for rhodesain of the starting compound 1 ( $K_i = 190$  nM) with the P3-modified analogues 4a–4c demonstrates that the exchange of *N*-methyl piperazine against aromatic residues with no or only limited basicity significantly enhances inhibition potency (e.g., cpd 4b with  $K_i = 12$  nM). This is also reflected by the scores obtained from docking for these compounds, for example, for 4b noncovalent affinity as well as the stability of the covalent complex are predicted to be higher (Table S1). Additionally, compounds 4a–4c show improved selectivity for rhodesain over the human cathepsins. Lead compound 1 shows a higher affinity for human CatL ( $K_i = 23$  nM) than for rhodesain ( $K_i = 190$  nM), while P3-modified compounds 4a and 4b slightly favor inhibition of rhodesain (3-fold). Furthermore, selectivity for rhodesain over CatB is dramatically enhanced by these structural variations. This is a remarkable improvement (2-fold) compared to the weak selectivity of starting compound 1. A further increase in potency for rhodesain is observed for compounds with an additional 4-methyl substituent at the phenylalanine aromatic ring (4d–4f), with compound 4e ( $K_i = 5$  nM) being the most potent inhibitor in the series of phenyl vinylsulfones. As suggested from noncovalent docking, this increase in potency

may be directly attributed to additional hydrophobic interactions of the 4-methyl group with lipophilic residues lining the S2 pocket (Ala208, Leu160, Figure 7), which is also reflected in

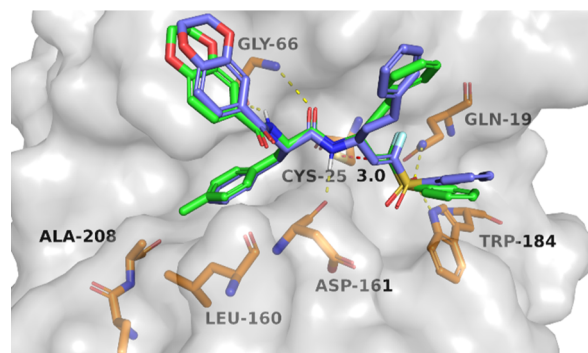


**Figure 7.** Noncovalent binding mode of compound 4b (light blue, FlexX score:  $-31.2$ , Hyde score:  $-10.0$  kcal mol<sup>-1</sup>) and 4e (green, FlexX score:  $-32.5$ , Hyde score:  $-11.7$  kcal mol<sup>-1</sup>) as predicted by FlexX. The electrophilic  $\beta$ -carbon of the fluorovinylsulfone warhead comes in close proximity to the nucleophilic sulfur of Cys25 (3.0 Å). The sulfone group forms hydrogen bonds with Gln19 and Trp184. The recognition unit forms hydrogen bonds to Gly66 and Asp161. The additional 4-methyl group of 4e at the phenylalanine aromatic ring points into a hydrophobic cavity between Ala208 and Leu160, resulting in additional lipophilic interactions compared to compound 4b.

higher scores compared to compounds 4a–4c (Table S1). Additionally, introduction of the 4-methyl substituent further increases selectivity against CatL (14-fold for 4d). In contrast, incorporation of a 3-methyl substituent (4g–4i) does reduce potency and selectivity compared to compounds 4a–4c. In particular, the combination of the 3-methyl substituent and the 3,5-difluorophenyl moiety (4i) is not advantageous: compound 4i displayed significantly reduced potency ( $K_i = 329$  nM). The considerable difference compared to compound 4e with a 4-methyl substituent ( $K_i = 10$  nM) cannot be explained exclusively with the slightly reduced docking scores (Table S1).

Within the set of benzyl vinylsulfones (3a–3i), the SAR relationships are very similar compared to phenyl vinylsulfones (4a–4i). Consequently, compounds 3d and 3e with a 4-methyl substituent and a 4-pyridyl or DHBD moiety, respectively, are the most potent and most selective inhibitors (3d:  $K_i = 15$  nM, 12-fold selectivity over CatL). Remarkably, compound 3d showed even lower activity against CatB (35% inhibition at 11  $\mu$ M) compared with its counterpart 4d. Again, compound 3i with a 3-methyl substituent and 3,5-difluorophenyl residue shows noticeably lower potency ( $K_i = 380$  nM). Comparison of inhibitory potency for benzyl and phenyl vinylsulfones with the same recognition unit (e.g., 3a vs 4a) reveals that the benzyl substituent at the warhead has a negative influence on inhibition potency. In general, benzyl vinylsulfones have slightly increased  $K_i$  values compared to their phenyl counterparts.

These findings cannot be correlated with scores from docking, which generally predicted a higher affinity for compounds with a benzyl group at P1'. Computational conclusions to explain these differences between theory and experiment would be desirable, but are difficult because the differences in  $K_i$  values result from an increase in binding energy of less than 1 kcal mol<sup>-1</sup> (e.g., 3d  $K_i = 0.015$   $\mu$ M, i.e.,  $\Delta G = -11.10$  kcal mol<sup>-1</sup> vs 4d  $K_i = 0.008$   $\mu$ M, i.e.,  $\Delta G = -11.49$  kcal mol<sup>-1</sup>), which is out of the scope of even high-level quantum chemical computations. Possibly, entropic

effects due to the higher flexibility of the benzyl group in the noncovalent enzyme inhibitor complex may contribute.

The results from dilution and dialysis assays revealed that benzyl vinylsulfones are faster reversible than their phenyl counterparts, which may be explained with a lower reaction energy for the covalent bond-forming step, resulting in a weaker covalent bond.

Comparison of the  $K_i$  values of starting compound **1** ( $K_i = 190$  nM) and the corresponding vinylsulfonate **2k** ( $K_i = 108$  nM) demonstrates a nearly 2-fold improvement in affinity for rhodesain. The increase in potency may be partly attributed to the enlarged substituent at P1'. The results from noncovalent docking suggest that the vinylsulfonate moiety extends further into the S1' pocket and forms nonpolar interactions with Trp184 (Figure 8), which is also reflected by the slightly

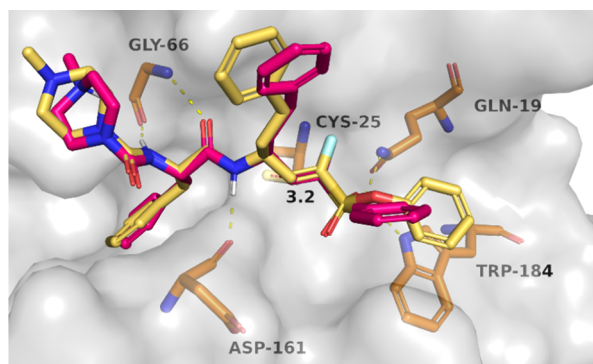


**Figure 8.** Overlay of noncovalent docking poses of compound **1** (magenta, FlexX score:  $-27.9$ , Hyde score:  $-6.2$  kcal mol $^{-1}$ ) and compound **2k** (gold, FlexX score:  $-28.4$ , Hyde score:  $-8.8$  kcal mol $^{-1}$ ). The enlarged vinylsulfonate moiety of compound **2k** extends further into the S1' pocket and the aromatic ring can form additional hydrophobic interactions with Trp184 ( $\pi$ - $\pi$ -stacking interactions).

enhanced scores. Again, substitution of the *N*-methyl piperazine against aromatic residues (cpds **2a–2i**) further improves affinity for rhodesain. Additionally, and in contrast to compound **2k**, compounds **2a–2i** show a biphasic, time-dependent inhibition mechanism.

Dilution and dialysis experiments demonstrated reversibility for compound **2d** (Figures 4 and 6), which is, however, significantly slower compared to vinylsulfonate **2k**, which supports the tight-binding properties of **2d**. The related vinylsulfones (**3d** and **4d**) do not show two-step inhibition, indicating that a combination of the properties of the fluorovinylsulfonate warhead with appropriate noncovalent interactions is required for tight binding. This is further supported by vinylsulfonate **2j** with a Cbz group at P3, which also does not show time-dependent inhibition. Among the tight-binding compounds, **2d** shows the highest potency for rhodesain with a dissociation constant of the initial encounter complex  $K_i = 24$  nM, and with a high-affinity complex formed in the second step ( $K_i^* = 3$  nM). Especially, the covalent complex is predicted to be very stable (Figure 9B). This is in excellent accordance with the high scores obtained from both docking approaches for compound **2d** (Table S1). Notably, compound **2d** showed good selectivity over the human cathepsins, with 26-fold selectivity against CatL and virtually no activity against CatB (38% at 11  $\mu$ M), which is a significant improvement compared to the starting compound **1**.

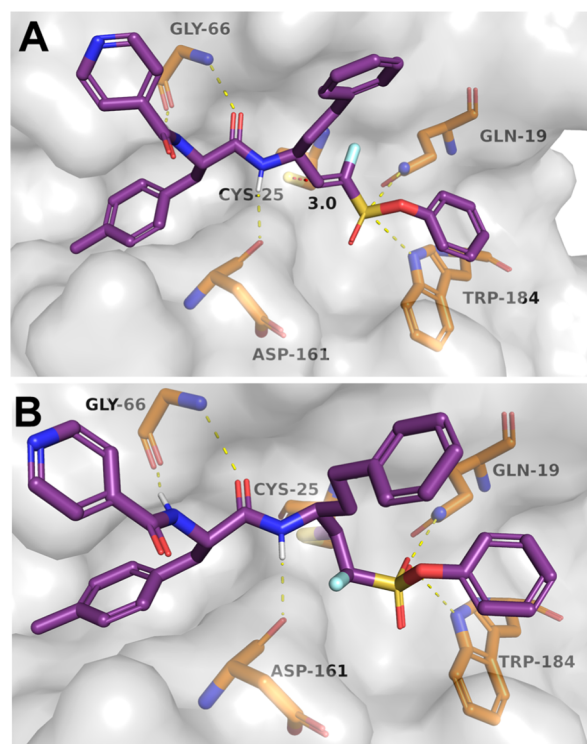


**Figure 9.** (A) Non-covalent docking pose of compound **2d** predicted with FlexX (FlexX score:  $-34.3$ , Hyde score:  $-38$ ). (B) Geometry of the covalent complex between rhodesain and compound **2d** as predicted with DOCKTITE [score (affinity  $\Delta G$ , kcal mol $^{-1}$ ):  $-6.2$ , DSX score:  $-195.5$ ]. The combination of the vinylsulfonate aromatic ring extending further into the S1' pocket and forming lipophilic interactions with Trp184, additional hydrophobic interactions of the 4-methyl group at phenylalanine aromatic ring with the S2 pocket and the preferred 4-pyridyl group at P3 results in a high affinity of compound **2d** for the binding site. This is reflected from higher scores obtained from both docking approaches compared to its analogues (Table S1).

Assuming that inhibitor binding to CatL and CatB is similar to rhodesain binding and that the binding mode is not largely altered for the compounds presented herein compared to **K11777**, which is also suggested by the docking (Figures 7–9), the underlying molecular mechanisms for selectivity can be explained by analysis of the known X-ray structures. Rhodensain shares an overall sequence identity of 44.7% and similarity of 59.1% with CatL and 27.9% identity and 47.4% similarity with CatB, as well as a highly similar fold with an  $C_\alpha$ -RMSD of 1.35 and 2.15 Å, respectively, known from crystal structures available in the PDB<sup>35</sup> (entries, rhodensain: 2p7u,<sup>11</sup> CatL: 2xu1,<sup>36</sup> and CatB: 3ai8).<sup>37</sup> For residues forming the binding site (defined as all amino acids within 6 Å of reference ligand **K11777**) identity/similarity even increase to 59.1%/70.2% for CatL and 40.4%/49.1% for CatB. Nevertheless, slight structural differences of residues forming the S1–S3 sites can be observed, explaining the selectivity profile of the compounds under investigation. Additionally, CatB, divergent from CatL and rhodensain, contains a so-called occluding loop (residues 104–124), which is crucial for this enzyme's exopeptidase activity.<sup>38</sup> This loop structure closes upon the S' sites. Neither phenyl- nor benzylfluorovinylsulfone nor fluorovinylsulfonate moieties of the compounds within this study reach far enough toward this sites to form interactions, but—in contrast—may even cause clashes with the residues of CatB (Figure 10A). Further focusing on the S1 site reveals one residue of the CatB occluding loop, which provides



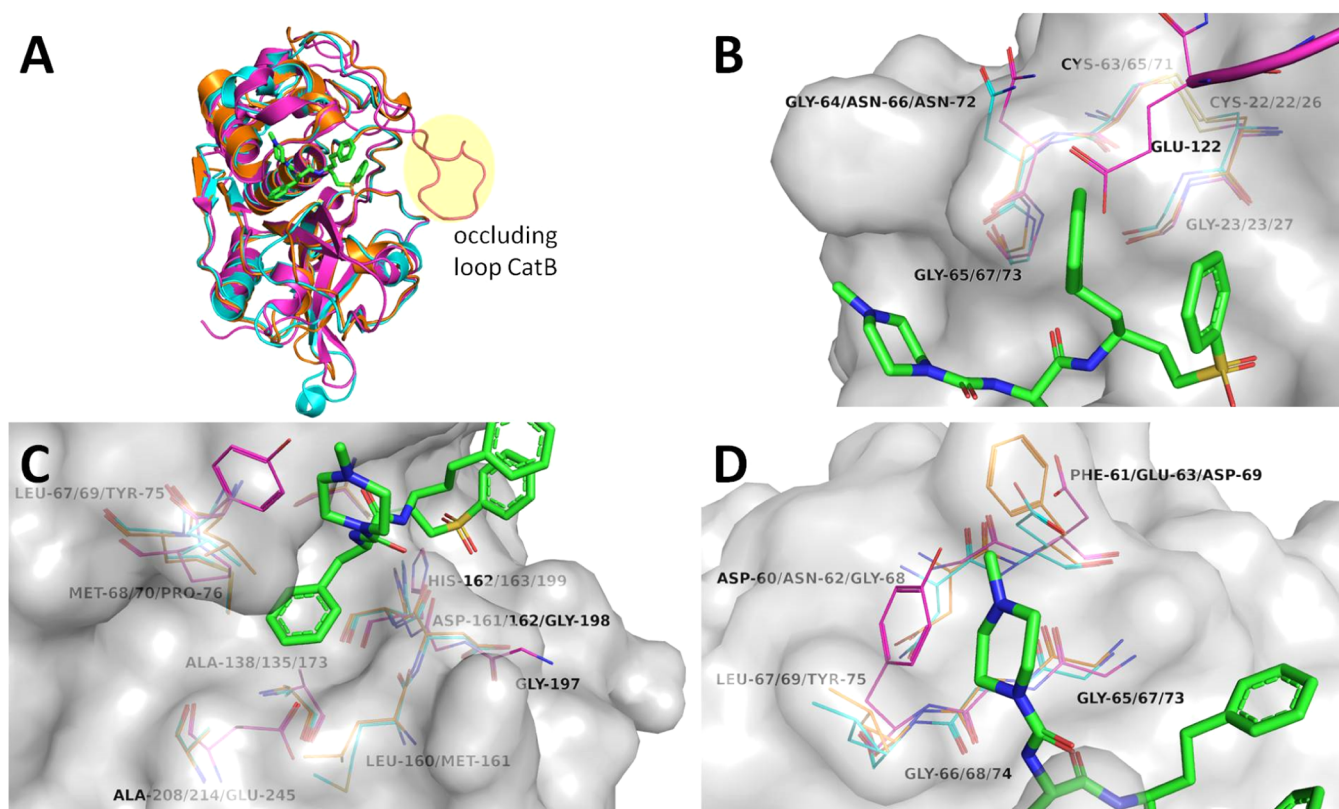


**Figure 10.** Structure comparison of rhodesain (orange carbon atoms, pdb entry 2p7u), CatL (cyan carbon atoms, pdb entry 2xu1), and CatB (magenta carbon atoms, pdb entry 3ai8) with inhibitor K11777 shown with green carbon atoms. Residue enumeration is rhodesain/CatL/CatB. For (B–D), the rhodesain surface is shown in gray for orientation. (A) Whole protease structures depicted as cartoons with the CatB occluding loop highlighted. (B) Close view of S1 site residues. CatB-unique occluding loop shown in the upper right with Glu122 as a selectivity determining feature over CatB. (C) Close view of S2 site residues. (D) Close view of S3 site residues reveals acidic Glu63 and Asp69 in cathepsins to form ionic interactions with the basic center of compound K11777, which is absent in compounds with more favorable selectivity profiles.

an explanation for selectivity (Figure 10B). Glu122 reaches toward the S1 pocket, not only making this site more polar, but also narrower, clashing with the homophenylalanine moiety of the inhibitors and thereby causing selectivity over CatB. Within the S2 pocket, the largest differences were found for CatB as well (Figure 10C). CatB Gly197 shows a different orientation than the corresponding residues Leu160 in rhodesain and Met161 in CatL. Additionally, Ala208/214 (enumeration is rhodesain/CatL) is exchanged to Glu246, Met69/70 to Pro76, and Leu67/69 to Tyr75. These differences all together result in a more open and polar pocket within CatB, which leads to a higher affinity for rhodesain and CatL for inhibitors carrying (3- or 4-methyl)-phenylalanine moieties. Additionally, the selectivity for rhodesain over CatL introduced by the 4-methyl substitution (compounds 2d, 3d, and 4d) is likely to be caused by non-polar interactions with Leu160 being more favorable compared to the CatL Met161, which is slightly more distant and potentially impaired in its flexibility upon binding. The most significant improvement in selectivity was the displacement of *N*-methyl piperazine by 4-pyridine or—less pronounced—by DHDB (compounds 2d, 2e, 3d, 3e, 4d, and 4e). Within the S3 site, acidic amino acids Glu63 and Asp69 are found in CatL and CatB, respectively, while in rhodesain Phe61 sits at the corresponding position (Figure 1D). By the removal of the positively charged *N*-methyl piperazine, the loss of potential ionic interactions only with the off-target cathepsins is, therefore, likely to improve the selectivity profile of these compounds. Additionally, the Tyr75 residue in CatB compared

to Leu in rhodesain and CatL results in a smaller S3 pocket and an enhanced selectivity over CatB, too.

In contrast to all other compounds in this study, the geometry of the double bond of compound (Z)-2a has a (Z)-configuration. Because (Z)-isomers are obtained as side products from HWE olefination, it was obvious to explore the influence of the geometry of the double bond on inhibitory potency. Compared to the (E)-isomer 2a ( $K_i^* = 15$  nM), compound (Z)-2a ( $K_i = 525$  nM) shows markedly reduced potency and forms no high-affinity complex, indicating that the (Z)-configuration of the double bond is not favorable.

Compounds with a modified P1 residue (4j–4l) showed reduced potency for rhodesain compared to the counterparts with homophenylalanine, which was already anticipated from non-covalent docking scores. Nevertheless, compound 4k, with methionine at P1 and the 4-pyridyl moiety at P3, is still a potent inhibitor of rhodesain ( $K_i = 56$  nM).

**MS Analysis.** Covalent protein–ligand interactions were verified by ESI MS for compounds 2a, (Z)-2a, and 2j and MALDI-TOF MS for K11777, 1, 2a, 2j, and 2k.

In all three cases (2a, (Z)-2a, and 2j), the protein–ligand adduct resulting from Michael addition was detected in the ESI mass spectra. The observed mass shift corresponds to the mass of the inhibitor [exemplified for compound 2a in Figure 11; for compounds (Z)-2a and 2j, see Figure S2], which shows covalent bond formation.

To further elucidate possible differences in binding mode related to compound variability, especially to confirm the

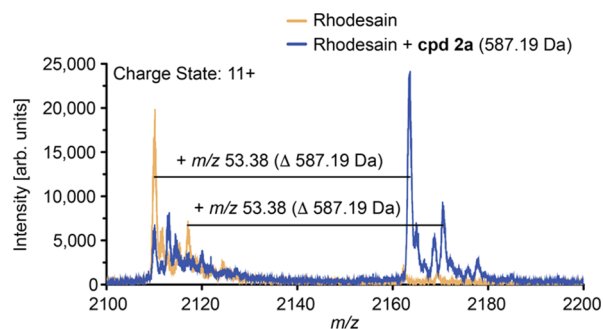


**Figure 11.** Intact protein–ligand adducts obtained by mass spectrometry for compound **2a**. The observed shift corresponds to the mass of the inhibitor considering the charge state of the protein ( $m/z = 11^+$ ).

covalent inhibition, a representative subset of compounds covering the majority of synthesized modifications was selected and analyzed by MALDI-TOF MS. The aim here was to analyze whether these modifications impede covalent bond formation between the catalytic thiolate and the vinyl moiety. ESI MS is a softer method in terms of transition to the gas phase, where non-covalent adducts can be found as well as covalent adducts. Depending on the matrix, MALDI-TOF MS can discriminate between covalent and non-covalent binding: the formation of non-covalent adducts can be suppressed by using an acidic matrix, which was attributed to the disruption of salt bridges and the subsequent destabilization of the non-covalent protein–ligand complex.<sup>39–41</sup> Therefore, MALDI-TOF MS was applied to further investigate the binding mode.<sup>40,42,43</sup>

In terms of warhead modification, vinyl sulfone **K11777**,  $\alpha$ -fluorovinylsulfone **1**, and  $\alpha$ -fluorovinylsulfonates **2a**, **2j**, and **2k** were evaluated. Furthermore, the selected subset differed in

their substituents in the P3 position, namely isonicotinyl amide (**2a**), benzylcarbamate (**2j**), and 4-methylpiperazine-1-carboxamide (**K11777**, **1**, and **2k**), while sharing the preceding Phe-Phe motif in P2 and P1, respectively. **K11777** was used as a known, structurally equivalent control compound for its analogous, though covalent irreversible binding mode. A non-covalent inhibitor of rhodesain (**42**) carrying a fluorodinitrobenzene moiety as an aromatic electrophile was chosen as a control substance for its different inhibition mode (Figure 12) compared to the vinylsulfones. The compound forms a tight  $\pi$ -complex with the catalytic thiolate, the adduct mass of which was detectable in ESI MS experiments with rhodesain.<sup>44</sup>

For all evaluated  $\alpha$ -fluorovinyl analogues (**1**, **2a**, **2j**, and **2k**), covalent adducts with rhodesain were observed by MALDI-TOF MS. The resulting spectra consisted of a broad peak corresponding to the protein (ca. 23.3 kDa),<sup>45–47</sup> and a second peak corresponding to the covalent protein–inhibitor adduct (ca. 23.8 kDa) that shows a mass shift corresponding to the mass of the respective compound (Figure 12). The observed multiplicity of the peaks was attributed to additions of matrix molecules [ $m(\text{sinapinic acid}) = 224 \text{ Da}$ ] to rhodesain, as similar phenomena are described in the literature.<sup>47</sup> The four fluorovinyl derivatives (**1**, **2a**, **2j**, and **2k**) behaved like the irreversible control substance **K11777**, while the non-covalent inhibitor (**42**) did not show any detectable adduct signals under the evaluated conditions. Apart from that, an adduct of **42** was found with ESI MS as published previously.<sup>39,40,44</sup> The identical behavior of **K11777** and the  $\alpha$ -fluorovinylsulfones/-sulfonates in the MALDI-TOF MS experiments could be observed using two different matrices, sinapinic acid and a mixture of  $\alpha$ -cyano-4-hydroxycinnamic acid and 2,5-dihydroxybenzoic acid,<sup>43</sup> respectively, the latter data are shown in the Figure S1. These findings, combined with the results from ESI MS and the dialysis

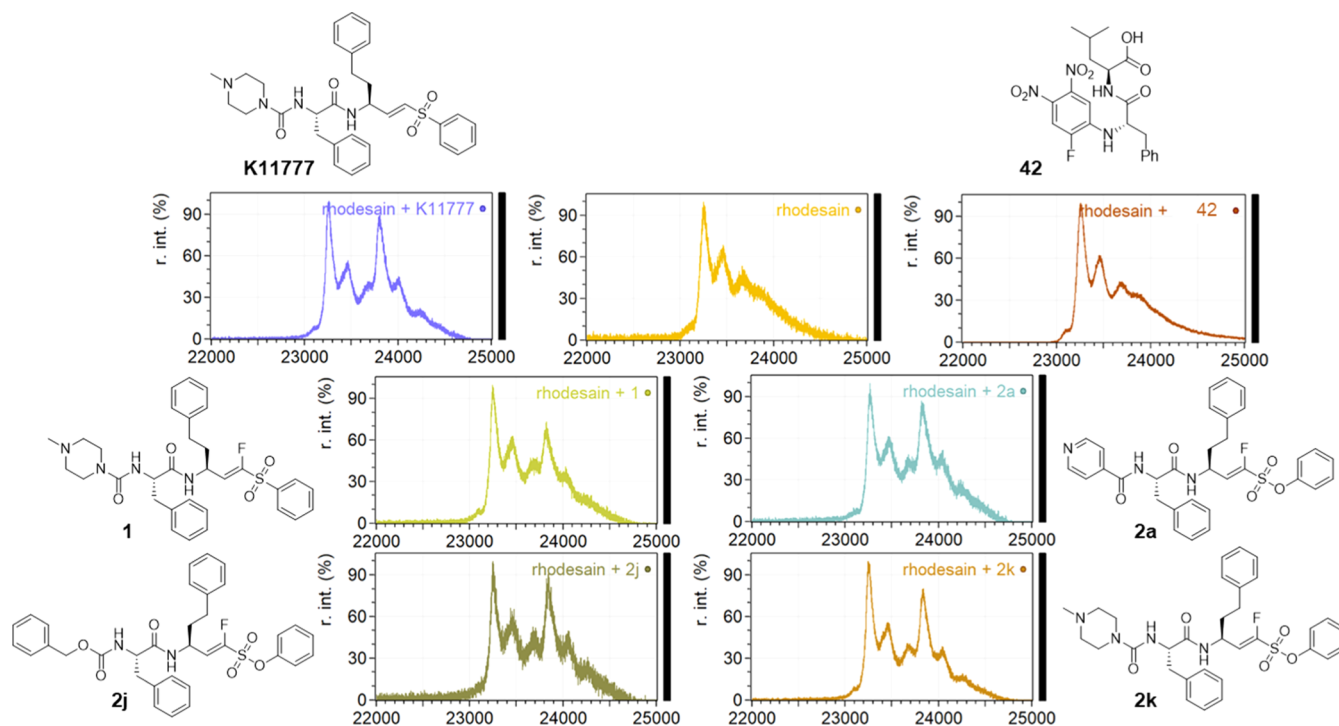


**Figure 12.** MALDI-TOF mass spectra of rhodesain (ca. 23 kDa) in the presence of different inhibitors (10-fold molar excess of inhibitor to protein). Sinapinic acid was used as the matrix substance. The figures show the relevant range of the spectrum to display  $[M + H]^+$ , which were baseline corrected.

and dilution assays, clearly show that the  $\alpha$ -fluorovinylsulfones and -sulfonates are indeed covalent reversible inhibitors of rhodesain.

**Comparison of the Inhibition Mechanisms of K11777 and 1 by QM/MM Modeling.** In our previous study,<sup>12</sup> the computed reaction energies of K11777 and 1 differed only marginally so that the computational results could hardly explain the transition from irreversible to reversible inhibition. In that study, both reaction pathways had been calculated starting from the X-ray structure of the covalent enzyme–inhibitor complex of K1177 with rhodesain (PDB: 2p7u) going backwards from the covalent toward the non-covalent complex. To generate the reaction path for 1, the hydrogen atom had been substituted for fluorine in the X-ray structure. It had been necessary to start the computations from the X-ray structure of the covalent complex because no experimental information on the non-covalent complex was available. Moreover, such procedures had been very successful to explain the stereo- and regioselectivity of various epoxide- and aziridine-based inhibitors and to predict improved inhibitors.<sup>48–50</sup> However, such approaches can be error-prone in cases when the geometries of the covalent and non-covalent enzyme–inhibitor complexes differ largely, especially when substitution leads to large differences in the non-covalent complex.

To obtain more reliable insights into possible differences between the non-covalent enzyme–inhibitor complexes of K11777 and 1, at first, non-covalent structures starting from the X-ray structure of K11777 with rhodesain (PDB: 2p7u) were calculated. For 1, the hydrogen atom in the  $\alpha$ -position was substituted by fluorine. These structures then were used as starting points for MD simulations (10 times 10 ns sequences for each compound). Exemplarily, Figure 13 presents the

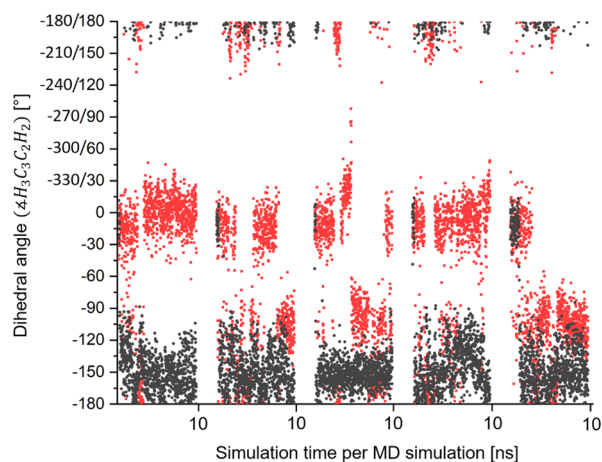


**Figure 13.** Variation of the dihedral angle  $\angle H^3C^3C^2H^2$  along the MD simulations (sequences of 10.0 ns, respectively) for K11777 with X = H (in red) and the fluorinated vinylsulfone with X = F (in black). Figure 13 defines the dihedral angle and gives the corresponding orientation of the warhead in the active site. Please note that  $\angle H^3C^3C^2H^2 = 150^\circ$  is equal to  $\angle H^3C^3C^2H^2 = -210^\circ$ .

fluctuations in the dihedral angle  $\angle H^3C^3C^2H^2$  (see Figure 14 for definition) for five different MD samplings. A variation of  $\angle H^3C^3C^2H^2$  from 0 to  $\pm 180^\circ$  describes the rotation of the inhibitor around the  $C^3C^2$  single bond, adjacent to the double bond. Due to this rotation, the  $C^1X$  bond ( $X = H, F$ ) moves from the Gly23-oriented side to the opposite side (Figure 14). For K11777, mainly values between  $-40$  and  $40^\circ$  ( $-320^\circ$ ) were

found for the  $\angle H^3C^3C^2H^2$  angle. In the following, we denominate alignments with  $-40^\circ < \angle H^3C^3C^2H^2 < 40^\circ$  (Figure 14) as “H-orientation”. For 1,  $\angle H^3C^3C^2H^2$  adopted values between  $-120$  and  $-190^\circ$  ( $170^\circ$ ), that is, the warhead of the compound oscillates around a position, where the F-atom is oriented toward the backbone NH groups of Cys25, Ser24, and the side-chain  $NH_2$  group of Gln19 (Figure 14b), but mainly adopts positions with  $\angle H^3C^3C^2H^2 > -180^\circ$ . In the following, geometries with  $-190^\circ < \angle H^3C^3C^2H^2 < -120^\circ$  are denominated “F-orientation”.

During the MD simulation, K11777 populated both H- ( $\approx 80\%$ ) and F-orientation ( $\approx 20\%$ ) indicating that both alignments are energetically quite similar. In contrast, 1 predominantly adopted the F-orientation due to attractive interactions with the NH backbone group of Cys25, the side chain  $NH_2$  group of Gln19 (known as the oxyanion hole of rhodesain), and the NH backbone group of Ser24. Similar variations in the structures upon fluorination were reported in the literature.<sup>51,52</sup>

While the orientation of the recognition unit (in Figure 14 given in purple) remained fixed in the torsional motion around  $\angle H^3C^3C^2H^2$ , the relative positions between the attacked double bond of the inhibitor and the involved side chains of Cys25 and His162 changed drastically as shown in Figure 15. In both cases, a syn-addition takes place because the thiolate group of Cys25 and the protonated imidazole ring of His162 are found to be on the same side of the double bond (Figure 15), but for the H-orientation, the CS bond of the Cys25 side chain is orthogonally oriented with respect to the  $C^1C^2$  double bond while it is oriented in parallel for the F-orientation. The position of the protonated imidazole ring of His162 also changed accordingly.

To calculate the influence of the different orientation of the warhead of K11777 and 1 on the inhibition mechanism (Figure 1), the corresponding reaction paths were computed. However, due to the large number of local minima for the non-covalent complex (the reactant) and the covalent complex (the product) in combination with the roughness of the underlying potential energy surface (PES), the appropriate picture of the inhibition reaction is not that of a single reaction path with one starting point, one transition state, and one product, but that of a very rough PES with various energetically similar pathways starting from and ending at slightly different reactants and products. To achieve representative pathways, we performed geometry optimizations starting from two selected snapshots of the MD simulation for each inhibitor and computed the reaction paths starting from the obtained minima. The geometrical parameters of the respective minima are given in Table S2.

To characterize the reaction mechanism, we first computed two-dimensional scans using the distances  $R(S_{\text{Cys}}-C_2)$  and  $R(H_{\text{His}}-C_1)$  as main reaction parameters (Figure 14). The resulting transition states served as starting points for subsequent IRC (intrinsic reaction paths) simulations,<sup>53</sup> the course of which generally gives good insights into the reaction mechanism (reaction barrier, reaction energy, and structural changes in the course of the reaction). More details are given in the Experimental Section. In Figure 15, representative IRCs for K11777 starting from the H-orientation and 1 starting from the F-orientation are compared. Figure 16 also sketches the geometry variations along the IRCs. Further information on the geometries is given in Table S3. Additional paths starting from other reactant minima showing similar shapes can also be found in the Supporting Information (Figures S4 and S7).



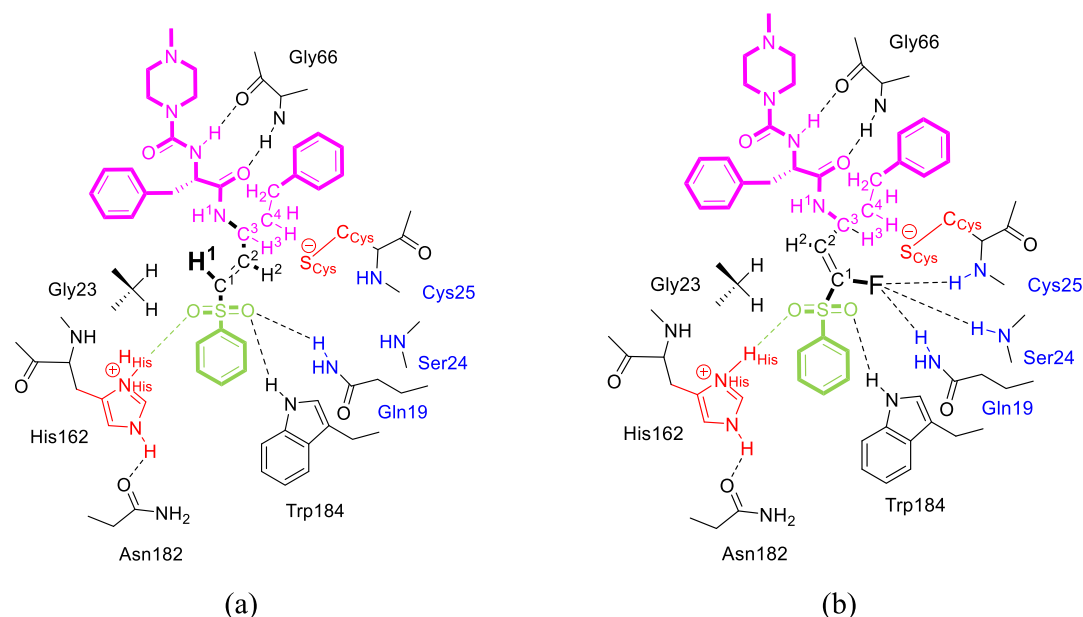


**Figure 14.** Sketch of the predominant orientation of the warheads (bold) in the active site during the MD simulations given in Figure 13. (a) H-orientation: predominant conformations of **K11777** ( $X = H$ ) with  $-40^\circ \leq \angle H^3C^3C^2H^2 \leq 40^\circ$  (b) F-orientation: predominant conformations for the fluorinated vinylsulfone **1**, with  $-190^\circ \leq \angle H^3C^3C^2H^2 \leq -120^\circ$ . For more information, see the text.

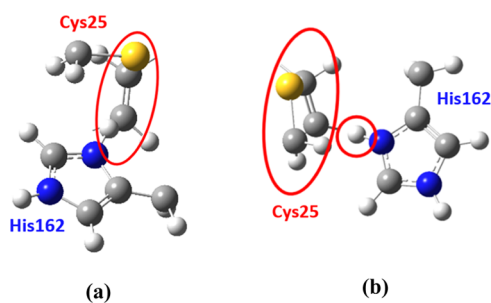


**Figure 15.** Relative orientation of Cys25 and His162 moieties with respect to the double bond of the vinylsulfone group attacked by Cys25, (a) for **K11777** ( $X = H$ ) in the H-orientation, and (b) for the fluorinated vinylsulfone ( $X = F$ ) in the F-orientation.

Figure 16 shows considerable differences in the IRCs of both compounds. While the reaction pathway for the inhibition of rhodesain by **K11777** passes over a barrier of about 12 kcal mol<sup>-1</sup> and has an exothermic reaction energy of about -20 kcal mol<sup>-1</sup>, we predict a thermoneutral reaction for the inhibition reaction of **1** with a very high barrier of 25 kcal mol<sup>-1</sup>. The small reaction barrier and the strong exothermicity nicely explain why **K11777** is an efficient irreversible inhibitor.

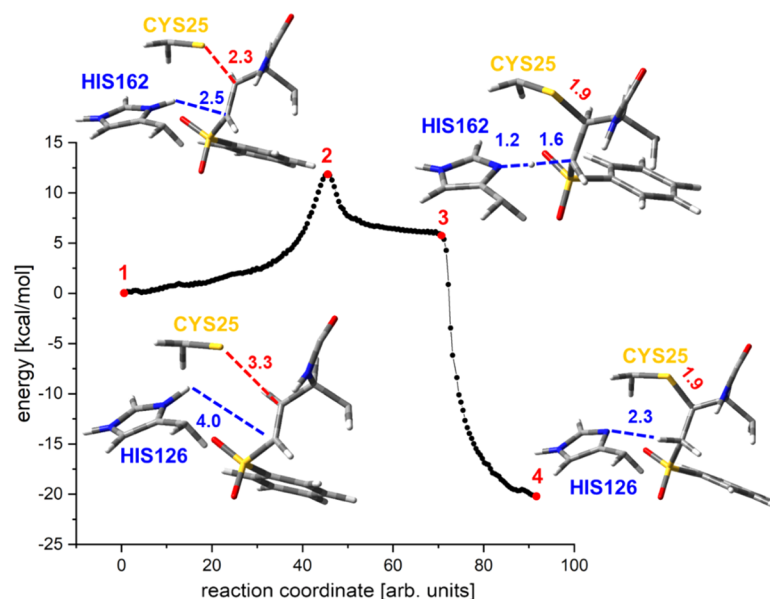
The different shapes of the reaction pathways presented in Figure 16 may result from the different orientation of the olefin in the active site or from changes in the electronic structure due to the fluorine substitution in **1**. To obtain more insights, the reaction of **K11777** from the F-orientation was computed. For this purpose, we first computed the energy profile of the torsional motion of the C<sup>1</sup>C<sup>2</sup> double bond around the dihedral angle  $\angle H^3C^3C^2H^2$  (Figure S3). As expected from the MD simulations, for **K11777**, the energy difference between the H- and the F-orientation was found to be small (1–2 kcal mol<sup>-1</sup>) so that the reaction could take place from both orientations. However, the two-dimensional scan starting from the F-orientation predicted barriers of about 33 kcal mol<sup>-1</sup> and nearly isothermal reactions ( $\Delta E_{\text{reac}} = -3$  kcal mol<sup>-1</sup>). This indicates

that the different starting orientations are leading forces for the observed differences. Attempts to generate IRCs failed, possibly because the paths energetically lie above the path given in Figure 15a.

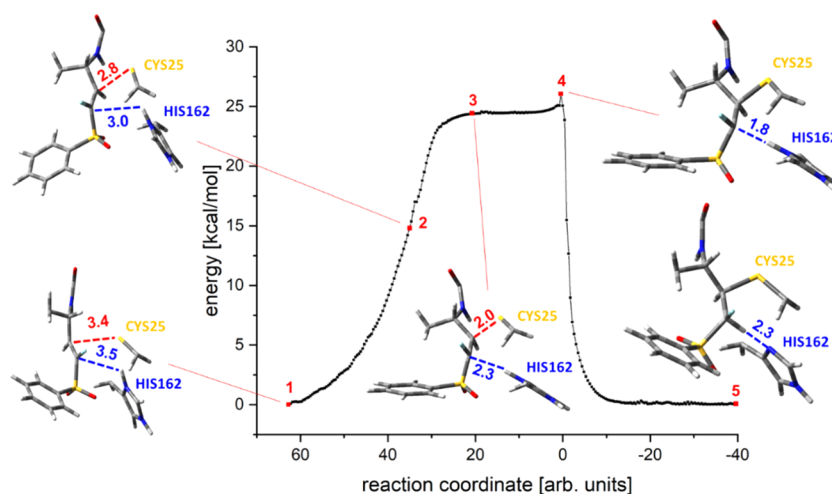
This finding could also indicate that a reaction of **1** starting from the H-orientation is more favorable. To answer this question, we calculated a two-step mechanism for inhibitor **1**. In the first step, **1** was found to twist from the F- into the H-orientation (variation of  $\angle H^3C^3C^2H^2$ ). Starting from the obtained local minimum, we then calculated the course of inhibition by compound **1** starting from the H-orientation as the second step of the overall inhibition reaction. The result of this two-step inhibition reaction is shown in Figure 17.

Figure 17 indicates that the shape of the reaction path of **1**, if it starts from the H-orientation, resembles the path found for **K11777** (Figure 16). Starting from the H-orientation (Figure 17, structure 3), the reaction proceeds over a barrier of about 18 kcal mol<sup>-1</sup> and has a reaction energy of about -12 kcal mol<sup>-1</sup>. However, the exothermicity of the whole reaction drops to only -4 kcal mol<sup>-1</sup>, due to the previously necessary transition from the F- to the H-orientation. Other reaction courses given in the Supporting Information provide a similar picture (Figures S8–S10).

Our investigation revealed that the differences between **K11777** and **1** are mainly due to the interaction between the fluorine atom and the oxyanion hole of rhodesain, which induces a flip of the olefin group of the warhead within the active site. This change in the orientation significantly complicates the further course of the inhibition reaction. As a result, for inhibitor **1**, a two-step mechanism becomes more favorable, which contains a torsional movement from the F- to the H-orientation before the actual covalent Michael-type reaction can take place leading to a considerably reduced exothermicity. These differences nicely explain the switch from the irreversible (**K11777**) to the reversible (**1**) inhibition mode and are in line with all experimental data, which indicate a covalent, but reversible bond formation for various fluorinated inhibitors.



(a)



(b)

**Figure 16.** Representative intrinsic reaction coordinate (IRC) simulation of the inhibition reaction of **K11777** (a) and **1** (b). Selected geometrical parameters of the indicated structures are summarized in Table S3.

**Antitrypanosomal Activity and Toxicity.** Selected compounds were tested for antitrypanosomal activity and cytotoxicity (Table 5). Trypanocidal activity was measured against *T. brucei brucei* TC211<sup>54,55</sup> or *T. brucei brucei* BS449, as described previously.<sup>56,57</sup> Cytotoxicity was measured for selected compounds in the macrophage cell line J774.1 and in HeLa cells as described before.<sup>12,55</sup> Most inhibitors tested showed significantly improved antitrypanosomal activity compared to starting compound **1**. This correlates very well with the higher inhibitory potency of the compounds for rhodesain. The compounds also displayed an improved safety profile by showing no relevant cytotoxicity in HeLa cells or in the J774.1 macrophage cell line. Most interestingly, from the hPhe series, the compounds with N-terminal DHBD group and 4-Me-Phe residue at the P2 position (**2e**, **4e**) exhibited highest

antitrypanosomal potency with the sulfonate **2e** being the most potent compound ( $EC_{50} = 0.14 \mu\text{M}$ ), similarly active to the irreversible **K11777**. Also, within the 4-Pyr series, the compounds with 4-Me-Phe residue (**2d**, **3d**, and **4d**) are more potent than those with Phe at P2 position (**2a**, **4a**). Probably, the higher lipophilicity and thus better membrane permeability of these compounds contribute to their better antitrypanosomal activity. No differences are observed between the various warheads (phenyl vinylsulfonate **2d**, benzyl vinylsulfone **3d**, and phenyl vinylsulfone **4d**). Within the N-Me-Pip series (**1**, **4j**, and **4l**), the compound with Cys(Bn) in the P1 position (**4l**) is most active ( $3.0 \mu\text{M}$ ) despite being a much less-potent inhibitor of rhodesain. This observation may be explained with the relatively high toxicity of the compound, which seems to be also

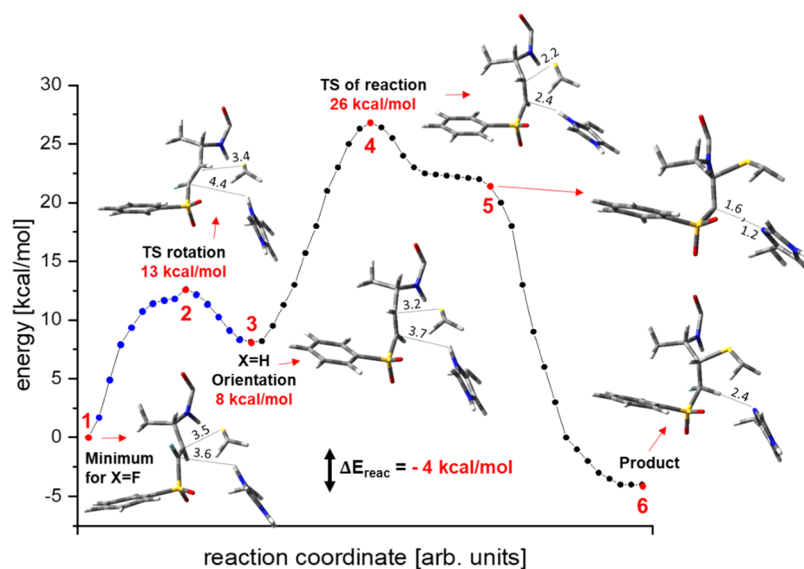
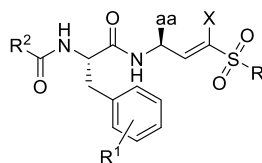


**Figure 17.** Reaction profile of the two-step inhibition reaction of **1**. The rotation about  $\angle\text{H}^3\text{C}^3\text{C}^2\text{H}^2$  is given in blue. Please note that the reaction path is put together from several IRCs. Selected geometrical parameters of the indicated structures are summarized in Table S3. See also Figure S6.

**Table 5.** Antitrypanosomal Activity and Cytotoxicity of Selected Compounds<sup>aa</sup>



cpd	substitution					<i>T. b. b.</i> EC <sub>50</sub> /μM		cytotoxicity CC <sub>50</sub> /μM	
	R	R <sup>1</sup>	R <sup>2</sup>	aa	X	48 h	J774.1	HeLa	
K11777	Ph	H	<i>N</i> -MePip	hPhe	H	0.18 ± 0.03 <sup>b,c</sup>	41 <sup>b</sup>	>10 <sup>d</sup>	
<b>1</b>	Ph	H	<i>N</i> -MePip	hPhe	F	12.5 ± 0.4 <sup>c</sup>	38	10 ± 2	
<b>2a</b>	OPh	H	4-Pyr	hPhe	F	4.8 ± 0.9 <sup>c</sup>	n.d.	>100	
<b>2d</b>	OPh	4-Me	4-Pyr	hPhe	F	1.9 ± 1.8 <sup>e</sup>	n.d.	>100	
<b>2e</b>	OPh	4-Me	DHBD	hPhe	F	0.14 ± 0.05 <sup>e</sup>	n.d.	>100	
<b>3d</b>	Bn	4-Me	4-Pyr	hPhe	F	1.4 ± 0.9 <sup>e</sup>	n.d.	>100	
<b>4a</b>	Ph	H	4-Pyr	hPhe	F	3.0 ± 0.4 <sup>c</sup>	>100	>100	
<b>4d</b>	Ph	4-Me	4-Pyr	hPhe	F	1.9 ± 1.2 <sup>c</sup>	n.d.	>100	
<b>4e</b>	Ph	4-Me	DHBD	hPhe	F	0.80 ± 0.5 <sup>e</sup>	n.d.	>100	
<b>4j</b>	Ph	H	<i>N</i> -MePip	Met	F	14.1 ± 0.6 <sup>c</sup>	43	77 ± 8	
<b>4l</b>	Ph	H	<i>N</i> -MePip	Cys(Bn)	F	3.0 ± 0.1 <sup>c</sup>	8.7	8 ± 0.4	

<sup>a</sup>n.d. not determined. <sup>b</sup>See ref 12. <sup>c</sup>*T. brucei brucei* TC211. <sup>d</sup>See ref 58. <sup>e</sup>*T. brucei brucei* BS449.

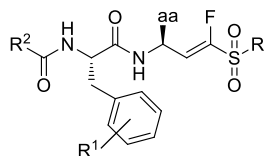
connected to the *N*-Me-Pip moiety (compounds K11777, **1**, **4j**, and **4l**).

**Selectivity over Serine and Threonine Proteases.** For selected compounds, inhibitory potency against other proteases (the threonine protease 20S proteasome and the serine protease NS2B/NS3 of the Dengue virus) was tested (Table 6). The activity of the compounds against the different catalytically active subunits of the proteasome (trypsin-like, caspase-like, and  $\alpha$ -chymotrypsin-like) was tested separately by the use of specific fluorogenic substrates (see Experimental Section). Most compounds showed no relevant inhibition (less than 50%) at concentrations of 11  $\mu\text{M}$ . Highest percentage inhibition was observed in the case of the caspase-like activity for compounds **2d** (44%) and **4a** (41%). Inhibitor **4l** was the only compound that showed relevant inhibition of the  $\alpha$ -chymotrypsin-like activity of the proteasome (71% at 11  $\mu\text{M}$ ).

**In Vitro Metabolism.** The metabolism of compounds **1** and **2d**-(H) was investigated using rat liver microsomes and an NADPH-generating system. The covalent cysteine protease inhibitor K11777 was used as a control. Previous in vitro metabolism studies by Jacobsen and co-workers revealed three metabolites of K11777 depicted in Figure 18.<sup>59</sup>

Compound **1** (fluorinated K11777) also showed *N*-demethylation (**1a**) and *N*-oxidation (**1b**) as shown in Figure S13. The metabolites were analyzed via LC-MS fragmentation. Additionally, the potential metabolites were synthesized as described in the Chemistry section, and their fragments and retention times were compared to those found in the metabolism studies to ensure the identity of the metabolites. In contrast to the reported metabolism of K11777, the  $\beta$ -hydroxy homophenylalanine derivative<sup>32</sup> did not occur, neither in the experiments with compound **1** nor in those with K11777.

Table 6. Inhibition Data for 20S Proteasome and Dengue NS2B/NS3 Protease for Selected Compounds



cpd	substitution				human 20S proteasome/% <sup>a</sup>			dengue
	R	R <sup>1</sup>	R <sup>2</sup>	aa	trypsin	caspace	$\alpha$ -chymotrps.	NS2B/NS3% <sup>a</sup>
1	Ph	H	N-MePip	hPhe	n.i.	16	13	n.i.
2a	OPh	H	4-Pyr	hPhe	n.i.	22	11	n.i.
2d	OPh	4-Me	4-Pyr	hPhe	10	44	20	n.i.
2e	OPh	4-Me	DHBD	hPhe	n.i.	31	22	11
3d	Bn	4-Me	4-Pyr	hPhe	n.i.	n.i.	n.i.	n.i.
4a	Ph	H	4-Pyr	hPhe	n.i.	41	10	n.i.
4b	Ph	H	DHBD	hPhe	n.i.	26	n.i.	n.d.
4d	Ph	4-Me	4-Pyr	hPhe	12	28	13	n.d.
4j	Ph	H	N-MePip	Met	n.i.	18	n.i.	n.d.
4l	Ph	H	N-MePip	Cys(Bn)	14	n.i.	71	13

<sup>a</sup>% inhibition at inhibitor concentrations of 11  $\mu$ M; n.i. = <10% inhibition at 11  $\mu$ M; and n.d. = not determined.

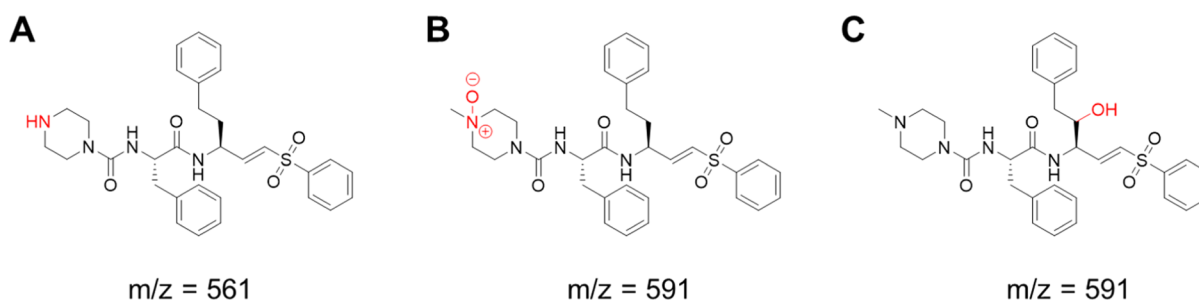
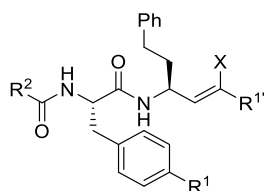


Figure 18. Metabolites of K11777 as published by Jacobsen and co-workers.<sup>59</sup> N-Demethylation at the N-methyl piperazine moiety (A) and N-oxidation (B) are the major metabolic reactions. Additionally, a  $\beta$ -hydroxy homophenylalanine metabolite was found (C).

Table 7. Assay Results of the Metabolites



cpd	substitution					rhodesain		
	R <sup>1</sup>	R <sup>2</sup>	R <sup>1'</sup>	X	K <sub>i</sub> /nm	k <sub>i</sub> /s <sup>-1</sup>	k <sub>2nd</sub> /m <sup>-1</sup> s <sup>-1</sup>	
1	H	N-MePip	SO <sub>2</sub> Ph	F	190 <sup>a,b</sup>	n.a.	n.a.	
1a	H	Pip	SO <sub>2</sub> Ph	F	192 $\pm$ 40 <sup>b</sup>	n.a.	n.a.	
2d-(H)	Me	4-Pyr	SO <sub>3</sub> Ph	H	0.45 $\pm$ 0.06	0.020	46 $\times$ 10 <sup>6</sup>	
2l	Me	4-Pyr-N-oxide	SO <sub>3</sub> Ph	H	1.50 $\pm$ 0.46	0.018	12 $\times$ 10 <sup>6</sup>	

<sup>a</sup>See ref 12. <sup>b</sup>K<sub>i</sub> calculated from the Cheng–Prusoff equation;<sup>32</sup> n.a. not applicable.

The metabolism studies of 2d-(H) only resulted in a single metabolite, the N-oxidized derivative 2l as shown in Figure S14. In order to verify the structure, the metabolite was synthesized as described in the Chemistry section and retention times and fragments were compared as described above.

The synthesized metabolites were also tested in the fluorometric enzyme assay in order to determine their K<sub>i</sub> values. The assays were performed as described in the Enzyme assays section and the results are shown in Table 7.

The demethylation of compound 1 to its metabolite 1a does not decrease its inhibitory activity significantly. Both, compound

2d-(H) and its metabolite 2l, show a good inhibition of rhodesain in the low nanomolar range. Therefore, it can be concluded that the metabolites retain most of the inhibitory potency of the parent drug.

**In Vivo Distribution.** Compound 1 as an example for a covalent reversible and compound 2d-(H) as an example for a covalent irreversible inhibitor were tested for their biodistribution in vivo in wild type CD1 mice. Their biodistribution after oral (p.o.) or intraperitoneal (i.p.) application was investigated by LC–MS analysis of plasma samples and brain tissues to determine the ability of the compounds to cross the blood–

brain barrier. The compounds were chosen for the in vivo assays based on their differences in the mode of inhibition (covalent reversible vs irreversible) and based on their physicochemical properties (Table 8), which are similar for compound **2d**-(H) and its fluorinated counterpart **2d**.

**Table 8. Comparison of 1, 2d, and 2d-(H) in Terms of Physicochemical Properties and the Mechanism of Inhibition**

cpd	inhibition mode	SlogP (calc.) <sup>a</sup>	TPSA [ $\text{\AA}^2$ ] (calc.) <sup>a</sup>
<b>1</b>	covalent reversible	3.96	98.82
<b>2d</b>	covalent reversible	5.07	114.46
<b>2d-(H)</b>	covalent irreversible	4.77	114.46

<sup>a</sup>Calculated using MOE.<sup>60</sup>

Compound **1** was found in plasma samples but not in the brain homogenate, whereas compound **2d**-(H) could be found in both, plasma and brain tissue after i.p. and p.o. administration, respectively (Figures 19, S15, and S16). Therefore, it can be concluded that **2d**-(H) is able to cross the blood–brain barrier due to its higher lipophilicity. An accumulation of this compound was also suggested because of a higher AUC after multiple oral administration compared to a single dose i.p. administration, thus making it a possible candidate for the treatment of stage-2 HAT.

Furthermore, the distribution of the compounds in the brain extracellular space was also investigated via microdialysis. Only compound **2d**-(H) could be found in the dialysate with recovery rates from the plasma concentration between 0.8 and 6% of plasma values after i.p. injection. This indicates that the lipophilic compound **2d**-(H) reaches higher concentrations intracellularly than in the extracellular fluid.

Notably, the mice treated with the compounds did not show any signs of toxication.

It can be concluded that the optimization of compound **1** through SAR studies not only enhanced the inhibitory potency against rhodesain and the selectivity over CatB and CatL but also resulted in a potential drug candidate for stage-2 HAT with a higher lipophilicity (calc.  $S \log P = 4.77$  compared to 3.96 for **1**) that is able to cross the blood brain barrier and accumulate in brain tissue.

## CONCLUSIONS

In this study, compound **1** ( $K_i = 190 \text{ nM}$ ,  $EC_{50} (T. brucei) = 12.5 \mu\text{M}$ ), which was recently identified as a covalent reversible cysteine protease inhibitor by the application of a quantum-chemical-based design protocol,<sup>12</sup> was optimized in terms of inhibitory potency and selectivity for rhodesain. Based on the results obtained from molecular docking and MD simulations, a series of compounds with a modified recognition unit and an altered substitution pattern of the warhead were synthesized. Introduction of aromatic residues at P3 significantly enhanced the potency for rhodesain (**4b**:  $K_i = 12 \text{ nM}$ ) and increased the trypanocidal activity against *T. brucei* [**4a**:  $EC_{50} (T. brucei) = 3.0 \mu\text{M}$ ]. Incorporation of a 4-methyl substituent at the phenylalanine aromatic ring additionally improved selectivity against human cathepsins (**4d**:  $K_i = 8 \text{ nM}$ , 12-fold selectivity over CatL, more than 200-fold selectivity over CatB). By alteration of the substitution pattern of the warhead, two new classes of covalent reversible cysteine protease inhibitors with distinct properties were obtained. The compounds from the series of benzyl fluorovinylsulfones (cpds **3a–3i**) showed a similar potency compared to the respective analogues with phenyl substituents (**4a–4i**) but were significantly more rapidly reversible in dilution and dialysis assays. Several compounds in the series of fluorovinylsulfonates (**2a–2i**) showed a biphasic inhibition mechanism, with the formation of a single digit nanomolar, high-affinity complex in the second step (**2d**:  $K_i^* = 3 \text{ nM}$ ). This complex was shown to dissociate markedly slower in dialysis experiments for compound **2d**. Therefore, compound **2d** represents a potent, tight binding, and slowly reversible inhibitor of rhodesain. Furthermore, compound **2d** shows selectivity over CatL (26-fold) and is only a weak inhibitor of CatB (38% at  $11 \mu\text{M}$ ). In addition, no relevant off-target activity against threonine and serine proteases was observed and the cytotoxicity profile improved considerably. Compounds with a DHBD moiety at the N-terminus and 4-Me-Phe in the P2 position (**2e**, **4e**) are not only nanomolar inhibitors of rhodesain, but are most promising with regard to their antitrypanosomal activity and cytotoxicity profile, with  $EC_{50}$  values comparable to those of the irreversible inhibitor K11777 ( $EC_{50} = 0.14–0.80 \mu\text{M}$ ) and no cytotoxic effects against HeLa cells ( $EC_{50} > 100 \mu\text{M}$ ).

Microsomal stability assays revealed N-oxidation of the 4-Pyr substituent in the P3 position of **2d**-(H). However, this does not seem to reduce the inhibitory potency. Moreover, the

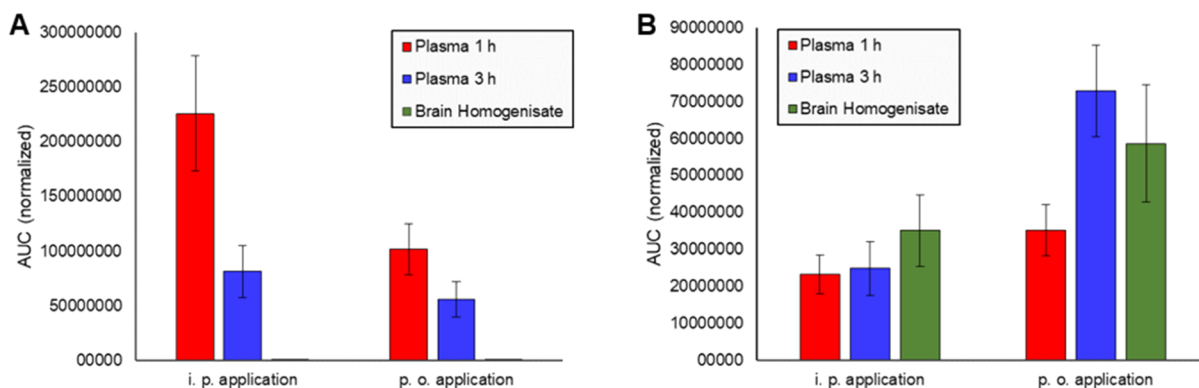


**Figure 19.** (A) Compound **1** was found in mouse plasma after 1 and 3 h, but not in the brain homogenate after i.p. and p.o. administration, respectively. (B) Compound **2d**-(H) showed plasma levels and distribution in brain tissue after both i.p. and p.o. administration. Both diagrams show the average AUC values of all tested mice (five for each compound and route of administration).



accumulation of **2d-(H)** in mouse brain tissue, which did not occur with **1**, indicates a correlation of CNS permeation with the physicochemical properties of the tested inhibitors, such as SlogP values. These findings confirm that the optimized covalent reversible fluorovinylsulfonates should be further investigated as possible candidates for the treatment of both stage-1 and -2 HAT.

Based on these features, the high-affinity, lipophilic, and selective reversible  $\alpha$ -fluorovinylsulfones and sulfonates as inhibitors of rhodesain may serve as a basis for the future development of effective and non-toxic drugs for the treatment of HAT.

In addition, we used mass spectrometry to demonstrate the formation of a covalent bond. Using QM/MM and MD computations, we could attribute the differences in inhibition mechanisms between **K11777** (irreversible) and **1** (reversible) to the interaction between the fluorine atom and the oxyanion hole of rhodesain. Due to this interaction, the olefin group of the warhead flips in the active site significantly complicating the further course of the inhibition reaction and leading to a considerably reduced exothermicity and thus a reversible inhibition.

## EXPERIMENTAL SECTION

**Syntheses. General.** All reagents and solvents were of analytical grade quality and purchased from Sigma-Aldrich, Alfa Aesar, Acros, or TCI. Chemicals were used without further purification. Solvents were purified by distillation and desiccated by standard methods if necessary.  $^1\text{H}$  and  $^{13}\text{C}$  spectra were recorded on a Bruker Fourier 300 using DMSO- $d_6$ ,  $\text{CDCl}_3$ , or  $\text{CD}_2\text{Cl}_2$  as a solvent. Chemical shifts  $\delta$  are given in parts per million (ppm) using residual proton peaks of the solvent as the internal standard ( $^1\text{H}/^{13}\text{C}$ : DMSO: 2.50/39.52 ppm,  $\text{CHCl}_3$ : 7.26/77.16 ppm,  $\text{CH}_2\text{Cl}_2$ : 5.32/54.00 ppm). The purity of the compounds was determined via HPLC-MS ( $\delta = 254$  nm). All compounds are >95% pure according to HPLC analysis. High-resolution mass spectra were obtained on a Waters Q-TOF-Ultima 3-instrument. Alternatively, the mass spectra were obtained from an LC-MS system consisting of a 1100 series HPLC system from Agilent with an Agilent Poroshell 120 EC- $\text{C}_{18}$  150  $\times$  2.10 mm, 4  $\mu\text{m}$  column. The mobile phase was 80% acetonitrile, 10%  $\text{H}_2\text{O}$ , and 10% of a 0.1% solution of formic acid in water. Detection wavelength was 254 nm. The molecular mass was detected using an Agilent 1100 series LC/MSD Trap with electron spray ionization (ESI) in positive mode. Purification with a preparative HPLC system was performed with a Varian PrepStar system (model 218) with an Agilent Zorbax XDB- $\text{C}_{18}$  21.2  $\times$  150 mm, 5  $\mu\text{m}$  column. Column chromatography was performed with silica gel (0.06–0.02 mm or 0.040–0.063 mm) obtained from Carl Roth. All reactions were monitored by thin-layer chromatography using Macherey-Nagel ALUGRAM Xtra SIL G/UV254 silica gel 60 plates for detection at 254 nm. Melting points were determined in open capillaries using a Stuart SMP10-instrument. Optical rotation  $[\alpha]_D^{25}$  was measured on an P3000 polarimeter from Krüss at 22  $^\circ\text{C}$  and is reported in  $\text{cm}^3 \text{g}^{-1} \text{dm}^{-1}$ .

**Synthesis of Starting Materials. Phenyl Methanesulfonate<sup>61</sup> (I).** Phenol (2.35 g, 1.0 equiv) was dissolved in EtOAc and cooled to 0  $^\circ\text{C}$ . TEA (6.93 mL, 2.0 equiv) and methanesulfonyl chloride (2.52 mL, 1.3 equiv) were added successively and the mixture was allowed to warm to rt. After stirring for 30 min, the solution was washed with water (3 $\times$ ) and brine (1 $\times$ ) and was dried with  $\text{Na}_2\text{SO}_4$ . Evaporation of the solvent yielded phenyl methanesulfonate (**I**) as a colorless powder (3.95 g, 92%). Spectral data matched those reported in the literature.<sup>28</sup>

**Diethyl((benzylthio)methyl)phosphonate<sup>28</sup> (II).** Benzyl mercaptan (0.84 mL, 1.0 equiv) was dissolved in THF and cooled to 0  $^\circ\text{C}$ . NaH (60% in mineral oil, 0.32 g, 1.0 equiv) was added in portions and the mixture was stirred for 15 min. Diethyl iodomethylphosphonate (1.24 mL, 1.0 equiv) was added dropwise and the mixture was stirred for 3.5 h at rt. THF was removed in vacuo and EtOAc was added. The organic phase was washed with water (2 $\times$ ) and brine (1 $\times$ ) and dried with

$\text{Na}_2\text{SO}_4$ . After evaporation of the solvent, the residue was purified by column chromatography (petroleum ether/EtOAc 1:1), yielding the title compound as a colorless liquid. Yield: 1.66 g (84%).  $^1\text{H}$  NMR (300 MHz,  $\text{CDCl}_3$ ):  $\delta$  7.43–7.21 (m, 5H), 4.25–4.08 (m, 4H), 3.90 (s, 2H), 2.54 (d,  $J_{\text{H-P}} = 12.9$  Hz, 2H), 1.34 (t,  $J = 7.1$  Hz, 6H).  $^{13}\text{C}$  NMR (75 MHz,  $\text{CDCl}_3$ ):  $\delta$  137.3, 129.4, 128.7, 127.4, 62.7 (d,  $J_{\text{C-P}} = 6.7$  Hz), 37.0 ( $J_{\text{C-P}} = 2.9$  Hz), 23.8 ( $J_{\text{C-P}} = 150$  Hz), 16.6 ( $J_{\text{C-P}} = 6.0$  Hz).  $^1\text{H}$  NMR data are consistent with the literature.<sup>12</sup>

**Diethyl((phenylsulfonyl)methyl)phosphonate<sup>12</sup> (III).** To a solution of methyl phenyl sulfone (3.81 g, 24 mmol) in dry THF, *n*-BuLi (2.5 M in hexane, 21.5 mL, 60 mmol) was added at 0  $^\circ\text{C}$  with stirring. After 30 min, diethyl chlorophosphate was added dropwise and the reaction mixture was stirred at 0  $^\circ\text{C}$  for 1 h. 25 mL of a saturated solution of ammonium chloride was added and the volatiles were evaporated. The residue was extracted with DCM and the combined extracts were washed with brine, dried with sodium sulfate, concentrated under reduced pressure, and purified by column chromatography (light petroleum/EtOAc 1:5) to afford the title compound as a colorless oil, which solidified upon standing (4.11 g, 52%). NMR data were consistent with the literature.<sup>28,62</sup>

**Phenyl(diethoxyphosphoryl)methanesulfonate (IV).** Phenyl methanesulfonate (**I**, 2.5 g, 1.0 equiv) was dissolved in THF and cooled to  $-78$   $^\circ\text{C}$ . KHMDS (1.0 M in THF, 15 mL, 1.1 equiv) was added dropwise and the mixture was stirred for an additional 15 min. Diethyl chlorophosphate (1.5 mL, 0.7 equiv) was added slowly and stirred for 1 h at  $-60$   $^\circ\text{C}$ . The reaction was quenched by addition of glacial AcOH (1 mL) and then allowed to warm to rt. THF was removed in vacuo and EtOAc was added to the residue. The solution was washed with water (2 $\times$ ) and brine (1 $\times$ ) and then dried with  $\text{Na}_2\text{SO}_4$ . Evaporation of the solvent gave a crude product, which was purified by column chromatography (petroleum ether/EtOAc 1:1 to 1:3), yielding the title compound as a colorless liquid (3.3 g, 74%).  $^1\text{H}$  NMR (300 MHz,  $\text{CDCl}_3$ ):  $\delta$  7.52–7.29 (m, 5H), 4.36–4.20 (m, 4H), 3.81 (d,  $J_{\text{H-P}} = 17$  Hz, 2H), 1.44–1.31 (m, 6H).  $^{13}\text{C}$  NMR (75 MHz,  $\text{CDCl}_3$ ):  $\delta$  149.4, 130.2, 127.8, 122.3, 64.2 (d,  $J_{\text{C-P}} = 6.5$  Hz), 47.3 (d,  $J_{\text{C-P}} = 139$  Hz), 16.4 (d,  $J_{\text{C-P}} = 6.3$  Hz).

**Diethyl((benzylsulfonyl)methyl)phosphonate<sup>28</sup> (V).** Compound **II** (2.55 g, 1.0 equiv) was dissolved in DCM and cooled to 0  $^\circ\text{C}$ . Subsequently, *m*CPBA (77%, 5.8 g, 3.0 equiv) was added in portions and the mixture was stirred for 12 h at rt. Then, the solution was filtered and washed with 1 M NaOH (4 $\times$ ), water (1 $\times$ ), and brine (1 $\times$ ) and dried with  $\text{Na}_2\text{SO}_4$ . After evaporation of the solvent, the title compound was obtained as a colorless oil. Yield: 2.82 g (99%).  $^1\text{H}$  NMR (300 MHz,  $\text{CDCl}_3$ ):  $\delta$  7.57–7.47 (m, 2H), 7.44–7.34 (m, 3H), 4.60 (s, 2H), 4.24 (dq,  $J = 8.1, 7.1$  Hz, 4H), 3.36 (d,  $J = 16$  Hz, 2H), 1.37 (dt,  $J = 7.1, 0.4$  Hz, 6H).  $^{13}\text{C}$  NMR (75 MHz,  $\text{CDCl}_3$ ):  $\delta$  131.2, 129.3, 129.2, 128.2, 63.9 (d,  $J_{\text{C-P}} = 6.5$  Hz), 60.4, 48.0 (d,  $J_{\text{C-P}} = 140$  Hz), 16.50 (d,  $J_{\text{C-P}} = 6.4$  Hz). Spectral data are consistent with the literature.<sup>12,63</sup>

**(S)-tert-Butyl(1-oxo-4-phenylbutan-2-yl)carbamate (VI).** L-Homophenylalanine (5.0 g, 28 mmol) was dissolved in THF (15 mL) and a solution of  $\text{Na}_2\text{CO}_3$  (3 g, 28 mmol) in 100 mL of water was added followed by di-*tert*-butyl dicarbonate (31 mmol) in 75 mL THF. The mixture was stirred overnight, diluted with water (100 mL), and extracted with  $\text{CH}_2\text{Cl}_2$ . The aqueous layer was acidified with  $\text{KHSO}_4$  to pH 3 and extracted with  $\text{CH}_2\text{Cl}_2$ . The combined organic extracts were dried with sodium sulfate and concentrated under reduced pressure to give crude boc-L-homophenylalanine (7.0 g, 89%). This crude material (4.91 g, 18 mmol) was dissolved in DCM (100 mL) and cooled to 0  $^\circ\text{C}$ . EDC-HCl (4.05 g, 21 mmol), HOBt (3.23 g, 21 mmol), and DIEA (13.5 mL, 78 mmol) were added and the mixture was stirred for 15 min before *N,O*-dimethylhydroxylamine hydrochloride (2.06 g, 21 mmol) was added. The mixture was allowed to warm to rt and was stirred for 18 h. DCM was removed under reduced pressure, water (60 mL) was added, and the suspension was extracted with EtOAc. The combined organic extracts were washed with saturated aq  $\text{NaHCO}_3$  (5 $\times$ ) and brine, dried with sodium sulfate, and concentrated under reduced pressure to give *tert*-butyl (S)-((1-(methoxy(methyl)amino)-1-oxo-4-phenylbutan-2-yl)carbamate as a crude yellow oil (5.64 g, 99%), which was used in the next step without further purification.  $^1\text{H}$  NMR (300 MHz, DMSO- $d_6$ ):  $\delta$  7.46–7.18 (m, 5H), 5.28 (d,  $J = 9.3$  Hz, 1H), 4.73

(s, 1H), 3.67 (s, 3H), 3.21 (s, 3H), 2.88–2.61 (m, 2H), 2.18–1.79 (m, 2H), 1.52 (s, 9H). The crude oil (4.05 g, 12.5 mmol) was dissolved in dry diethyl ether (130 mL) and cooled to 0 °C. LiAlH<sub>4</sub> (0.59 g, 15.7 mmol) was added portion wise. The mixture was stirred for 30 min and subsequently quenched by addition of aqueous KHSO<sub>4</sub> (0.33 M, 65 mL). The organic phase was separated, and the aqueous phase was extracted with diethyl ether. The combined organic extracts were washed with 3 M HCl, saturated aq NaHCO<sub>3</sub>, and brine, dried with sodium sulfate, concentrated under reduced pressure, and purified by column chromatography (light petroleum/EtOAc 3:1), yielding the title compound as a colorless solid (2.44 g, 74%). <sup>1</sup>H NMR (300 MHz, CDCl<sub>3</sub>): δ 9.55 (s, 1H), 7.40–7.13 (m, 5H), 5.08 (d, J = 4.1 Hz, 1H), 4.26 (q, J = 5.9 Hz, 1H), 2.87–2.63 (m, 2H), 2.35–2.06 (m, 1H), 2.02–1.77 (m, 2H), 1.47 (s, 9H). <sup>13</sup>C NMR (75 MHz, CDCl<sub>3</sub>): δ 199.6, 155.6, 140.7, 128.8, 128.7, 126.5, 80.4, 59.7, 31.6, 31.2, 28.4. NMR data are consistent with the literature.<sup>64</sup>

**(S)-tert-Butyl(4-(methylthio)-1-oxobutan-2-yl)carbamate (VII).** Boc-L-Met-OH (2.43 g, 1.0 equiv) was dissolved in DCM and cooled to 0 °C. HOBt (1.49 g, 1.0 equiv) and DIEA (5.0 mL, 3.0 equiv) were added successively, and the mixture was stirred until all materials were solubilized. To this mixture, TBTU (3.12 g, 1.0 equiv) was added in one portion and then stirred for 15 min at 0 °C. N,O-Dimethylhydroxylamine hydrochloride (1.0 g, 1.1 equiv) was added in one portion and the mixture was stirred for 12 h at rt. DCM was removed in vacuo, and the residue was diluted with EtOAc. The organic layer was washed with water (5×), conc. NaHCO<sub>3</sub> (2×), and 1 M aq HCl (2×) and dried with Na<sub>2</sub>SO<sub>4</sub>. After evaporation of the solvent, the residue was purified by column chromatography (petroleum ether/EtOAc 2:1), yielding tert-butyl (S)-(1-methoxy(methylamino)-4-(methylthio)-1-oxobutan-2-yl)carbamate as a colorless oil (2.42 g, 85%). <sup>1</sup>H NMR (300 MHz, CDCl<sub>3</sub>): δ 5.23 (d, J = 7.7 Hz, 1H), 4.78 (s, 1H), 3.77 (s, 3H), 3.20 (s, 3H), 2.68–2.42 (m, 2H), 2.08 (s, 3H), 2.05–1.92 (m, 1H), 1.89–1.71 (m, 1H), 1.42 (s, 9H). <sup>13</sup>C NMR (75 MHz, CDCl<sub>3</sub>): δ 172.7, 155.7, 79.9, 61.8, 50.0, 32.6, 32.3, 30.3, 28.5, 15.6. This material (2.42 g, 1.0 equiv) was dissolved in THF and cooled to 0 °C. LiAlH<sub>4</sub> (0.41 g, 1.3 equiv) was added in portions and stirred for 30 min. The mixture was diluted with 50 mL diethyl ether and then 1 M KHSO<sub>4</sub> (50 mL) was added carefully. The layers were separated, and the aqueous phase was extracted twice with diethyl ether. The combined organic layers were washed with 1 M HCl (2×), saturated aq NaHCO<sub>3</sub>, and brine, and then dried with Na<sub>2</sub>SO<sub>4</sub>. After evaporation of the solvent, the residue was purified by column chromatography (petroleum ether/EtOAc 2:1) to give the title compound as a colorless solid (1.49 g, 77%). <sup>1</sup>H NMR (300 MHz, CDCl<sub>3</sub>): δ 9.63 (s, 1H), 5.21 (s, 1H), 4.39–4.11 (m, 1H), 2.56 (t, J = 7.2 Hz, 2H), 2.34–2.13 (m, 1H), 2.07 (s, 3H), 1.99–1.83 (m, 1H), 1.44 (s, 9H). <sup>13</sup>C NMR (75 MHz, CDCl<sub>3</sub>): δ 199.2, 155.6, 80.4, 59.1, 29.9, 28.8, 28.4, 15.5. NMR data are consistent with the literature.<sup>65</sup>

**(R)-tert-Butyl(1-(benzylthio)-3-oxopropan-2-yl)carbamate (VIII).** L-Cysteine hydrochloride (5.20 g, 1.0 equiv) was dissolved in 60 mL 2 M NaOH and 150 mL EtOH. To the mixture, 5.64 g (3.92 mL, 1.0 equiv) benzyl bromide is added dropwise. After stirring for 1 h, the mixture is neutralized by addition of conc. HCl. The precipitate is collected by filtration and washed with water, diethyl ether, and ethanol. S-Benzyl L-cysteine is obtained as a colorless solid and directly used for the next step (6.4 g, 91%). <sup>1</sup>H NMR (300 MHz, D<sub>2</sub>O): δ 7.50–7.24 (m, 5H), 4.17 (q, J = 6.5 Hz, 1H), 3.88–3.71 (s, 2H), 3.09–2.87 (m, 2H). <sup>13</sup>C NMR (75 MHz, D<sub>2</sub>O): δ 171.7, 138.2, 129.3, 129.1, 127.8, 51.8, 35.5, 30.7. S-Benzyl L-cysteine (3.0 g, 1.0 equiv) was dissolved in THF (50 mL), and K<sub>2</sub>CO<sub>3</sub> (2.94 g, 1.5 equiv) and water (50 mL) were added. Di-tert-butyl-dicarbonate (3.25 g, 1.05 equiv) dissolved in 50 mL THF was added dropwise and stirred for 12 h at rt. THF was removed in vacuo and the residue was extracted twice with DCM. The aqueous layer was acidified to pH 3 by addition of 1 M KHSO<sub>4</sub> and extracted with DCM (3×). The combined organic layers were washed with brine (2×), dried with Na<sub>2</sub>SO<sub>4</sub>, and evaporated under reduced pressure to give crude boc-S-benzyl L-cysteine as a colorless oil (3.05 g, 69%). <sup>1</sup>H NMR (300 MHz, DMSO-d<sub>6</sub>): δ 7.38–7.03 (m, 5H), 4.14–4.02 (m, 1H), 3.71 (s, 2H), 2.67 (m, 2H), 1.35 (s, 9H). <sup>13</sup>C NMR (75 MHz, DMSO-d<sub>6</sub>): δ 172.6, 155.4, 138.3, 128.9, 128.4, 126.9, 78.3, 53.2,

39.5, 35.2, 32.4, 28.2. This material (3.05 g, 1.0 equiv) was dissolved in DCM and cooled to 0 °C. HOBt (1.49 g, 1.0 equiv) and DIEA (5.0 mL, 3.0 equiv) were added successively, and the mixture was stirred until all materials were solubilized. To this mixture, TBTU (3.40 g, 1.0 equiv) was added in one portion and then stirred for 15 min at 0 °C. N,O-Dimethylhydroxylamine hydrochloride (1.0 g, 1.1 equiv) was added in one portion and the mixture was stirred for 12 h at rt. DCM was removed in vacuo, and the residue was diluted with EtOAc. The organic layer was washed with water (5×), conc. NaHCO<sub>3</sub> (2×), and 1 M aq HCl (2×) and dried with Na<sub>2</sub>SO<sub>4</sub>. After evaporation of the solvent, the residue was purified by column chromatography (petroleum ether/EtOAc 2:1), yielding (R)-tert-butyl (3-(benzylthio)-1-(methoxy(methylamino)-1-oxopropan-2-yl)carbamate as a colorless oil (3.25 g, 95%). <sup>1</sup>H NMR (300 MHz, CDCl<sub>3</sub>): δ 7.42–7.15 (m, 5H), 5.28 (d, J = 8.6 Hz, 1H), 4.84–4.59 (m, 1H), 3.67 (s, 3H), 3.21 (s, 3H), 2.83–2.54 (m, 2H), 2.15–1.77 (m, 2H), 1.50 (s, 9H). <sup>13</sup>C NMR (75 MHz, CDCl<sub>3</sub>): δ 173.2, 155.7, 141.3, 128.7, 128.5, 126.1, 61.6, 50.2, 38.8, 34.7, 31.8, 28.5. The above compound (3.0 g, 1.0 equiv) was dissolved in diethyl ether and cooled to 0 °C. LiAlH<sub>4</sub> (0.42 g, 1.3 equiv) was added in portions and stirred for 30 min. The mixture was diluted with 50 mL diethyl ether and then 1 M KHSO<sub>4</sub> (50 mL) was added carefully. The layers were separated, and the aqueous phase was extracted twice with diethyl ether. The combined organic layers were washed with 1 M HCl (2×), saturated aq NaHCO<sub>3</sub>, and brine, and then dried with Na<sub>2</sub>SO<sub>4</sub>. After evaporation of the solvent, the residue was purified by column chromatography (petroleum ether/EtOAc 2:1) to give the title compound as a colorless solid (1.70 g, 68%). <sup>1</sup>H NMR (300 MHz, CDCl<sub>3</sub>): δ 9.46 (s, 2H), 7.32–7.21 (m, 13H), 5.29 (d, J = 21.5 Hz, 2H), 4.32–4.16 (m, 2H), 3.67 (s, 5H), 2.86–2.70 (m, 5H), 1.39 (s, 24H). <sup>13</sup>C NMR (75 MHz, CDCl<sub>3</sub>): δ 198.8, 137.7, 129.1, 128.8, 127.3, 80.6, 77.2, 59.3, 37.1, 30.8, 28.4. NMR data are consistent with the literature.<sup>12</sup>

**(S)-2-(4-Methylpiperazin-1-ium-1-carboxamido)-3-phenylpropanoate<sup>2-</sup> (IX).** L-Phenylalanine methyl ester hydrochloride (2.0 g, 1.0 equiv) was suspended in CH<sub>2</sub>Cl<sub>2</sub> and 25 mL of a saturated aqueous solution of NaHCO<sub>3</sub> was added. At 0 °C, triphosgene (0.92 g, 0.3 equiv) was added and the mixture was allowed to stir for 30 min at this temperature. Subsequently, the organic phase was separated, and the aqueous phase was extracted with three portions of DCM. The combined organic extracts were washed with brine, dried with Na<sub>2</sub>SO<sub>4</sub>, and concentrated under reduced pressure. The residue was dissolved in THF and cooled to 0 °C. N-Methyl piperazine (0.93 g, 1.03 mL, 1.0 equiv) was added dropwise. After stirring for 1 h, THF was removed under reduced pressure and the residue was diluted with EtOAc. Aqueous work-up was performed with water (1×), saturated aq NaHCO<sub>3</sub> (1×), and brine (1×). The organic layer was dried with Na<sub>2</sub>SO<sub>4</sub> and evaporated. The crude product was purified by column chromatography (CH<sub>2</sub>Cl<sub>2</sub>/MeOH 9:1), giving methyl (4-methylpiperazine-1-carboxyl)-L-phenylalaninate as a colorless oil. Yield: <sup>1</sup>H NMR (300 MHz, CDCl<sub>2</sub>): δ 7.30–7.10 (m, 3H), 7.04 (d, J = 7.3 Hz, 2H), 4.77 (d, J = 7.3 Hz, 1H), 4.61 (m, 1H), 3.61 (s, 3H), 3.29–3.11 (m, 4H), 3.00 (m, 2H), 2.22 (t, J = 5.0 Hz, 4H), 2.16 (s, 3H). This material (3.0 g, 9.4 mmol) was dissolved in THF (20 mL) and LiOH (1.4 g, 33.4 mmol) in 10 mL water was added. The mixture was stirred for 18 h at rt and the volatiles were removed under reduced pressure. Water was added to the residue and the pH was adjusted to 2 with 1 M aq HCl. The title compound was crystallized at 4 °C along with some LiCl and collected by filtration. Recrystallization from methanol gave the pure compound as a colorless powder. <sup>1</sup>H NMR (300 MHz, DMSO-d<sub>6</sub>): δ 7.33–7.05 (m, 5H), 6.68 (d, J = 7.9 Hz, 1H), 4.28–4.09 (m, 1H), 3.50–3.16 (m, 4H), 2.98 (m, 2H), 2.46–2.30 (m, 4H), 2.25 (s, 3H). <sup>13</sup>C NMR (75 MHz, DMSO-d<sub>6</sub>): δ 174.6, 157.1, 139.0, 129.4, 128.0, 126.1, 56.0, 53.1, 44.8, 42.7, 39.5, 36.9.

**Isonicotinoyl-L-phenylalanine<sup>66</sup> (X).** To a solution of L-phenylalanine ethyl ester hydrochloride (2.50 g, 10.88 mmol) and TEA (4.5 mL, 32.65 mmol) in DCM, isonicotinoyl chloride hydrochloride (1.93 g, 10.88 mmol) was added in small portions. The mixture was stirred for 3 h, washed with a saturated solution of NaHCO<sub>3</sub>, dried with Na<sub>2</sub>SO<sub>4</sub>, and concentrated under reduced pressure. Ethyl isonicotinoyl-L-phenylalaninate (2.84 g, yield 87%) was obtained as a yellowish oil,



which crystallized upon standing and was used in the next step without further purification.  $^1\text{H}$  NMR (300 MHz,  $\text{DMSO}-d_6$ ):  $\delta$  9.18 (d,  $J = 7.7$  Hz, 1H), 8.73 (d,  $J = 5.2$  Hz, 2H), 7.69 (d,  $J = 5.2$  Hz, 2H), 7.37–7.12 (m, 5H), 4.75–4.57 (m, 1H), 4.10 (q,  $J = 7.1$  Hz, 2H), 3.05–3.21 (m, 2H), 1.14 (t,  $J = 7.1$  Hz, 3H).  $^{13}\text{C}$  NMR (75 MHz,  $\text{DMSO}-d_6$ ):  $\delta$  171.3, 165.0, 150.3, 140.6, 137.4, 129.1, 128.3, 126.6, 121.3, 60.7, 54.4, 45.7, 39.5, 36.2, 14.0. The above compound (2.84 g, 9.53 mmol) was dissolved in water (30 mL) and THF (30 mL), then LiOH (1.20 g, 28.6 mmol) was added. The mixture was stirred for 2 h before the organic solvent was removed under reduced pressure and the aqueous residue was neutralized with 1 M aq HCl. The title compound was crystallized at 4 °C along with LiCl. Recrystallization from methanol gave the pure product as a colorless powder (1.59 g, 62%).  $^1\text{H}$  NMR (300 MHz,  $\text{DMSO}-d_6$ ):  $\delta$  8.76–8.57 (m, 2H), 8.22 (d,  $J = 7.3$  Hz, 1H), 7.71–7.57 (m, 2H), 7.25–6.99 (m, 5H), 4.26 (td,  $J = 7.4, 4.6$  Hz, 1H), 3.27–2.95 (m, 3H).  $^{13}\text{C}$  NMR (75 MHz,  $\text{DMSO}-d_6$ ):  $\delta$  171.9, 163.4, 150.2, 142.1, 139.5, 129.4, 127.7, 125.6, 121.0, 56.1, 37.2.

**11-(Tritylthio)undecanoic Acid (XI).** Triphenylmethyl chloride (0.63 g, 1.0 equiv) was dissolved in DCM (5 mL). There to, a solution of 11-mercaptoundecanoic acid (MUA) (0.5 g, 1.0 equiv) in DCM (15 mL) was added dropwise. The mixture was stirred for 2 h at rt. DCM was removed by distillation, and the residue was purified by column chromatography (petroleum ether/EtOAc 2:1).  $^1\text{H}$  NMR (300 MHz,  $\text{CDCl}_3$ ):  $\delta$  7.40 (d,  $J = 7.6$  Hz, 6H), 7.31–7.09 (m, 9H), 2.32 (t,  $J = 7.1$  Hz, 2H), 2.11 (t,  $J = 7.3$  Hz, 2H), 1.60 (q,  $J = 7.4$  Hz, 2H), 1.46–0.95 (m, 14H).  $^{13}\text{C}$  NMR (75 MHz,  $\text{CDCl}_3$ ):  $\delta$  179.7, 145.2, 129.8, 127.9, 126.6, 66.5, 34.1, 32.2, 29.5, 29.32, 29.27, 29.16, 29.12, 28.7, 24.8. NMR data are consistent with the literature.<sup>12</sup>

**tert-Butyl (S)-4-((1-Ethoxy-1-oxo-3-phenylpropan-2-yl)-carbamoyl)piperazine-1-carboxylate (XII).** To a stirred solution of 0.798 g 1-boc piperazine in THF, a suspension of 0.860 g (S)-ethyl-2-isocyanate-3-phenylpropanoate in THF was added dropwise. The mixture was stirred for 18 h and the solvent was removed under reduced pressure. The residue was extracted with EtOAc and the combined extracts were washed with a saturated solution of  $\text{NaHCO}_3$  and brine, dried with  $\text{Na}_2\text{SO}_4$ , and concentrated under reduced pressure, resulting in a colorless oil (0.81 g, 50%).  $^1\text{H}$  NMR (300 MHz,  $\text{CDCl}_3$ ):  $\delta$  7.49–7.33 (m, 3H), 7.29–7.18 (m, 2H), 5.10–4.83 (m, 1H), 4.28 (dq,  $J = 15.5, 7.2$  Hz, 2H), 3.70–3.57 (m, 1H), 3.57–3.48 (m, 4H), 3.48–3.35 (m, 4H), 3.29–3.22 (m, 2H), 1.60 (s, 9H), 1.39 (td,  $J = 7.1, 3.3$  Hz, 3H).  $^{13}\text{C}$  NMR (75 MHz,  $\text{CDCl}_3$ ):  $\delta$  172.6, 156.5, 154.6, 136.3, 129.3, 128.5, 127.0, 80.2, 61.4, 60.4, 54.37, 43.9, 38.4, 28.4, 21.1, 14.2.

**(4-(tert-Butoxycarbonyl)piperazine-1-carbonyl)-L-phenylalanine (XIII).** 0.81 g of compound XII was dissolved in THF and cooled to 0 °C. A solution of 0.29 g LiOH in water was added dropwise and the mixture was stirred for 3 h at room temperature. The solvent was removed under reduced pressure and the pH of the residue was adjusted to 2 with 1 M HCl. The residue was extracted with ethyl acetate and the combined extracts were washed with brine, dried with  $\text{Na}_2\text{SO}_4$ , and concentrated under reduced pressure. The crude product was dissolved in diethyl ether, *n*-pentane was added, and the product was crystallized at 4 °C, giving a colorless solid (0.56 g, 74%).  $^1\text{H}$  NMR (300 MHz,  $\text{CDCl}_3$ ):  $\delta$  9.39 (s, 1H), 7.25–7.14 (m, 3H), 7.14–7.04 (m, 2H), 5.05 (d,  $J = 7.1$  Hz, NH), 4.61 (q,  $J = 6.2$  Hz, 1H), 3.30 (dd,  $J = 7.9, 4.0$  Hz, 4H), 3.24–3.09 (m, 4H), 3.04 (dd,  $J = 14.0, 6.8$  Hz, 2H), 1.39 (s, 9H).  $^{13}\text{C}$  NMR (75 MHz,  $\text{CDCl}_3$ ):  $\delta$  174.7, 157.5, 154.8, 136.4, 129.5, 128.7, 127.2, 80.6, 54.9, 43.7, 37.5, 28.5.

**Preparation of Phosphonates 5–7. Diethyl(fluoro-phenylsulfonyl)methylphosphonate<sup>12,67</sup> (5).** To a stirred solution of phosphonate III (1.54 g, 1.0 equiv) in THF, KHMDS (1 M in THF, 6.59 mL, 1.25 equiv) was added dropwise at –80 °C. After 30 min at this temperature, Selectfluor (2.80 g, 1.5 equiv) in 10 mL DMF was added and the reaction mixture was stirred for 3 h, slowly warming to 0 °C. 15 mL of a saturated solution of ammonium chloride was added and the volatiles were evaporated. The residue was extracted with DCM and the combined extracts were washed with a saturated solution of  $\text{NaHCO}_3$  and brine, dried with  $\text{Na}_2\text{SO}_4$ , concentrated under reduced pressure, and purified by column chromatography (light petroleum/EtOAc 1:6) to afford the title compound as a colorless solid. Yield: 1.0 g (62%).  $^1\text{H}$  NMR (300 MHz,  $\text{CDCl}_3$ ):  $\delta$  8.01 (d,  $J = 7.5$  Hz, 2H), 7.74

(t,  $J = 7.4$  Hz, 1H), 7.61 (t,  $J = 7.7$  Hz, 2H), 5.38 (dd,  $J_{\text{H-F}} = 45.5$  Hz,  $J_{\text{H-P}} = 6.6$  Hz, 1H), 4.40–4.18 (m, 4H), 1.35 (t,  $J = 7.1$  Hz, 6H). NMR data were consistent with the literature.<sup>12</sup>

**Phenyl(diethoxyphosphoryl)fluoromethanesulfonate (6).** Phosphonate IV (1.73 g, 1.0 equiv) was dissolved in THF (15 mL) and cooled to –78 °C. KHMDS (1 M in THF, 7.0 mL, 1.25 equiv) was added dropwise and the mixture was stirred for an additional 30 min. Selectfluor (3.0 g, 1.5 equiv) was added in one portion and the mixture was stirred for 5 min. Then, DMF (12 mL) was added in one portion and the mixture was allowed to warm to 0 °C. After stirring for 3 h, the reaction was quenched with conc. aq  $\text{NH}_4\text{Cl}$  (5 mL) and THF was removed in vacuo. EtOAc was added and the organic phase was washed with water (3 $\times$ ) and brine (2 $\times$ ) and dried with  $\text{Na}_2\text{SO}_4$ . The solvent was removed under reduced pressure and the residue was purified by column chromatography (petroleum ether/EtOAc 1:1), yielding the title compound as a colorless oil (0.95 g, 52%).  $^1\text{H}$  NMR (300 MHz,  $\text{CDCl}_3$ ):  $\delta$  7.50–7.39 (m, 2H), 7.39–7.28 (m, 3H), 5.63 (dd,  $J_{\text{H-F}} = 45$  Hz,  $J_{\text{H-P}} = 7.2$  Hz, 1H), 4.45–4.25 (m, 4H), 1.39 (tdd,  $J = 7.1, 2.0, 0.7$  Hz, 6H).  $^{13}\text{C}$  NMR (75 MHz,  $\text{CDCl}_3$ ):  $\delta$  149.6, 130.3, 128.0, 122.2, 93.4 (dd,  $J_{\text{C-F}} = 232$  Hz,  $J_{\text{C-P}} = 162$  Hz), 65.7 (dd,  $J_{\text{C-F}} = 10.7$  Hz,  $J_{\text{C-P}} = 6.7$  Hz), 16.44 (d,  $J_{\text{C-P}} = 5.8$  Hz).

**Diethyl((benzylsulfonyl)fluoromethyl)phosphonate (7).** Phosphonate V (3.77 g, 1.0 equiv) was dissolved in THF (40 mL) and cooled to –78 °C. KHMDS (1 M in THF, 15.4 mL, 1.25 equiv) was added dropwise and the mixture was stirred for an additional 30 min. Selectfluor (6.55 g, 1.5 equiv) was added in one portion and the mixture was stirred for 5 min. Then, DMF (24 mL) was added in one portion and the mixture was allowed to warm to 0 °C. After stirring for 3 h, the reaction was quenched with conc.  $\text{NH}_4\text{Cl}$  (5 mL) and THF was removed in vacuo. EtOAc was added and the organic phase was washed with water (3 $\times$ ) and brine (2 $\times$ ) and dried with  $\text{Na}_2\text{SO}_4$ . The solvent was removed under reduced pressure and the residue was purified by column chromatography (DCM/EtOAc 9:1), yielding the title compound as a colorless oil (1.92 g, 48%).  $^1\text{H}$  NMR (300 MHz,  $\text{CDCl}_3$ ):  $\delta$  7.51–7.32 (m, 5H), 5.28 (dd,  $J_{\text{H-F}} = 45$  Hz,  $J_{\text{H-P}} = 7.1$  Hz, 1H), 4.67–4.49 (m, 2H), 4.42–4.21 (m, 4H), 1.39 (td,  $J = 7.1, 0.7$  Hz, 6H).  $^{13}\text{C}$  NMR (75 MHz,  $\text{CDCl}_3$ ):  $\delta$  131.4, 129.5, 129.2, 125.8, 95.2 (dd,  $J_{\text{C-F}} = 228$  Hz,  $J_{\text{C-P}} = 161$  Hz), 65.4 (dd,  $J_{\text{C-F}} = 6.3$  Hz,  $J_{\text{C-P}} = 6.2$  Hz), 57.5, 16.5 (d,  $J_{\text{C-P}} = 5.8$  Hz).

**HWE Olefination (Compounds 8–12). Procedure A.** The specified phosphonate (1.0 equiv) was dissolved in THF and cooled to 0 °C. NaH (60% in mineral oil, 1.1 equiv) was added in portions and the mixture was stirred for 15 min. The corresponding boc-protected aminoaldehyde (1.0 equiv) was added in one portion, and the mixture was allowed to warm to rt. After stirring for 1 h, EtOAc was added and the organic phase was extracted with water, saturated aq  $\text{NaHCO}_3$ , and brine and finally dried with  $\text{Na}_2\text{SO}_4$ . Evaporation of the solvent under reduced pressure provided the boc-protected vinylsulfones as a crude mixture of *E/Z* isomers. Purification and separation of the isomers were achieved by column chromatography. The products were obtained as colorless solids.

**Procedure B.** The specified phosphonate (1.0 equiv) was dissolved in THF and cooled to –78 °C. KHMDS (1 M in THF, 1.0 equiv) or LHMDS (1 M in THF, 1.0 equiv) was added dropwise and it was stirred for additional 20 min. The respective aldehyde (1.0 equiv) was added in one portion and the mixture was allowed to warm to rt over a period of 1 h. After stirring for an additional hour at rt, EtOAc was added and the organic phase was extracted with water (2 $\times$ ) and brine (1 $\times$ ). Evaporation of the solvent under reduced pressure gave the crude product as *E/Z* isomers. Purification by column chromatography allowed the isolation of the desired (*E*)-isomers. The products were obtained as colorless solids.

**tert-Butyl (S,E)-(1-Fluoro-5-phenyl-1-(phenylsulfonyl)pent-1-en-3-yl)carbamate<sup>12</sup> (8).** Prepared following procedure A using 0.35 g of phosphonate 5, 0.3 g boc-homophenylalanine or boc-homophenylalanine aldehyde or boc-hPhe-H (VI), and 0.05 g NaH in 6 mL THF. Column chromatography: petroleum ether/EtOAc 3:1. (*E*)-isomer: Yield 0.20 g (41%).  $^1\text{H}$  NMR (300 MHz,  $\text{CDCl}_3$ ):  $\delta$  7.95 (d,  $J = 7.6$  Hz, 2H), 7.70 (t,  $J = 7.4$  Hz, 1H), 7.58 (t,  $J = 7.6$  Hz, 2H), 7.36–7.16 (m, 3H), 7.12 (d,  $J = 7.1$  Hz, 2H), 6.19 (dd,  $J_{\text{H-F}} = 32.3$  Hz,  $J_{\text{H-H}} = 7.1$  Hz,

1H), 4.61 (s, 1H), 4.46 (s, 1H), 2.74–2.52 (m, 2H), 2.00–1.77 (m, 2H), 1.39 (s, 9H). <sup>13</sup>C NMR (75 MHz, CDCl<sub>3</sub>): δ 154.9, 154.7 (d, *J*<sub>C–F</sub> = 300 Hz), 140.5, 137.2, 134.7, 129.61, 128.8, 128.7, 128.4, 126.4, 118.4 (d, *J*<sub>C–F</sub> = 4.6 Hz), 80.3, 46.4 (d, *J*<sub>C–F</sub> = 2.7 Hz), 36.2, 32.0, 28.3. (*Z*)-isomer: Yield 0.10 g (21%). <sup>1</sup>H NMR (300 MHz, CDCl<sub>3</sub>): δ 8.09 (d, *J* = 4.2 Hz, 2H), 7.69 (t, *J* = 7.4 Hz, 1H), 7.57 (t, *J* = 7.7 Hz, 2H), 7.37–7.12 (m, 5H), 5.81 (dd, *J*<sub>H–F</sub> = 21 Hz, *J*<sub>H–H</sub> = 10 Hz, 1H), 5.35–5.18 (m, 1H), 4.70 (s, 1H), 2.89–2.62 (m, 2H), 2.14–1.86 (m, 2H), 1.46 (s, 9H). <sup>13</sup>C NMR (75 MHz, CDCl<sub>3</sub>): δ 155.0, 152.7 (d, *J*<sub>C–F</sub> = 293 Hz), 141.0, 137.7, 134.7, 129.5, 129.1, 128.7, 128.5, 126.3, 121.4 (d, *J*<sub>C–F</sub> = 11 Hz), 80.0, 46.6 (d, *J*<sub>C–F</sub> = 5 Hz), 37.3, 32.3, 28.5.

**Phenyl (*S,E*)-3-((*tert*-Butoxycarbonyl)amino)-1-fluoro-5-phenylpent-1-ene-1-sulfonate (9).** Prepared following procedure A using 0.66 g of phosphonate 6, 0.53 g boc-homophenylalaninal or boc-homophenylalanine aldehyde or boc-hPhe-H (VI), and 0.09 g NaH in 12 mL THF. Column chromatography: petroleum ether/EtOAc 5:1. (*E*)-isomer: Yield 0.38 g (43%). <sup>1</sup>H NMR (300 MHz, CDCl<sub>3</sub>): δ 7.46–7.32 (m, 2H), 7.32–7.15 (m, 6H), 7.10 (d, *J* = 7.0 Hz, 2H), 5.91 (dd, *J*<sub>H–F</sub> = 31.3 Hz, *J*<sub>H–H</sub> = 8.6 Hz, 1H), 4.68–4.27 (m, 2H), 2.66–2.43 (m, 2H), 1.97–1.66 (m, 2H), 1.43 (s, 9H). <sup>13</sup>C NMR (75 MHz, CDCl<sub>3</sub>): δ 154.8, 150.8, 148.9 (d, *J*<sub>C–F</sub> = 296 Hz), 140.2, 130.2, 128.8, 128.4, 128.0, 126.5, 122.4 (d, *J*<sub>C–F</sub> = 4.1 Hz), 122.3, 80.4, 46.3 (d, *J*<sub>C–F</sub> = 2.1 Hz), 35.9, 31.9, 28.4. (*Z*)-isomer: yield 0.22 g (22%). <sup>1</sup>H NMR (300 MHz, CDCl<sub>3</sub>): δ 7.44–7.32 (m, 2H), 7.32–7.13 (m, 6H), 7.04 (d, *J* = 7.2 Hz, 2H), 6.14 (br, 1H), 4.88–4.44 (br, 2H), 2.59–2.46 (m, 1H), 2.46–2.29 (m, 1H), 1.84 (br, 1H), 1.42 (br, 1H), 1.43 (s, 9H). <sup>13</sup>C NMR (75 MHz, CDCl<sub>3</sub>): δ 154.8, 149.3, 147.5 (d, *J*<sub>C–F</sub> = 296 Hz), 140.7, 130.1, 128.5, 128.4, 128.1, 126.3, 124.1 (d, *J*<sub>C–F</sub> = 9.9 Hz), 122.4, 80.4, 47.1 (d, *J*<sub>C–F</sub> = 3.6 Hz), 36.3, 32.0, 28.4.

**Phenyl (*S,E*)-3-((*tert*-Butoxycarbonyl)amino)-5-phenylpent-1-ene-1-sulfonate (9-(H)).** Prepared following procedure B using 1.45 g of phosphonate IV, 1.24 g boc-homophenylalaninal or boc-homophenylalanine aldehyde or boc-hPhe-H (VI), and 6.0 mL 1 M LHMDS in 25 mL THF. Column chromatography: cyclohexane/EtOAc 5:1. (*E*)-isomer: Yield 0.80 g (41%). <sup>1</sup>H NMR (300 MHz, CDCl<sub>3</sub>): δ 7.43–7.35 (m, 2H), 7.35–7.27 (m, 3H), 7.27–7.20 (m, 3H), 7.18–7.10 (m, 2H), 6.76 (dd, *J* = 15.1, 5.1 Hz, 1H), 6.48 (dd, *J* = 15.1, 1.5 Hz, 1H), 4.58 (d, *J* = 8.2 Hz, 1H), 4.33 (s, 1H), 2.77–2.52 (m, 2H), 1.98–1.72 (m, 2H), 1.49 (s, 9H). <sup>13</sup>C NMR (75 MHz, CDCl<sub>3</sub>): δ 154.9, 150.4, 149.6, 140.2, 130.0, 128.8, 128.4, 127.4, 126.6, 124.4, 122.6, 80.5, 51.0, 35.6, 32.0, 28.4.

***tert*-Butyl (*S,E*)-1-(*Benzylsulfonyl*)-1-fluoro-5-phenylpent-1-en-3-ylcarbamate (10).** Synthesized following procedure B using 0.92 g phosphonate 7, 0.74 g boc-homophenylalaninal or boc-homophenylalanine aldehyde or boc-hPhe-H (VI), and 2.8 mL LHMDS (1 M in THF) in 14 mL THF. Column chromatography: DCM/EtOAc 100:1. (*E*)-isomer: yield: 0.57 g (47%). <sup>1</sup>H NMR (300 MHz, CDCl<sub>3</sub>): δ 7.39–7.16 (m, 8H), 7.10 (d, *J* = 7.0 Hz, 2H), 5.76 (dd, *J*<sub>H–F</sub> = 32.8 Hz, *J*<sub>H–H</sub> = 8.1 Hz, 1H), 4.59–4.38 (m, 2H), 4.35 (s, 2H), 2.62–2.38 (m, 2H), 1.91–1.64 (m, 3H), 1.45 (s, 9H). <sup>13</sup>C NMR (75 MHz, CDCl<sub>3</sub>): δ 154.8, 152.1 (d, *J*<sub>C–F</sub> = 300 Hz), 140.5, 131.0, 129.5, 129.2, 128.7, 128.4, 126.8, 126.4, 120.9 (d, *J*<sub>C–F</sub> = 3.1 Hz), 80.3, 58.9, 46.1, 36.2, 31.8, 28.5. The (*Z*)-isomer was not isolated.

***tert*-Butyl (*S,E*)-1-(*Fluoro-5*-(methylthio)-1-(phenylsulfonyl)pent-1-en-3-yl)carbamate (11).** Synthesized following procedure B using 0.93 g phosphonate 5, 0.75 g boc-Met-H, and 3.15 mL LHMDS (1 M in THF) in 20 mL THF. Column chromatography: Petroleum ether/EtOAc 3:1. (*E*)-isomer: Yield 0.88 g (75%). <sup>1</sup>H NMR (300 MHz, CDCl<sub>3</sub>): δ 7.94 (d, *J* = 7.8 Hz, 2H), 7.70 (t, *J* = 7.3 Hz, 1H), 7.58 (t, *J* = 7.6 Hz, 2H), 6.21 (br d, *J*<sub>H–F</sub> = 31.5 Hz, 1H), 4.74 (br s, 1H), 4.55 (br s, 1H), 2.57–2.40 (m, 2H), 2.07 (s, 3H), 2.00–1.78 (m, 2H), 1.37 (s, 9H). <sup>13</sup>C NMR (75 MHz, CDCl<sub>3</sub>): δ 154.9, 154.7 (d, *J*<sub>C–F</sub> = 300 Hz), 137.1, 134.7, 129.6, 128.8, 118.0 (d, *J*<sub>C–F</sub> = 4.6 Hz), 80.4, 46.0 (d, *J*<sub>C–F</sub> = 1.0 Hz), 33.8, 30.2, 28.3, 15.7. The (*Z*)-isomer was not further characterized.

***tert*-Butyl (*R,E*)-1-(*Benzylthio*)-4-fluoro-4-(phenylsulfonyl)but-3-en-2-yl)carbamate (12).** Synthesized following procedure B using 0.55 g phosphonate 5, 0.55 g boc-L-Cys(Bn)-H, and 1.85 mL LHMDS (1 M in THF) in 10 mL THF. Column chromatography: Petroleum ether/EtOAc 3:1. (*E*)-isomer: yield 0.44 g (54%). <sup>1</sup>H NMR (300 MHz,

CDCl<sub>3</sub>): δ 8.00–7.92 (m, 3H), 7.75–7.53 (m, 5H), 7.30–7.27 (m, 3H), 6.23 (dd, *J*<sub>H–F</sub> = 31.8 Hz, *J*<sub>H–H</sub> = 8.5 Hz, 1H), 4.83 (s, 1H), 4.59 (s, 1H), 3.70 (s, 2H), 2.73–2.44 (m, 2H), 1.39 (s, 9H). <sup>13</sup>C NMR (75 MHz, CDCl<sub>3</sub>): δ 156.9, 154.8, 137.5, 137.1, 135.0, 134.7, 129.7, 129.6, 129.2, 129.0, 128.9, 128.8, 127.5, 117.5, 80.5, 46.0, 36.7, 35.4, 28.4.

**Peptide Chemistry. Coupling Protocols. Procedure C.** The specified carboxylic acid (1.0 equiv) and HOBt (1.0 equiv) were dissolved in DCM (8 mL) and cooled to 0 °C. DIEA (3.0 equiv) was added slowly, and the mixture was stirred until all materials were solubilized. TBTU (1.0 equiv) was added in one portion and the mixture was stirred for 15 min at 0 °C. The specific amine (1.0 equiv) was dissolved in DCM and added dropwise to the reaction mixture. After stirring for 12 h at rt, DCM was removed in vacuo and the residue was dissolved in EtOAc. The organic phase was washed with water (5×), conc. NaHCO<sub>3</sub> (2×), and 1 M aq HCl (2×) and then dried with Na<sub>2</sub>SO<sub>4</sub>. Evaporation of the solvent gave the crude product, which was purified by column chromatography.

**Procedure D.** The specified carboxylic acid (1.0 equiv) and TBTU (1.0 equiv) were dissolved in DCM and cooled to 0 °C. DIEA (3.0 equiv) was added and the mixture was stirred for 15 min. The respective amine (1.0 equiv) was added in one portion. After stirring for 12 h at rt, DCM was removed in vacuo, and the residue was dissolved in EtOAc. The organic phase was washed with water (5×), conc. NaHCO<sub>3</sub> (2×), and 1 M aq HCl (2×) and then dried with Na<sub>2</sub>SO<sub>4</sub>. Evaporation of the solvent gave the crude product, which was purified by column chromatography.

**Procedure E.** The respective carboxylic acid (IX or X, 1.0 equiv) and HOBt (1.0 equiv) were dissolved in DMF (5 mL) and cooled to 0 °C. DIEA (3.0 equiv) was added and the mixture was stirred for 15 min. The respective amine (1.0 equiv) was added in one portion and the mixture was stirred for 12 h at rt. EtOAc was added and aqueous work-up was performed with 5% aq LiCl (5×), water (2×), and saturated aq NaHCO<sub>3</sub> (2×). After evaporation of the solvent, the residue was purified by column chromatography.

**Removal of Boc Groups. Procedure F.** Boc-protected compounds (8–10) were dissolved in 4 M HCl/dioxane solution (5–10 mL). After stirring for 30 min at rt, dioxane was evaporated in vacuo and the residue was washed several times with diethyl ether. The precipitate was collected and dried under reduced pressure. The amines were obtained as hydrochloride salts and were sufficiently pure to be used in the next step without further purification.

**Procedure G.** Boc-protected compounds (11–12) were dissolved in DCM (10 mL) and cooled to 0 °C. 1 mL TFA was added dropwise, and the resulting mixture was stirred for 1 h. After evaporation to dryness in high vacuum, the residue was washed with diethyl ether and collected by filtration. The amines were obtained as TFA salt and directly used for the next step.

**(*S,E*)-1-Fluoro-5-phenyl-1-(phenylsulfonyl)pent-1-en-3-amine Hydrochloride (13).** Prepared following procedure F using 0.60 g of compound 8 in 12 mL 4 M HCl/dioxane. Yield: 0.47 g (93%). <sup>1</sup>H NMR (300 MHz, DMSO-*d*<sub>6</sub>): δ 8.65 (s, 3H), 8.03 (d, *J* = 7.8 Hz, 2H), 7.89 (t, *J* = 7.3 Hz, 1H), 7.77 (t, *J* = 7.6 Hz, 2H), 7.32–7.13 (m, 3H), 7.06 (d, *J* = 7.3 Hz, 2H), 6.54 (dd, *J*<sub>H–F</sub> = 33 Hz, *J*<sub>H–H</sub> = 9.8 Hz, 1H), 4.09–3.90 (m, 1H), 2.62–2.34 (m, 2H), 2.25–2.07 (m, 1H), 2.07–1.89 (m, 1H). <sup>13</sup>C NMR (75 MHz, DMSO-*d*<sub>6</sub>): δ 155.2 (d, *J*<sub>C–F</sub> = 301 Hz), 139.9, 135.9, 135.6, 130.2, 128.54, 128.45, 128.1, 126.2, 114.5 (d, *J*<sub>C–F</sub> = 3.7 Hz), 45.0 (d, *J*<sub>C–F</sub> = 2.7 Hz), 33.4 (d, *J*<sub>C–F</sub> = 1.4 Hz), 30.5.

**Phenyl (*S,E*)-3-Amino-1-fluoro-5-phenylpent-1-ene-1-sulfonate Hydrochloride (14).** Prepared following procedure F using 0.3 g of compound 9 in 7 mL 4 M HCl/dioxane. Yield: 0.23 g (89%). <sup>1</sup>H NMR (300 MHz, DMSO-*d*<sub>6</sub>): δ 8.72 (s, 3H), 7.56–7.47 (m, 2H), 7.47–7.37 (m, 3H), 7.31 (t, *J* = 7.2 Hz, 2H), 7.26–7.19 (m, 1H), 7.19–7.09 (m, 2H), 6.42 (dd, *J*<sub>H–F</sub> = 32 Hz, *J*<sub>H–H</sub> = 9.7 Hz, 1H), 4.15 (td, *J* = 9.2, 5.3 Hz, 1H), 2.48–2.32 (m, 2H), 2.19–2.01 (m, 1H), 2.00–1.81 (m, 1H). <sup>13</sup>C NMR (75 MHz, DMSO-*d*<sub>6</sub>): δ 149.3 (d, *J*<sub>C–F</sub> = 300 Hz), 148.6, 140.0, 130.6, 128.5, 128.4, 128.1, 126.3, 122.0, 118.4 (d, *J*<sub>C–F</sub> = 3.2 Hz), 45.2 (d, *J*<sub>C–F</sub> = 2.2 Hz), 40.4, 33.3, 30.4.

**Phenyl (*S,Z*)-3-Amino-1-fluoro-5-phenylpent-1-ene-1-sulfonate Hydrochloride (14-(Z)).** Prepared following procedure F using 0.2 g of compound 9-(Z) in 7 mL 4 M HCl/dioxane. Yield: 0.16 g (93%). <sup>1</sup>H



NMR (300 MHz, DMSO- $d_6$ ):  $\delta$  8.68 (s, 3H), 7.59–7.45 (m, 2H), 7.44–7.13 (m, 6H), 7.08–6.98 (m, 2H), 6.73 (dd,  $J_{H-F}$  = 21.2 Hz,  $J_{H-H}$  = 10.6 Hz, 1H), 4.27 (q,  $J$  = 7.8, 1H), 2.29–2.02 (m, 2H), 1.95–1.80 (m, 1H), 1.68–1.47 (m, 1H).  $^{13}\text{C}$  NMR (75 MHz, DMSO- $d_6$ ):  $\delta$  148.3, 148.1 (d,  $J_{C-F}$  = 288 Hz), 140.1, 130.6, 128.7, 128.4, 128.0, 126.1, 122.1, 120.6 (d,  $J$  = 16 Hz), 45.9 (d,  $J_{C-F}$  = 6.7 Hz), 34.3, 30.2.

**Phenyl (S,E)-3-Amino-5-phenylpent-1-ene-1-sulfonate Hydrochloride (14-(H)).** Prepared following procedure F using 0.78 g of compound 9-(H) in 14 mL 4 M HCl/dioxane. Yield: 0.34 g (51%).  $^1\text{H}$  NMR (300 MHz, DMSO- $d_6$ ):  $\delta$  8.64 (s, 3H), 7.50–7.41 (m, 2H), 7.41–7.34 (m, 2H), 7.34–7.24 (m, 3H), 7.24–7.17 (m, 1H), 7.16–7.10 (m, 2H), 6.81 (dd,  $J_{H-H}$  = 15.3, 6.8 Hz, 1H), 4.15–3.95 (m, 1H), 2.61–2.38 (m, 2H), 2.10–1.84 (m, 2H).  $^{13}\text{C}$  NMR (75 MHz, DMSO- $d_6$ ):  $\delta$  149.0, 145.3, 140.3, 130.1, 128.5, 128.2, 127.6, 127.6, 126.2, 122.6, 50.1, 33.3, 30.4.

**(S,E)-1-(Benzylsulfonyl)-1-fluoro-5-phenylpent-1-en-3-amine Hydrochloride (15).** Prepared following procedure F using 0.46 g of compound 10 in 10 mL 4 M HCl/dioxane. Yield: 0.37 g (95%).  $^1\text{H}$  NMR (300 MHz, DMSO- $d_6$ ):  $\delta$  8.66 (s, 3H), 7.48–7.27 (m, 7H), 7.26–7.09 (m, 3H), 6.13 (dd,  $J_{H-F}$  = 33 Hz,  $J_{H-H}$  = 9.9 Hz, 1H), 4.87 (s, 2H), 4.04 (td,  $J$  = 9.3, 5.0 Hz, 1H), 2.39 (t,  $J$  = 8.1 Hz, 2H), 2.13–1.97 (m, 1H), 1.91–1.74 (m, 1H).  $^{13}\text{C}$  NMR (75 MHz, DMSO- $d_6$ ):  $\delta$  154.1 (d,  $J_{C-F}$  = 304 Hz), 140.2, 131.2, 129.0, 128.7, 128.5, 128.2, 127.0, 126.2, 115.7 (d,  $J_{C-F}$  = 2.9 Hz), 57.6, 45.0 (d,  $J_{C-F}$  = 2.2 Hz), 33.5, 30.4.

**(S,E)-1-Fluoro-5-(methylthio)-1-(phenylsulfonyl)pent-1-en-3-aminium 2,2,2-Trifluoroacetate (16).** Prepared following procedure G with 0.88 g compound 11. Yield: 0.60 g (65%).  $^1\text{H}$  NMR (300 MHz, DMSO- $d_6$ ):  $\delta$  7.89–7.82 (m, 2H), 7.82–7.63 (m, 1H), 7.57–7.52 (m, 2H), 6.21 (d,  $J_{H-F}$  = 32 Hz, 1H), 4.46 (m, 1H), 2.69–2.41 (m, 2H), 2.06 (s, 3H), 2.05–1.75 (m, 2H).

**(R,E)-1-(Benzylthio)-4-fluoro-4-(phenylsulfonyl)but-3-en-2-aminium 2,2,2-Trifluoroacetate (17).** Prepared following procedure G with 0.44 g compound 12. Yield: 0.37 g (81%).  $^1\text{H}$  NMR (300 MHz, DMSO- $d_6$ ):  $\delta$  8.04 (s, 3H), 7.95–7.84 (m, 2H), 7.77–7.55 (m, 4H), 7.25–7.19 (m, 4H), 6.44 (dd,  $J_{H-F}$  = 30 Hz,  $J_{H-H}$  = 9.1 Hz, 1H), 4.20–4.01 (m, 1H), 3.71 (s, 2H), 2.91–2.62 (m, 2H).  $^{13}\text{C}$  NMR (75 MHz, DMSO- $d_6$ ):  $\delta$  161.4, 160.8, 155.5, 136.6, 135.5, 135.0, 129.9, 129.7, 129.2, 129.1, 128.9, 127.9, 117.3, 113.5, 111.1, 77.2, 46.2, 36.2, 33.3.

**tert-Butyl ((S)-1-((S,E)-1-Fluoro-5-phenyl-1-(phenylsulfonyl)pent-1-en-3-yl)amino)-1-oxo-3-phenylpropan-2-yl)carbamate (18).** Synthesized following procedure C with 0.180 g compound 13, 0.135 g boc-L-Phe-OH, 0.162 g TBTU, 0.078 g HOBt, and 0.265 mL DIEA. Purification by column chromatography (petroleum ether/EtOAc 3:1). Yield: 0.21 g (73%).  $^1\text{H}$  NMR (300 MHz,  $\text{CDCl}_3$ ):  $\delta$  8.00–7.89 (m, 2H), 7.79–7.68 (m, 1H), 7.67–7.55 (m, 2H), 7.39–7.12 (m, 8H), 7.10–7.00 (m, 2H), 6.00 (dd,  $J_{H-F}$  = 32 Hz,  $J_{H-H}$  = 8.5 Hz, 1H), 5.82 (d,  $J$  = 8.0 Hz, 1H), 4.91 (s, 1H), 4.69 (quint,  $J$  = 7.7 Hz, 1H), 4.20 (q,  $J$  = 7.5 Hz, 1H), 3.04 (dd,  $J$  = 13.7, 6.6 Hz, 1H), 2.95 (dd,  $J$  = 13.7, 7.6 Hz, 1H), 2.52 (t,  $J$  = 7.2 Hz, 2H), 1.96–1.75 (m, 2H), 1.40 (s, 9H).  $^{13}\text{C}$  NMR (75 MHz,  $\text{CDCl}_3$ ):  $\delta$  170.8, 155.6, 154.8 (d,  $J_{C-F}$  = 301 Hz), 140.4, 137.1, 136.6, 134.8, 129.7, 129.4, 129.0, 128.8, 128.7, 128.4, 127.3, 126.4, 117.3 (d,  $J_{C-F}$  = 4.7 Hz), 80.6, 56.2, 45.0, 38.4, 35.7, 31.8, 28.4.

**Phenyl (S,E)-3-((S)-2-((tert-Butoxycarbonyl)amino)-3-phenylpropanamido)-1-fluoro-5-phenylpent-1-ene-1-sulfonate (19).** Synthesized following procedure C with 0.160 g compound 14, 0.114 g boc-L-Phe-OH, 0.138 g TBTU, 0.066 g HOBt, and 0.225 mL DIEA. Purification by column chromatography (petroleum ether/EtOAc 3:1). Yield: 0.20 g (78%).  $^1\text{H}$  NMR (300 MHz,  $\text{CDCl}_3$ ):  $\delta$  7.47–7.35 (m, 2H), 7.35–7.10 (m, 9H), 7.08–6.95 (m, 4H), 5.65 (d,  $J$  = 7.9 Hz, 1H), 5.60 (dd,  $J_{H-F}$  = 32 Hz,  $J_{H-H}$  = 8.3 Hz, 1H), 5.02 (d,  $J$  = 7.1 Hz, 1H), 4.68 (q,  $J$  = 7.4 Hz, 1H), 4.18 (dd,  $J$  = 8.6, 5.6 Hz, 1H), 3.04 (dd,  $J$  = 13.4, 6.2 Hz, 1H), 2.85 (dd,  $J$  = 13.4, 8.4 Hz, 1H), 2.55–2.35 (m, 2H), 1.83–1.60 (m, 2H), 1.41 (s, 9H).  $^{13}\text{C}$  NMR (75 MHz,  $\text{CDCl}_3$ ):  $\delta$  170.8, 155.8, 149.4, 149.0 (d,  $J_{C-F}$  = 297 Hz), 147.0, 140.1, 136.5, 130.2, 129.3, 129.0, 128.8, 128.4, 128.0, 127.4, 126.6, 122.5, 121.3 (d,  $J_{C-F}$  = 5.1 Hz), 80.6, 56.2, 44.8, 38.7, 35.3, 31.7, 28.4.

**Phenyl (S,Z)-3-((S)-2-((tert-Butoxycarbonyl)amino)-3-phenylpropanamido)-1-fluoro-5-phenylpent-1-ene-1-sulfonate (19-(Z)).** Synthesized following procedure C with 0.128 g compound 14-(Z), 0.091 g boc-L-Phe-OH, 0.110 g TBTU, 0.053 g HOBt, and 0.204 mL DIEA.

Purification by column chromatography (petroleum ether/EtOAc 3:1). Yield: 0.150 g (81%).  $^1\text{H}$  NMR (300 MHz,  $\text{CDCl}_3$ ):  $\delta$  7.46–7.08 (m, 13H), 6.97 (d,  $J$  = 6.8 Hz, 2H), 5.94–5.59 (m, 2H), 4.96 (s, 1H), 4.80 (q,  $J$  = 8.2 Hz, 1H), 4.25–4.11 (m, 1H), 3.14–2.87 (m, 2H), 2.44–2.17 (m, 2H), 1.82–1.61 (m, 1H), 1.53–1.42 (m, 1H), 1.41 (s, 9H).  $^{13}\text{C}$  NMR (75 MHz,  $\text{CDCl}_3$ ):  $\delta$  171.0, 155.6, 149.2, 148.0 (d,  $J_{C-F}$  = 289 Hz), 140.6, 136.7, 130.2, 129.5, 128.9, 128.6, 128.4, 128.1, 127.2, 126.3, 123.0, 123.0 (d,  $J_{C-F}$  = 12 Hz), 80.6, 56.1, 46.1 (d,  $J_{C-F}$  = 5.9 Hz), 38.5, 35.7, 31.8, 28.4.

**tert-Butyl ((S)-1-((S,E)-1-(Benzylsulfonyl)-1-fluoro-5-phenylpent-1-en-3-yl)amino)-1-oxo-3-phenylpropan-2-yl)carbamate (20).** Synthesized following procedure C with 0.230 g compound 15, 0.165 g boc-L-Phe-OH, 0.200 g TBTU, 0.095 g HOBt, and 0.325 mL DIEA. Purification by column chromatography (petroleum ether/EtOAc 3:1). Yield: 0.30 g (85%).  $^1\text{H}$  NMR (300 MHz,  $\text{CDCl}_3$ ):  $\delta$  7.42–7.15 (m, 11H), 7.13–6.97 (m, 4H), 5.68 (d,  $J$  = 8.0 Hz, 1H), 5.53 (dd,  $J_{H-F}$  = 33 Hz,  $J_{H-H}$  = 8.9 Hz, 1H), 4.99 (br s, 1H), 4.68 (quint,  $J$  = 7.8 Hz, 1H), 4.35 (s, 2H), 4.18 (q,  $J$  = 7.9 Hz, 1H), 3.03 (dd,  $J$  = 13.5, 6.4 Hz, 1H), 2.91 (dd,  $J$  = 13.5, 8.0 Hz, 1H), 2.49–2.29 (m, 2H), 1.70–1.56 (m, 2H), 1.42 (s, 9H).  $^{13}\text{C}$  NMR (75 MHz,  $\text{CDCl}_3$ ):  $\delta$  170.6, 155.6, 152.3 (d,  $J_{C-F}$  = 301 Hz), 140.3, 136.6, 131.0, 129.5, 129.4, 129.2, 129.0, 128.7, 128.4, 127.3, 126.7, 126.5, 119.7 (d,  $J_{C-F}$  = 4.0 Hz), 80.6, 58.8, 56.2, 44.7 (d,  $J_{C-F}$  = 1.3 Hz), 38.6, 35.5 (d,  $J_{C-F}$  = 1.4 Hz), 31.7, 28.4.

**tert-Butyl ((S)-1-((S,E)-1-Fluoro-5-phenyl-1-(phenylsulfonyl)pent-1-en-3-yl)amino)-1-oxo-3-(m-tolyl)propan-2-yl)carbamate (21).** Synthesized following procedure C with 0.220 g compound 13, 0.173 g boc-L-Phe(3-Me)-OH, 0.198 g TBTU, 0.095 g HOBt, and 0.330 mL DIEA. Purification by column chromatography (petroleum ether/EtOAc 3:1). Yield: 0.28 g (77%).  $^1\text{H}$  NMR (300 MHz,  $\text{CDCl}_3$ ):  $\delta$  8.00–7.88 (m, 2H), 7.76–7.65 (m, 1H), 7.64–7.53 (m, 2H), 7.31–7.12 (m, 4H), 7.11–6.88 (m, 5H), 6.04 (dd,  $J_{H-F}$  = 32.1 Hz,  $J_{H-H}$  = 8.4 Hz, 1H), 5.93 (d,  $J$  = 8.0 Hz, 1H), 4.92 (s, 1H), 4.78–4.59 (m, 1H), 4.21 (q,  $J$  = 7.3 Hz, 1H), 3.01 (dd,  $J$  = 13.8, 6.6 Hz, 1H), 2.92 (dd,  $J$  = 13.8, 7.5 Hz, 1H), 2.58–2.46 (m, 2H), 2.31 (s, 3H), 1.93–1.77 (m, 2H), 1.41 (s, 9H).  $^{13}\text{C}$  NMR (75 MHz,  $\text{CDCl}_3$ ):  $\delta$  170.9, 155.62, 154.9 (d,  $J_{C-F}$  = 303 Hz), 140.4, 138.7, 137.1, 136.5, 134.8, 130.1, 129.7, 128.9, 128.8, 128.7, 128.4, 128.1, 126.4, 126.4, 117.4 (d,  $J_{C-F}$  = 3.6 Hz), 80.6, 56.2, 45.2, 38.2, 35.8, 31.8, 28.4, 21.5.

**Phenyl (S,E)-3-((S)-2-((tert-Butoxycarbonyl)amino)-3-(m-tolyl)propanamido)-1-fluoro-5-phenylpent-1-ene-1-sulfonate (22).** Synthesized following procedure C with 0.280 g compound 14, 0.210 g boc-L-Phe(3-Me)-OH, 0.242 g TBTU, 0.115 g HOBt, and 0.40 mL DIEA. Purification by column chromatography (petroleum ether/EtOAc 3:1). Yield: 0.34 g (75%).  $^1\text{H}$  NMR (300 MHz,  $\text{CDCl}_3$ ):  $\delta$  7.40 (t,  $J$  = 7.3 Hz, 2H), 7.35–7.08 (m, 7H), 7.08–7.00 (m, 3H), 6.91 (s, 1H), 6.80 (d,  $J$  = 7.3 Hz, 1H), 5.78 (d,  $J$  = 7.7 Hz, 1H), 5.65 (dd,  $J_{H-F}$  = 31.4 Hz,  $J_{H-H}$  = 8.3 Hz, 1H), 5.04 (s, 1H), 4.70 (quint,  $J$  = 8.2, 7.0 Hz, 1H), 4.18 (quint,  $J$  = 8.7, 8.0 Hz, 1H), 3.01 (dd,  $J$  = 13.3, 6.1 Hz, 1H), 2.83 (dd,  $J$  = 13.3, 8.6 Hz, 1H), 2.55–2.37 (m, 2H), 2.28 (s, 3H), 1.81–1.65 (m, 2H), 1.42 (s, 9H).  $^{13}\text{C}$  NMR (75 MHz,  $\text{CDCl}_3$ ):  $\delta$  170.9, 155.6, 149.4, 149.0 (d,  $J_{C-F}$  = 297 Hz), 140.2, 138.7, 136.5, 130.2, 130.0, 128.9, 128.8, 128.4, 128.1, 128.0, 126.5, 126.4, 122.4, 121.3 (d,  $J_{C-F}$  = 4.9 Hz), 80.6, 56.2, 44.9 (d,  $J_{C-F}$  = 1.2 Hz), 38.5, 35.4 (d,  $J_{C-F}$  = 0.9 Hz), 31.7, 28.4, 21.4.

**tert-Butyl ((S)-1-((S,E)-1-(Benzylsulfonyl)-1-fluoro-5-phenylpent-1-en-3-yl)amino)-1-oxo-3-(m-tolyl)propan-2-yl)carbamate (23).** Synthesized following procedure C with 0.230 g compound 15, 0.174 g boc-L-Phe(3-Me)-OH, 0.200 g TBTU, 0.095 g HOBt, and 0.325 mL DIEA. Purification by column chromatography (petroleum ether/EtOAc 3:1). Yield: 0.28 g (69%).  $^1\text{H}$  NMR (300 MHz,  $\text{CDCl}_3$ ):  $\delta$  7.41–7.12 (m, 9H), 7.04 (d,  $J$  = 7.3 Hz, 3H), 6.94 (s, 1H), 6.85 (d,  $J$  = 7.3 Hz, 1H), 5.73 (d,  $J$  = 7.8 Hz, 1H), 5.56 (dd,  $J_{H-F}$  = 32.8 Hz,  $J_{H-H}$  = 8.8 Hz, 1H), 4.99 (s, 1H), 4.69 (quint,  $J$  = 8.3, 7.8 Hz, 1H), 4.34 (s, 2H), 4.18 (q,  $J$  = 8.7 Hz, 1H), 3.01 (dd,  $J$  = 13.6, 6.5 Hz, 1H), 2.87 (dd,  $J$  = 13.6, 7.9 Hz, 1H), 2.49–2.33 (m, 2H), 2.30 (s, 3H), 1.72–1.57 (m, 2H), 1.42 (s, 9H).  $^{13}\text{C}$  NMR (75 MHz,  $\text{CDCl}_3$ ):  $\delta$  170.7, 155.6, 152.3 (d,  $J_{C-F}$  = 301 Hz), 140.4, 138.7, 136.5, 131.1, 130.1, 129.5, 129.2, 128.9, 128.7, 128.4, 128.1, 126.7, 126.5, 119.8 (d,  $J_{C-F}$  = 4.2 Hz), 80.6, 58.8, 56.2, 44.8 (d,  $J_{C-F}$  = 1.3 Hz), 38.4, 35.6, 31.7, 28.4, 21.5.



*tert*-Butyl ((*S*)-1-(((*S*,*E*)-1-Fluoro-5-phenyl-1-(phenylsulfonyl)pent-1-en-3-yl)amino)-1-oxo-3-(*p*-tolyl)propan-2-yl)carbamate (**24**). Synthesized following procedure C with 0.200 g compound **13**, 0.173 g boc-*L*-Phe(4-Me)-OH, 0.198 g TBTU, 0.095 g HOBt, and 0.30 mL DIEA. Purification by column chromatography (petroleum ether/EtOAc 3:1). Yield: 0.25 g (77%). <sup>1</sup>H NMR (300 MHz, CDCl<sub>3</sub>): δ 7.94 (d, *J* = 7.8 Hz, 2H), 7.70 (t, *J* = 7.2 Hz, 1H), 7.59 (t, *J* = 7.6 Hz, 2H), 7.35–6.92 (m, 9H), 6.03 (dd, *J*<sub>H-F</sub> = 32.0 Hz, *J*<sub>H-H</sub> = 8.4 Hz, 1H), 5.89 (d, *J* = 8.0 Hz, 1H), 4.93 (s, 1H), 4.70 (quint, *J* = 7.4 Hz, 1H), 4.20 (q, *J* = 7.2 Hz, 1H), 3.01 (dd, *J* = 13.6, 6.4 Hz, 1H), 2.91 (dd, *J* = 13.6, 7.6 Hz, 1H), 2.52 (t, *J* = 7.5 Hz, 2H), 2.33 (s, 3H), 1.95–1.77 (m, 2H), 1.41 (s, 9H). <sup>13</sup>C NMR (75 MHz, CDCl<sub>3</sub>): δ 170.9, 155.6, 154.8 (d, *J*<sub>C-F</sub> = 301 Hz), 140.4, 137.2, 137.0, 134.7, 133.4, 129.70, 129.65, 129.3, 128.8, 128.7, 128.4, 126.4, 117.4 (d, *J*<sub>C-F</sub> = 4.4 Hz), 80.5, 56.2, 45.0, 38.0, 35.8, 31.8, 28.4, 21.2.

Phenyl (*S*,*E*)-3-((*S*)-2-((*tert*-Butoxycarbonyl)amino)-3-(*p*-tolyl)propanamido)-1-fluoro-5-phenylpent-1-ene-1-sulfonate (**25**). Synthesized following procedure C with 0.292 g compound **14**, 0.220 g boc-*L*-Phe(4-Me)-OH, 0.252 g TBTU, 0.121 g HOBt, and 0.410 mL DIEA. Purification by column chromatography (petroleum ether/EtOAc 3:1). Yield: 0.39 g (83%). <sup>1</sup>H NMR (300 MHz, CDCl<sub>3</sub>): δ 7.47–7.35 (m, 2H), 7.35–7.15 (m, 6H), 7.10–6.98 (m, 4H), 6.92 (d, *J* = 8.0 Hz, 2H), 5.75 (d, *J* = 7.9 Hz, 1H), 5.62 (dd, *J*<sub>H-F</sub> = 31 Hz, *J*<sub>H-H</sub> = 9.0 Hz, 1H), 5.05 (d, *J* = 7.8 Hz, 1H), 4.70 (quint, *J* = 7.7 Hz, 1H), 4.20–4.08 (m, 1H), 3.00 (dd, *J* = 13.5, 6.1 Hz, 1H), 2.81 (dd, *J* = 13.5, 8.3 Hz, 1H), 2.53–2.36 (m, 2H), 2.29 (s, 3H), 1.83–1.62 (m, 2H), 1.41 (s, 9H). <sup>13</sup>C NMR (75 MHz, CDCl<sub>3</sub>): δ 170.9, 155.6, 149.4, 149.0 (d, *J*<sub>C-F</sub> = 297 Hz), 140.2, 137.0, 133.3, 130.2, 129.7, 129.2, 128.8, 128.4, 128.0, 126.5, 122.4, 121.4, 121.3, 80.6, 56.3, 44.8 (d, *J*<sub>C-F</sub> = 1.5 Hz), 38.3, 35.4, 31.7, 28.4, 21.1.

Phenyl (*S*,*E*)-3-((*S*)-2-((*tert*-Butoxycarbonyl)amino)-3-(*p*-tolyl)propanamido)-5-phenylpent-1-ene-1-sulfonate (**25**-(*H*)). Synthesized following procedure C with 0.34 g compound **14**-(*H*), 0.28 g boc-*L*-Phe(4-Me)-OH, 0.32 g TBTU, 0.14 g HOBt, and 0.70 mL DIEA. Purification by column chromatography (cyclohexane/EtOAc 4:1). Yield: 0.24 g (42%). <sup>1</sup>H NMR (300 MHz, CDCl<sub>3</sub>): δ 7.42–7.32 (m, 2H), 7.31–7.02 (m, 12H), 6.52 (dd, *J*<sub>H-H</sub> = 15.2, 4.6 Hz, 1H), 5.92 (dd, *J*<sub>H-H</sub> = 37.5, 11.8 Hz, 2H), 5.00 (s, 1H), 4.63–4.47 (m, 1H), 4.31–4.18 (q, 1H), 3.08–2.89 (m, 2H), 2.62–2.42 (m, 2H), 2.31 (s, 3H), 1.88–1.60 (m, 2H), 1.43 (s, 9H). <sup>13</sup>C NMR (75 MHz, CDCl<sub>3</sub>): δ 171.1, 149.5, 149.1, 140.1, 137.3, 133.0, 129.8 (d, *J* = 3.6 Hz), 129.1 (d, *J* = 6.7 Hz), 128.6, 128.3, 127.3, 126.4, 124.4, 122.6, 56.5, 49.2, 35.1, 31.7, 28.3, 21.0. mp 93–95 °C.

*tert*-Butyl ((*S*)-1-(((*S*,*E*)-1-(Benzylsulfonyl)-1-fluoro-5-phenylpent-1-en-3-yl)amino)-1-oxo-3-(*p*-tolyl)propan-2-yl)carbamate (**26**). Synthesized following procedure C with 0.230 g compound **15**, 0.174 g boc-*L*-Phe(4-Me)-OH, 0.200 g TBTU, 0.095 g HOBt, and 0.325 mL DIEA. Purification by column chromatography (petroleum ether/EtOAc 3:1). Yield: 0.290 g (79%). <sup>1</sup>H NMR (300 MHz, CDCl<sub>3</sub>): δ 7.43–7.14 (m, 8H), 7.12–6.99 (m, 4H), 6.96 (d, *J* = 7.4 Hz, 2H), 5.66 (d, *J* = 7.8 Hz, 1H), 5.54 (dd, *J*<sub>H-F</sub> = 32.9 Hz, *J*<sub>H-H</sub> = 8.7 Hz, 1H), 4.98 (s, 1H), 4.69 (quint, *J* = 8.3 Hz, 1H), 4.34 (s, 2H), 4.15 (q, *J* = 7.8, 7.4 Hz, 1H), 3.01 (dd, *J* = 13.6, 5.9 Hz, 1H), 2.85 (dd, *J* = 13.6, 8.0 Hz, 1H), 2.54–2.33 (m, 2H), 2.30 (s, 3H), 1.70–1.55 (m, 3H), 1.42 (s, 9H). <sup>13</sup>C NMR (75 MHz, CDCl<sub>3</sub>): δ 170.7, 155.6, 152.3 (d, *J*<sub>C-F</sub> = 301 Hz), 140.4, 137.0, 133.4, 131.0, 129.7, 129.5, 129.3, 129.2, 128.7, 128.4, 126.7, 126.5, 119.8 (d, *J*<sub>C-F</sub> = 4.0 Hz), 80.5, 58.8, 56.2, 44.7 (d, *J*<sub>C-F</sub> = 1.6 Hz), 38.1, 35.6, 31.7, 28.4, 21.2.

(*S*)-1-(((*S*,*E*)-1-Fluoro-5-phenyl-1-(phenylsulfonyl)pent-1-en-3-yl)amino)-1-oxo-3-phenylpropan-2-aminium Chloride (**27**). Synthesized by following procedure F with 0.21 g of compound **18** in 10 mL 4 M HCl/dioxane. Yield: 0.19 g (99%). The crude product was used without further purification and characterization for the next step.

(*S*)-1-(((*S*,*E*)-1-Fluoro-1-(phenoxysulfonyl)-5-phenylpent-1-en-3-yl)amino)-1-oxo-3-phenylpropan-2-aminium Chloride (**28**). Synthesized by following procedure F with 0.20 g of compound **19** in 8 mL 4 M HCl/dioxane. Yield: 0.18 g (99%). The crude product was used without further purification and characterization for the next step.

(*S*)-1-(((*S*,*Z*)-1-Fluoro-1-(phenoxysulfonyl)-5-phenylpent-1-en-3-yl)amino)-1-oxo-3-phenylpropan-2-aminium Chloride (**28**-(*Z*)). Synthesized by following procedure F with 0.15 g of compound **19**

(*Z*) in 8 mL 4 M HCl/dioxane. Yield: 0.13 g (99%). The crude product was used without further purification and characterization for the next step.

(*S*)-1-(((*S*,*E*)-1-(Benzylsulfonyl)-1-fluoro-5-phenylpent-1-en-3-yl)amino)-1-oxo-3-phenylpropan-2-aminium Chloride (**29**). Synthesized by following procedure F with 0.30 g of compound **20** in 10 mL 4 M HCl/dioxane. Yield: 0.26 g (99%). The crude product was used without further purification and characterization for the next step.

(*S*)-1-(((*S*,*E*)-1-Fluoro-5-phenyl-1-(phenylsulfonyl)pent-1-en-3-yl)amino)-1-oxo-3-(*m*-tolyl)propan-2-aminium Chloride (**30**). Synthesized by following procedure F with 0.28 g of compound **21** in 8 mL 4 M HCl/dioxane. Yield: 0.25 g (99%). The crude product was used without further purification and characterization for the next step.

(*S*)-1-(((*S*,*E*)-1-Fluoro-1-(phenoxysulfonyl)-5-phenylpent-1-en-3-yl)amino)-1-oxo-3-(*m*-tolyl)propan-2-aminium Chloride (**31**). Synthesized by following procedure F with 0.34 g of compound **22** in 10 mL 4 M HCl/dioxane. Yield: 0.30 g (99%). The crude product was used without further purification and characterization for the next step.

(*S*)-1-(((*S*,*E*)-1-(Benzylsulfonyl)-1-fluoro-5-phenylpent-1-en-3-yl)amino)-1-oxo-3-(*m*-tolyl)propan-2-aminium Chloride (**32**). Synthesized by following procedure F with 0.28 g of compound **23** in 8 mL 4 M HCl/dioxane. Yield: 0.25 g (99%). The crude product was used without further purification and characterization for the next step.

(*S*)-1-(((*S*,*E*)-1-Fluoro-5-phenyl-1-(phenylsulfonyl)pent-1-en-3-yl)amino)-1-oxo-3-(*p*-tolyl)propan-2-aminium Chloride (**33**). Synthesized by following procedure F with 0.25 g of compound **24** in 8 mL 4 M HCl/dioxane. Yield: 0.22 g (99%). The crude product was used without further purification and characterization for the next step.

(*S*)-1-(((*S*,*E*)-1-Fluoro-1-(phenoxysulfonyl)-5-phenylpent-1-en-3-yl)amino)-1-oxo-3-(*p*-tolyl)propan-2-aminium Chloride (**34**). Synthesized by following procedure F with 0.39 g of compound **25** in 10 mL 4 M HCl/dioxane. Yield: 0.34 g (99%). The crude product was used without further purification and characterization for the next step.

(*S*)-1-Oxo-1-(((*S*,*E*)-1-(phenoxysulfonyl)-5-phenylpent-1-en-3-yl)amino)-3-(*p*-tolyl)propan-2-aminium Chloride (**34**-(*H*)). Synthesized by following procedure F with 0.20 g of compound **25**-(*H*) in 4 mL 4 M HCl/dioxane. Yield: 0.15 g (89%), colorless solid. <sup>1</sup>H NMR (300 MHz, DMSO-*d*<sub>6</sub>): δ 9.06 (d, *J* = 8.4 Hz, 1H), 8.57 (s, 3H), 7.48–7.38 (m, 2H), 7.37–7.21 (m, 5H), 7.20–6.97 (m, 7H), 6.58 (dd, *J* = 15.3, 4.4 Hz, 1H), 6.21 (dt, *J* = 15.3, 2.1 Hz, 1H), 4.46 (s, 1H), 4.17 (s, 1H), 3.17–2.94 (m, 2H), 2.63–2.50 (m, 2H), 2.23 (d, *J* = 2.7 Hz, 3H), 1.82–1.62 (m, 2H). <sup>13</sup>C NMR (75 MHz, DMSO-*d*<sub>6</sub>): δ 167.8, 150.5, 149.1, 141.1, 136.4, 131.7, 130.0, 129.2 (d, *J* = 5.5 Hz), 128.3 (d, *J* = 6.1 Hz), 127.4, 125.9, 123.4, 122.6, 53.5, 49.2, 34.3, 31.1, 20.7.

(*S*)-1-(((*S*,*E*)-1-(Benzylsulfonyl)-1-fluoro-5-phenylpent-1-en-3-yl)amino)-1-oxo-3-(*p*-tolyl)propan-2-aminium Chloride (**35**). Synthesized by following procedure F with 0.29 g of compound **26** in 10 mL 4 M HCl/dioxane. Yield: 0.26 g (99%). The crude product was used without further purification and characterization for the next step.

Phenyl (*S*,*E*)-1-Fluoro-3-((*S*)-2-(isonicotinamido)-3-phenylpropanamido)-5-phenylpent-1-ene-1-sulfonate (**2a**). Synthesized by following procedure E with 0.14 g of compound **14**, 0.10 g compound **X**, 0.13 g TBTU, 0.062 g HOBt, and 0.21 mL DIEA. Column chromatography: petroleum ether/EtOAc 1:3 to 0:1. Yield: 0.16 g (73%), colorless solid. mp 71–73 °C. <sup>1</sup>H NMR (300 MHz, CDCl<sub>3</sub>): δ 8.70 (d, *J* = 5.9 Hz, 2H), 7.64 (d, *J* = 6.0 Hz, 2H), 7.51 (d, *J* = 7.6 Hz, 1H), 7.45–7.34 (m, 2H), 7.34–7.11 (m, 9H), 7.12–7.02 (m, 2H), 6.97 (d, *J* = 6.6 Hz, 2H), 6.22 (d, *J* = 7.6 Hz, 1H), 5.61 (dd, *J*<sub>H-F</sub> = 31.0 Hz, *J*<sub>H-H</sub> = 9.2 Hz, 1H), 4.80–4.62 (m, 2H), 3.22 (dd, *J* = 13.3, 6.2 Hz, 1H), 2.96 (dd, *J* = 13.3, 9.0 Hz, 1H), 2.52–2.27 (m, 2H), 1.82–1.55 (m, 2H). <sup>13</sup>C NMR (75 MHz, CDCl<sub>3</sub>): δ 170.2, 164.8, 149.3, 149.2 (d, *J*<sub>C-F</sub> = 297 Hz), 147.2, 142.1, 139.9, 136.0, 130.3, 129.3, 129.1, 128.8, 128.3, 128.1, 127.7, 126.6, 122.4, 121.8, 120.94 (d, *J*<sub>C-F</sub> = 4.8 Hz), 55.7, 44.9 (d, *J*<sub>C-F</sub> = 1.9 Hz), 38.9, 35.3, 31.7. mp 71–73 °C. LC–MS (ESI, *m/z*): [*M* + *H*]<sup>+</sup> calcd for C<sub>32</sub>H<sub>30</sub>FN<sub>3</sub>O<sub>5</sub>S, 588.20; found, 588.3. Purity: 97%. [*α*]<sub>D</sub><sup>25</sup> 10° (c 0.5, CHCl<sub>3</sub>).

Phenyl (*S*,*Z*)-1-Fluoro-3-((*S*)-2-(isonicotinamido)-3-phenylpropanamido)-5-phenylpent-1-ene-1-sulfonate (**2a**-(*Z*)). Synthesized by following procedure E with 0.10 g of compound **14**-(*Z*), 0.073 g compound **X**, 0.086 g TBTU, 0.041 g HOBt, and 0.14 mL DIEA. Column chromatography: petroleum ether/EtOAc 1:3. Yield: 0.12 g

(79%), colorless solid.  $^1\text{H}$  NMR (300 MHz,  $\text{CDCl}_3$ ):  $\delta$  8.65 (d,  $J = 5.5$  Hz, 2H), 7.85 (d,  $J = 7.4$  Hz, 1H), 7.60 (d,  $J = 5.3$  Hz, 2H), 7.44–7.07 (m, 14H), 6.98–6.83 (m, 2H), 6.38 (d,  $J = 7.2$  Hz, 1H), 5.58 (dd,  $J_{\text{H-F}} = 20.5$  Hz,  $J_{\text{H-H}} = 10.1$  Hz, 1H), 4.96 (dt,  $J = 14.8$ , 6.6 Hz, 1H), 4.77 (q,  $J = 7.7$  Hz, 1H), 3.24 (dd,  $J = 13.5$ , 6.6 Hz, 1H), 3.08 (dd,  $J = 13.4$ , 8.7 Hz, 1H), 2.37–2.22 (m, 1H), 2.20–2.08 (m, 1H), 1.69–1.52 (m, 1H), 1.43–1.32 (m, 1H).  $^{13}\text{C}$  NMR (75 MHz,  $\text{CDCl}_3$ ):  $\delta$  170.7, 164.9, 149.3, 149.1, 148.25 (d,  $J_{\text{C-F}} = 290$  Hz), 141.9, 140.3, 136.4, 130.2, 129.5, 129.0, 128.6, 128.7, 128.2, 127.5, 126.4, 122.5 (d,  $J_{\text{C-F}} = 11.4$  Hz), 122.3, 121.8, 55.8, 45.9 (d,  $J_{\text{C-F}} = 5.5$  Hz), 38.6, 35.8 (d,  $J_{\text{C-F}} = 2.3$  Hz), 31.6. mp 173–175 °C. LC–MS (ESI,  $m/z$ ):  $[\text{M} + \text{H}]^+$  calcd for  $\text{C}_{32}\text{H}_{30}\text{FN}_3\text{O}_5\text{S}$ , 588.20; found, 588.3. Purity: 95%.  $[\alpha]_{\text{D}}^{22}$  13° (c 0.5,  $\text{CHCl}_3$ ).

**Phenyl (S,E)-3-((S)-2-(2,3-Dihydrobenzo[b][1,4]dioxine-6-carboxamido)-3-phenylpropanamido)-1-fluoro-5-phenylpent-1-ene-1-sulfonate (2b).** Synthesized by following procedure D with 0.10 g of compound 28, 0.035 g 1,4-benzodioxane-6-carboxylic acid, 0.062 g TBTU, and 0.10 mL DIEA. Column chromatography: petroleum ether/EtOAc 2:1. Yield: 0.088 g (71%), colorless solid.  $^1\text{H}$  NMR (300 MHz,  $\text{CDCl}_3$ ):  $\delta$  7.46–7.35 (m, 2H), 7.35–7.10 (m, 11H), 7.04 (d,  $J = 6.5$  Hz, 2H), 6.96–6.80 (m, 4H), 6.60 (d,  $J = 7.4$  Hz, 1H), 5.60 (dd,  $J_{\text{H-F}} = 31.0$  Hz,  $J_{\text{H-H}} = 9.0$  Hz, 1H), 4.82 (q,  $J = 7.4$  Hz, 1H), 4.67 (quint,  $J = 7.8$  Hz, 1H), 4.34–4.19 (m, 4H), 3.17 (dd,  $J = 13.2$ , 6.2 Hz, 1H), 2.96 (dd,  $J = 13.2$ , 8.6 Hz, 1H), 2.45–2.26 (m, 2H), 1.72–1.52 (m, 2H).  $^{13}\text{C}$  NMR (75 MHz,  $\text{CDCl}_3$ ):  $\delta$  170.9, 167.0, 149.4, 149.0 (d,  $J_{\text{C-F}} = 297$  Hz), 147.0, 143.6, 140.1, 136.3, 130.2, 129.4, 129.0, 128.6, 128.3, 128.0, 127.4, 126.4, 122.4, 121.4 (d,  $J_{\text{C-F}} = 4.4$  Hz), 120.7, 117.5, 116.8, 64.7, 64.3, 55.2, 44.8 (d,  $J_{\text{C-F}} = 2.0$  Hz), 38.9, 35.2 (d,  $J_{\text{C-F}} = 1.5$  Hz), 31.6. mp 167–168 °C. LC–MS (ESI,  $m/z$ ):  $[\text{M} + \text{H}]^+$  calcd for  $\text{C}_{35}\text{H}_{33}\text{FN}_2\text{O}_7\text{S}$ , 645.2; found, 645.3. Purity: 98%.  $[\alpha]_{\text{D}}^{22}$  12° (c 1,  $\text{CHCl}_3$ ).

**Phenyl (S,E)-1-Fluoro-3-((S)-2-(isonicotinamido)-3-(p-tolyl)propanamido)-5-phenylpent-1-ene-1-sulfonate (2d).** Synthesized by following procedure D with 0.12 g of compound 34, 0.028 g isonicotinic acid, 0.073 g TBTU, and 0.12 mL DIEA. Column chromatography: petroleum ether/EtOAc 1:3. Yield: 0.10 g (77%), colorless solid.  $^1\text{H}$  NMR (300 MHz,  $\text{CDCl}_3$ ):  $\delta$  8.69 (d,  $J = 3.5$  Hz, 2H), 7.56 (d,  $J = 3.5$  Hz, 2H), 7.44–7.36 (m, 3H), 7.36–7.12 (m, 7H), 7.06 (d,  $J = 7.7$  Hz, 2H), 7.01–6.88 (m, 4H), 6.29 (d,  $J = 7.7$  Hz, 1H), 5.62 (dd,  $J_{\text{H-F}} = 31.0$  Hz,  $J_{\text{H-H}} = 9.1$  Hz, 1H), 4.81–4.63 (m, 2H), 3.16 (dd,  $J = 13.4$ , 5.7 Hz, 1H), 2.92 (dd,  $J = 12.9$ , 9.6 Hz, 1H), 2.47–2.30 (m, 2H), 2.27 (s, 3H), 1.80–1.56 (m, 3H).  $^{13}\text{C}$  NMR (75 MHz,  $\text{CDCl}_3$ ):  $\delta$  170.3, 165.3, 150.4, 149.3, 149.2 (d,  $J_{\text{C-F}} = 297$  Hz), 141.0, 139.9, 137.4, 132.8, 130.2, 129.8, 129.2, 128.8, 128.2, 128.1, 126.6, 122.4, 121.2, 120.9 (d,  $J_{\text{C-F}} = 5.2$  Hz), 55.6, 44.8 (d,  $J_{\text{C-F}} = 1.6$  Hz), 38.6, 35.4, 31.6, 21.1. mp 78–79 °C. LC–MS (ESI,  $m/z$ ):  $[\text{M} + \text{H}]^+$  calcd for  $\text{C}_{33}\text{H}_{32}\text{FN}_3\text{O}_5\text{S}$ , 602.21; found, 602.3. Purity: 97%.  $[\alpha]_{\text{D}}^{22}$  8° (c 0.5, MeOH).

**Phenyl (S,E)-3-((S)-2-(isonicotinamido)-3-((p-tolyl)propanamido)-5-phenylpent-1-ene-1-sulfonate (2d-(H)).** Synthesized by following procedure D with 0.21 g of compound 34-(H), 0.054 g isonicotinic acid, 0.014 g TBTU, and 0.28 mL DIEA. Column chromatography: cyclohexane/EtOAc 1:3. Yield: 0.080 g (35%), colorless solid.  $^1\text{H}$  NMR (300 MHz,  $\text{CDCl}_3$ ):  $\delta$  8.71 (d,  $J = 13.0$  Hz, 2H), 7.65 (d,  $J = 21.2$  Hz, 2H), 7.52–7.41 (m, 1H), 7.42–7.32 (m, 1H), 7.32–7.23 (m, 3H), 7.22–7.15 (m, 4H), 7.15–7.03 (m, 2H), 7.02–6.90 (m, 2H), 6.71–6.59 (m, 1H), 6.51 (dd,  $J = 15.2$ , 5.1 Hz, 1H), 6.32 (d,  $J = 7.7$  Hz, 1H), 5.99 (dd,  $J = 15.2$ , 1.5 Hz, 1H), 4.92–4.73 (m, 1H), 4.53 (s, 1H), 3.29–3.13 (m, 1H), 3.07 (dd,  $J = 13.5$ , 8.9 Hz, 1H), 2.60–2.40 (m, 2H), 2.32 (s, 3H), 1.83–1.58 (m, 3H).  $^{13}\text{C}$  NMR (75 MHz,  $\text{CDCl}_3$ ):  $\delta$  170.5, 164.5, 149.4, 148.7, 139.9, 137.6, 132.7, 129.9, 129.1, 128.7, 128.3, 127.4, 126.5, 124.6, 122.5, 126.6, 55.9, 49.6, 35.1, 31.7, 21.1. mp 84–86 °C. LC–MS (ESI,  $m/z$ ):  $[\text{M} + \text{H}]^+$  calcd for  $\text{C}_{33}\text{H}_{33}\text{N}_3\text{O}_5\text{S}$ , 584.21; found, 584.3. Purity: 98%.  $[\alpha]_{\text{D}}^{22}$  11° (c 0.5, MeOH).

**Phenyl (S,E)-3-((S)-2-(2,3-Dihydrobenzo[b][1,4]dioxine-6-carboxamido)-3-(p-tolyl)propanamido)-1-fluoro-5-phenylpent-1-ene-1-sulfonate (2e).** Synthesized by following procedure D with 0.100 g of compound 34, 0.034 g 1,4-benzodioxane-6-carboxylic acid, 0.060 g TBTU, and 0.10 mL DIEA. Column chromatography: petroleum

ether/EtOAc 2:1. Yield: 0.094 g (78%), colorless solid.  $^1\text{H}$  NMR (300 MHz,  $\text{CDCl}_3$ ):  $\delta$  7.46–7.35 (m, 2H), 7.34–7.23 (m, 5H), 7.23–7.12 (m, 4H), 7.03 (d,  $J = 7.9$  Hz, 2H), 6.97–6.88 (m, 4H), 6.88–6.78 (m, 2H), 6.58 (d,  $J = 7.7$  Hz, 1H), 5.61 (dd,  $J_{\text{H-F}} = 31.2$  Hz,  $J_{\text{H-H}} = 9.1$  Hz, 1H), 4.85–4.60 (m, 2H), 4.34–4.20 (m, 4H), 3.12 (dd,  $J = 13.3$ , 6.1 Hz, 1H), 2.91 (dd,  $J = 13.3$ , 8.6 Hz, 1H), 2.44–2.30 (m, 2H), 2.26 (s, 3H), 1.72–1.55 (m, 2H).  $^{13}\text{C}$  NMR (75 MHz,  $\text{CDCl}_3$ ):  $\delta$  170.9, 166.8, 149.4, 148.9 (d,  $J_{\text{C-F}} = 296$  Hz), 147.1, 143.6, 140.1, 137.1, 133.2, 130.2, 129.6, 129.3, 128.6, 128.3, 128.0, 126.4, 122.4, 121.5 (d,  $J_{\text{C-F}} = 4.6$  Hz), 120.6, 117.5, 116.8, 64.7, 64.3, 55.3, 44.7 (d,  $J_{\text{C-F}} = 1.7$  Hz), 38.5, 35.3, 31.6, 21.1. mp 92–93 °C. LC–MS (ESI,  $m/z$ ):  $[\text{M} + \text{H}]^+$  calcd for  $\text{C}_{36}\text{H}_{35}\text{FN}_2\text{O}_7\text{S}$ , 659.22; found, 659.3. Purity: 95%.  $[\alpha]_{\text{D}}^{22}$  26° (c 1, MeOH).

**Phenyl (S,E)-3-((S)-2-(3,5-Difluorobenzamido)-3-(p-tolyl)propanamido)-1-fluoro-5-phenylpent-1-ene-1-sulfonate (2f).** Synthesized by following procedure D with 0.10 g of compound 34, 0.030 g 3,5-difluorobenzoic acid, 0.060 g TBTU, and 0.10 mL DIEA. Column chromatography: petroleum ether/EtOAc 3:1. Yield: 0.097 g (81%), colorless solid.  $^1\text{H}$  NMR (300 MHz,  $\text{CDCl}_3$ ):  $\delta$  7.46–7.10 (m, 12H), 7.04 (d,  $J = 7.8$  Hz, 2H), 6.99–6.84 (m, 5H), 6.23 (d,  $J = 7.7$  Hz, 1H), 5.58 (dd,  $J_{\text{H-F}} = 31.0$  Hz,  $J_{\text{H-H}} = 9.2$  Hz, 1H), 4.80–4.60 (m, 2H), 3.15 (dd,  $J = 13.3$ , 6.0 Hz, 1H), 2.91 (dd,  $J = 13.3$ , 9.1 Hz, 1H), 2.49–2.31 (m, 2H), 2.26 (s, 3H), 1.73–1.56 (m, 2H).  $^{13}\text{C}$  NMR (75 MHz,  $\text{CDCl}_3$ ):  $\delta$  170.6, 164.9 (t,  $J_{\text{C-F}} = 2.6$  Hz), 163.0 (dd,  $J_{\text{C-F}} = 251$ , 12 Hz), 149.3, 149.2 (d,  $J_{\text{C-F}} = 297$  Hz), 140.0, 137.4, 136.8 (t,  $J_{\text{C-F}} = 8.5$  Hz), 132.9, 130.2, 129.8, 129.2, 128.7, 128.3, 128.1, 126.6, 122.4, 121.0 (d,  $J = 5.0$  Hz), 110.5 (dd,  $J_{\text{C-F}} = 26.2$ , 8.8 Hz), 107.4 (t,  $J_{\text{C-F}} = 25.4$  Hz), 55.8, 44.9 (d,  $J_{\text{C-F}} = 2.4$  Hz), 38.5, 35.4 (d,  $J_{\text{C-F}} = 1.6$  Hz), 31.7, 21.1. mp 175–177 °C. LC–MS (ESI,  $m/z$ ):  $[\text{M} + \text{H}]^+$  calcd for  $\text{C}_{34}\text{H}_{31}\text{F}_2\text{N}_2\text{O}_7\text{S}$ , 637.20; found, 637.2. Purity: >99%.  $[\alpha]_{\text{D}}^{22}$  7° (c 0.5,  $\text{CHCl}_3$ ).

**Phenyl (S,E)-1-Fluoro-3-((S)-2-(isonicotinamido)-3-(m-tolyl)propanamido)-5-phenylpent-1-ene-1-sulfonate (2g).** Synthesized by following procedure D with 0.11 g of compound 31, 0.026 g isonicotinic acid, 0.067 g TBTU, and 0.11 mL DIEA. Column chromatography: petroleum ether/EtOAc 1:3. Yield: 0.096 g (77%), colorless solid.  $^1\text{H}$  NMR (300 MHz,  $\text{CDCl}_3$ ):  $\delta$  8.62 (d,  $J = 4.6$  Hz, 2H), 7.49 (d,  $J = 4.0$  Hz, 2H), 7.39–7.03 (m, 11H), 6.97 (d,  $J = 7.3$  Hz, 1H), 6.94–6.81 (m, 3H), 6.74 (d,  $J = 7.3$  Hz, 1H), 6.10 (d,  $J = 7.5$  Hz, 1H), 5.57 (dd,  $J_{\text{H-F}} = 31.0$  Hz,  $J_{\text{H-H}} = 9.1$  Hz, 1H), 4.74–4.50 (m, 2H), 3.11 (dd,  $J = 13.1$ , 5.7 Hz, 1H), 2.88–2.78 (m, 1H), 2.39–2.21 (m, 2H), 2.17 (s, 3H), 1.72–1.49 (m, 2H).  $^{13}\text{C}$  NMR (75 MHz,  $\text{CDCl}_3$ ):  $\delta$  170.2, 165.3, 150.3, 149.33, 149.25 (d,  $J_{\text{C-F}} = 297$  Hz), 147.3, 141.2, 139.9, 138.9, 136.0, 130.2, 130.0, 129.0, 128.8, 128.5, 128.2, 128.1, 126.6, 126.4, 122.4, 121.2, 120.9 (d,  $J_{\text{C-F}} = 5.0$  Hz), 55.5, 45.0 (d,  $J_{\text{C-F}} = 2.0$  Hz), 38.9, 35.4, 31.6, 21.4. mp 67–68 °C. LC–MS (ESI,  $m/z$ ):  $[\text{M} + \text{H}]^+$  calcd for  $\text{C}_{33}\text{H}_{32}\text{FN}_3\text{O}_5\text{S}$ , 602.21; found, 602.3. Purity: >99%.  $[\alpha]_{\text{D}}^{22}$  8° (c 0.5,  $\text{CHCl}_3$ ).

**Phenyl (S,E)-3-((S)-2-(2,3-Dihydrobenzo[b][1,4]dioxine-6-carboxamido)-3-(m-tolyl)propanamido)-1-fluoro-5-phenylpent-1-ene-1-sulfonate (2h).** Synthesized by following procedure D with 0.10 g of compound 31, 0.034 g 1,4-benzodioxane-6-carboxylic acid, 0.060 g TBTU, and 0.10 mL DIEA. Column chromatography: petroleum ether/EtOAc 2:1. Yield: 0.088 g (72%), colorless solid.  $^1\text{H}$  NMR (300 MHz,  $\text{CDCl}_3$ ):  $\delta$  7.37–7.27 (m, 2H), 7.27–6.99 (m, 10H), 6.94 (d,  $J = 7.7$  Hz, 1H), 6.91–6.80 (m, 3H), 6.80–6.70 (m, 3H), 6.52 (d,  $J = 7.7$  Hz, 1H), 5.57 (dd,  $J_{\text{H-F}} = 31.1$  Hz,  $J_{\text{H-H}} = 9.1$  Hz, 1H), 4.73 (q,  $J = 7.9$  Hz, 1H), 4.59 (quint,  $J = 7.6$  Hz, 1H), 4.26–4.09 (m, 4H), 3.07 (dd,  $J = 13.4$ , 6.3 Hz, 1H), 2.85 (dd,  $J = 13.4$ , 8.5 Hz, 1H), 2.38–2.19 (m, 2H), 2.15 (s, 3H), 1.65–1.46 (m, 2H).  $^{13}\text{C}$  NMR (75 MHz,  $\text{CDCl}_3$ ):  $\delta$  170.9, 166.9, 149.4, 149.0 (d,  $J_{\text{C-F}} = 297$  Hz), 147.1, 143.6, 140.1, 138.7, 136.3, 130.2, 130.1, 128.8, 128.6, 128.3, 128.2, 128.0, 126.8, 126.5, 126.4, 122.4, 121.4 (d,  $J_{\text{C-F}} = 3.6$  Hz), 120.6, 117.5, 116.8, 64.7, 64.3, 55.2, 44.9 (d,  $J_{\text{C-F}} = 1.1$  Hz), 38.8, 35.3, 31.6, 21.4. mp 126–128 °C. LC–MS (ESI,  $m/z$ ):  $[\text{M} + \text{H}]^+$  calcd for  $\text{C}_{36}\text{H}_{35}\text{FN}_2\text{O}_7\text{S}$ , 659.22; found, 659.3. Purity: 98%.  $[\alpha]_{\text{D}}^{22}$  3° (c 0.5, MeOH).

**Phenyl (S,E)-3-((S)-2-(3,5-Difluorobenzamido)-3-(m-tolyl)propanamido)-1-fluoro-5-phenylpent-1-ene-1-sulfonate (2i).** Synthesized by following procedure D with 0.10 g of compound 31, 0.030 g 3,5-difluorobenzoic acid, 0.060 g TBTU, and 0.10 mL DIEA. Column



chromatography: petroleum ether/EtOAc 3:1. Yield: 0.075 g (62%), colorless solid.  $^1\text{H}$  NMR (300 MHz,  $\text{CDCl}_3$ ):  $\delta$  7.36–7.27 (m, 2H), 7.28–7.03 (m, 10H), 7.03–6.94 (m, 2H), 6.94–6.80 (m, 4H), 6.74 (d,  $J = 7.4$  Hz, 1H), 5.82 (d,  $J = 7.7$  Hz, 1H), 5.54 (dd,  $J_{\text{H-F}} = 30.9$  Hz,  $J_{\text{H-H}} = 9.1$  Hz, 1H), 4.68–4.52 (m, 2H), 3.10 (dd,  $J = 13.4, 6.0$  Hz, 1H), 2.80 (dd,  $J = 13.3, 9.1$  Hz, 1H), 2.41–2.21 (m,  $J = 7.2$  Hz, 2H), 2.19 (s, 3H), 1.68–1.57 (m, 2H).  $^{13}\text{C}$  NMR (75 MHz,  $\text{CDCl}_3$ ):  $\delta$  170.3, 165.0 (t,  $J_{\text{C-F}} = 2.7$  Hz), 163.0 (dd,  $J_{\text{C-F}} = 25.1, 12$  Hz), 149.4, 149.3 (d,  $J_{\text{C-F}} = 298$  Hz), 139.9, 139.0, 137.0, 136.9, 136.8, 136.1, 130.2, 130.0, 129.1, 128.8, 128.5, 128.3, 128.1, 126.6, 126.4, 122.4, 120.9 (d,  $J_{\text{C-F}} = 5.0$  Hz), 110.5 (dd,  $J_{\text{C-F}} = 26, 8.7$  Hz), 107.5 (t,  $J_{\text{C-F}} = 25$  Hz), 55.6, 45.0 (d,  $J_{\text{C-F}} = 2.3$  Hz), 38.8, 35.4, 31.6, 21.4. mp 129–130 °C. LC–MS (ESI,  $m/z$ ):  $[\text{M} + \text{H}]^+$  calcd for  $\text{C}_{34}\text{H}_{31}\text{F}_3\text{N}_2\text{O}_5\text{S}$ , 637.20; found, 637.3. Purity: 96%.  $[\alpha]_{\text{D}}^{22} 9^\circ$  (c 0.5, MeOH).

**Phenyl (S,E)-3-((S)-2-(((Benzylloxy)carbonyl)amino)-3-phenylpropanamido)-1-fluoro-5-phenylpent-1-ene-1-sulfonate (2j)**. Synthesized by following procedure E with 0.090 g of compound 14, 0.076 g Cbz-L-Phe-OH, 0.082 g TBTU, 0.039 g HOBt, and 0.13 mL DIEA. Column chromatography: petroleum ether/EtOAc 2:1. Yield: 0.12 g (78%), colorless solid.  $^1\text{H}$  NMR (300 MHz,  $\text{CDCl}_3$ ):  $\delta$  7.48–7.14 (m, 17H), 7.06–6.92 (m, 4H), 5.56 (dd,  $J_{\text{H-F}} = 31.1$  Hz,  $J_{\text{H-H}} = 9.0$  Hz, 2H), 5.32 (d,  $J = 5.7$  Hz, 1H), 5.06 (s, 2H), 4.68 (quint,  $J = 7.5$  Hz, 1H), 4.22 (d,  $J = 6.6$  Hz, 1H), 3.07 (dd,  $J = 13.4, 6.0$  Hz, 1H), 2.83 (dd,  $J = 13.4, 8.6$  Hz, 1H), 2.52–2.30 (m, 2H), 1.80–1.64 (m, 2H).  $^{13}\text{C}$  NMR (75 MHz,  $\text{CDCl}_3$ ):  $\delta$  170.3, 156.4, 149.4, 149.0 (d,  $J_{\text{C-F}} = 297$  Hz), 140.1, 136.2, 136.1, 130.2, 129.3, 129.1, 128.8, 128.7, 128.5, 128.3, 128.2, 128.0, 127.5, 126.6, 122.5, 121.1 (d,  $J_{\text{C-F}} = 4.6$  Hz), 67.4, 56.6, 44.9 (d,  $J_{\text{C-F}} = 1.1$  Hz), 38.9, 35.2, 31.7. mp 127–128 °C. LC–MS (ESI,  $m/z$ ):  $[\text{M} + \text{H}]^+$  calcd for  $\text{C}_{34}\text{H}_{33}\text{FN}_2\text{O}_6\text{S}$ , 617.21; found, 617.4. Purity: >99%.  $[\alpha]_{\text{D}}^{22} 17^\circ$  (c 0.5,  $\text{CHCl}_3$ ).

**Phenyl (S,E)-1-Fluoro-3-((S)-2-(4-methylpiperazine-1-carboxamido)-3-phenylpropanamido)-5-phenylpent-1-ene-1-sulfonate (2k)**. Synthesized by following procedure E with 0.11 g of compound 14, 0.086 g compound IX, 0.095 g TBTU, and 0.155 mL DIEA. Column chromatography: DCM/MeOH 95:5. Yield: 0.096 g (59%), colorless solid.  $^1\text{H}$  NMR (300 MHz,  $\text{CDCl}_3$ ):  $\delta$  7.45–7.35 (m, 2H), 7.35–7.14 (m, 10H), 7.06–6.93 (m, 4H), 6.62 (d,  $J = 7.6$  Hz, 1H), 5.62 (dd,  $J_{\text{H-F}} = 31.2$  Hz,  $J_{\text{H-H}} = 9.1$  Hz, 1H), 5.21 (d,  $J = 7.6$  Hz, 1H), 4.66 (quint,  $J = 7.7$  Hz, 1H), 4.45 (q,  $J = 7.9$  Hz, 1H), 3.42–3.24 (m, 4H), 3.05 (dd,  $J = 13.4, 6.5$  Hz, 1H), 2.88 (dd,  $J = 13.4, 8.4$  Hz, 1H), 2.49–2.33 (m, 6H), 2.31 (s, 3H), 1.78–1.52 (m, 3H).  $^{13}\text{C}$  NMR (75 MHz,  $\text{CDCl}_3$ ):  $\delta$  171.8, 156.9, 149.4, 148.9 (d,  $J_{\text{C-F}} = 297$  Hz), 140.2, 136.8, 130.2, 129.4, 128.9, 128.7, 128.4, 128.0, 127.3, 126.5, 122.4, 121.5 (d,  $J_{\text{C-F}} = 5.1$  Hz), 56.1, 54.4, 45.9, 44.7, 43.6, 39.1, 35.4, 31.6. mp 109–110 °C. LC–MS (ESI,  $m/z$ ):  $[\text{M} + \text{H}]^+$  calcd for  $\text{C}_{32}\text{H}_{37}\text{FN}_4\text{O}_5\text{S}$ , 608.26; found, 609.3. Purity: >99%.  $[\alpha]_{\text{D}}^{22} 10^\circ$  (c 0.5,  $\text{CHCl}_3$ ).

**N-((S)-1-(((S,E)-1-(Benzylsulfonyl)-1-fluoro-5-phenylpent-1-en-3-yl)amino)-1-oxo-3-phenylpropan-2-yl)isonicotinamide (3a)**. Synthesized by following procedure E with 0.11 g of compound 15, 0.080 g compound X, 0.095 g TBTU, 0.045 g HOBt, and 0.155 mL DIEA. Column chromatography: pure EtOAc. Yield: 0.14 g (81%), colorless solid.  $^1\text{H}$  NMR (300 MHz,  $\text{DMSO}-d_6$ ):  $\delta$  8.97 (d,  $J = 7.9$  Hz, 1H), 8.71 (d,  $J = 4.4$  Hz, 2H), 8.35 (d,  $J = 7.8$  Hz, 1H), 7.70 (d,  $J = 4.4$  Hz, 2H), 7.44–7.08 (m, 15H), 5.81 (dd,  $J_{\text{H-F}} = 34.1$  Hz,  $J_{\text{H-H}} = 8.8$  Hz, 1H), 4.75 (s, 2H), 4.70–4.50 (m, 2H), 3.19–2.87 (m, 2H), 2.49–2.39 (m, 3H), 1.86–1.56 (m, 2H).  $^{13}\text{C}$  NMR (75 MHz,  $\text{DMSO}$ ):  $\delta$  170.4, 164.8, 151.4 (d,  $J_{\text{C-F}} = 298$  Hz), 150.2, 140.9, 140.9, 137.9, 131.0, 129.1, 128.8, 128.6, 128.30, 128.29, 128.1, 127.5, 126.4, 125.9, 121.4, 120.4 (d,  $J_{\text{C-F}} = 3.8$  Hz), 57.6, 55.0, 43.7 (d,  $J_{\text{C-F}} = 2.0$  Hz), 37.0, 35.0, 30.9. mp 169–171 °C. LC–MS (ESI,  $m/z$ ):  $[\text{M} + \text{H}]^+$  calcd for  $\text{C}_{33}\text{H}_{32}\text{FN}_3\text{O}_4\text{S}$ , 586.22; found, 586.4. Purity: 96%.  $[\alpha]_{\text{D}}^{22} 9^\circ$  (c 0.5, MeOH).

**N-((S)-1-(((S,E)-1-(Benzylsulfonyl)-1-fluoro-5-phenylpent-1-en-3-yl)amino)-1-oxo-3-phenylpropan-2-yl)-2,3-dihydrobenzo[b][1,4]-dioxine-6-carboxamide (3b)**. Synthesized by following procedure D with 0.100 g of compound 29, 0.036 g 1,4-benzodioxane-6-carboxylic acid, 0.064 g TBTU, and 0.104 mL DIEA. Column chromatography: petroleum ether/EtOAc 2:1 to pure EtOAc. Yield: 0.096 g (75%), colorless solid.  $^1\text{H}$  NMR (300 MHz,  $\text{DMSO}-d_6$ ):  $\delta$  8.44 (d,  $J = 8.1$  Hz, 1H), 8.24 (d,  $J = 8.0$  Hz, 1H), 7.45–7.09 (m, 17H), 6.89 (d,  $J = 8.3$  Hz,

1H), 5.82 (dd,  $J_{\text{H-F}} = 34.2$  Hz,  $J_{\text{H-H}} = 9.0$  Hz, 1H), 4.74 (s, 2H), 4.65–4.47 (m, 2H), 4.34–4.16 (m, 4H), 3.11–2.91 (m, 2H), 2.48–2.35 (m, 2H), 1.87–1.54 (m, 2H).  $^{13}\text{C}$  NMR (75 MHz,  $\text{DMSO}-d_6$ ):  $\delta$  171.0, 165.4, 151.3 (d,  $J_{\text{C-F}} = 297$  Hz), 146.1, 142.8, 140.9, 138.2, 131.0, 129.1, 128.7, 128.6, 128.3, 128.1, 127.5, 127.0, 126.2, 125.9, 120.9, 120.5 (d,  $J_{\text{C-F}} = 3.9$  Hz), 116.6, 116.5, 64.3, 64.0, 57.6, 55.0, 43.6 (d,  $J_{\text{C-F}} = 2.4$  Hz), 36.9, 35.0, 30.9. mp 204–206 °C (decomposition). LC–MS (ESI,  $m/z$ ):  $[\text{M} + \text{H}]^+$  calcd for  $\text{C}_{36}\text{H}_{35}\text{FN}_3\text{O}_6\text{S}$ , 643.23; found, 643.3. Purity: >99%.  $[\alpha]_{\text{D}}^{22} 7^\circ$  (c 0.5,  $\text{CHCl}_3/\text{MeOH}$  1:1).

**N-((S)-1-(((S,E)-1-(Benzylsulfonyl)-1-fluoro-5-phenylpent-1-en-3-yl)amino)-1-oxo-3-phenylpropan-2-yl)-3,5-difluorobenzamide (3c)**. Synthesized by following procedure D with 0.120 g of compound 29, 0.037 g 3,5-difluorobenzoic acid, 0.075 g TBTU, and 0.12 mL DIEA. Column chromatography: petroleum ether/EtOAc 3:1. Yield: 0.094 g (65%), colorless solid.  $^1\text{H}$  NMR (300 MHz,  $\text{DMSO}-d_6$ ):  $\delta$  8.86 (d,  $J = 8.2$  Hz, 1H), 8.35 (d,  $J = 7.9$  Hz, 1H), 7.56–7.41 (m, 3H), 7.41–7.10 (m, 16H), 5.81 (dd,  $J_{\text{H-F}} = 34.2$  Hz,  $J_{\text{H-H}} = 9.1$  Hz, 1H), 4.75 (s, 2H), 4.69–4.51 (m, 2H), 3.09 (dd,  $J = 13.7, 5.1$  Hz, 1H), 2.97 (dd,  $J = 13.7, 10.1$  Hz, 1H), 2.49–2.40 (m, 2H), 1.86–1.57 (m, 2H).  $^{13}\text{C}$  NMR (75 MHz,  $\text{DMSO}-d_6$ ):  $\delta$  170.48, 163.7 (t,  $J_{\text{C-F}} = 2.8$  Hz), 162.2 (dd,  $J_{\text{C-F}} = 25.1, 12$  Hz), 151.4 (d,  $J_{\text{C-F}} = 298$  Hz), 140.9, 137.9, 137.4 (t,  $J_{\text{C-F}} = 8.5$  Hz), 137.3, 131.0, 129.1, 128.8, 128.6, 128.3, 128.1, 127.5, 126.4, 126.0, 120.4 (d,  $J_{\text{C-F}} = 4.1$  Hz), 110.8 (dd,  $J_{\text{C-F}} = 27, 8.7$  Hz), 106.9 (t,  $J_{\text{C-F}} = 26$  Hz), 57.6, 55.2, 43.7 (d,  $J_{\text{C-F}} = 2.3$  Hz), 37.0, 35.0, 30.9. mp 194–196 °C (decomposition). LC–MS (ESI,  $m/z$ ):  $[\text{M} + \text{H}]^+$  calcd for  $\text{C}_{34}\text{H}_{31}\text{F}_3\text{N}_2\text{O}_4\text{S}$ , 621.2; found, 621.3. Purity: >99%.  $[\alpha]_{\text{D}}^{22} 6^\circ$  (c 0.5,  $\text{CHCl}_3$ ).

**N-((S)-1-(((S,E)-1-(Benzylsulfonyl)-1-fluoro-5-phenylpent-1-en-3-yl)amino)-1-oxo-3-(p-tolyl)propan-2-yl)isonicotinamide (3d)**. Synthesized by following procedure D with 0.11 g of compound 35, 0.026 g isonicotinic acid, 0.067 g TBTU, and 0.11 mL DIEA. Column chromatography: petroleum ether/EtOAc 1:3. Yield: 0.091 g (73%), colorless solid.  $^1\text{H}$  NMR (300 MHz,  $\text{CDCl}_3$ ):  $\delta$  8.69 (d,  $J = 6.0$  Hz, 2H), 7.61–7.53 (m, 2H), 7.43–7.28 (m, 6H), 7.25–7.14 (m, 3H), 7.07 (d,  $J = 7.8$  Hz, 2H), 7.01–6.88 (m, 4H), 6.19 (d,  $J = 7.9$  Hz, 1H), 5.55 (dd,  $J_{\text{H-F}} = 32.6$  Hz,  $J_{\text{H-H}} = 9.2$  Hz, 1H), 4.76–4.59 (m, 2H), 4.36 (s, 2H), 3.14 (dd,  $J = 13.5, 6.0$  Hz, 1H), 2.93 (dd,  $J = 13.4, 8.6$  Hz, 1H), 2.44–2.19 (m, 5H), 1.75–1.50 (m, 2H).  $^{13}\text{C}$  NMR (75 MHz,  $\text{CDCl}_3$ ):  $\delta$  170.2, 165.1, 152.5 (d,  $J_{\text{C-F}} = 301$  Hz), 141.3, 140.1, 137.3, 132.8, 131.0, 129.8, 129.5, 129.3, 129.2, 128.7, 128.3, 126.7, 126.5, 121.3, 119.4 (d,  $J_{\text{C-F}} = 4.3$  Hz), 58.7, 55.6, 44.7 (d,  $J_{\text{C-F}} = 2.2$  Hz), 38.4, 35.6 (d,  $J_{\text{C-F}} = 1.6$  Hz), 31.6, 21.2. mp 181–183 °C. LC–MS (ESI,  $m/z$ ):  $[\text{M} + \text{H}]^+$  calcd for  $\text{C}_{34}\text{H}_{34}\text{FN}_3\text{O}_4\text{S}$ , 600.24; found, 600.4. Purity: 95%.  $[\alpha]_{\text{D}}^{22} 13^\circ$  (c 0.5, MeOH).

**N-((S)-1-(((S,E)-1-(Benzylsulfonyl)-1-fluoro-5-phenylpent-1-en-3-yl)amino)-1-oxo-3-(p-tolyl)propan-2-yl)-2,3-dihydrobenzo[b][1,4]-dioxine-6-carboxamide (3e)**. Synthesized by following procedure D with 0.110 g of compound 35, 0.037 g 1,4-benzodioxane-6-carboxylic acid, 0.067 g TBTU, and 0.108 mL DIEA. Column chromatography: petroleum ether/EtOAc 1:1 to 0:1. Yield: 0.10 g (76%), colorless solid.  $^1\text{H}$  NMR (300 MHz,  $\text{DMSO}-d_6$ ):  $\delta$  8.41 (d,  $J = 8.0$  Hz, 1H), 8.23 (d,  $J = 8.0$  Hz, 1H), 7.43–7.23 (m, 9H), 7.23–7.11 (m, 5H), 7.04 (d,  $J = 7.9$  Hz, 2H), 6.89 (d,  $J = 8.4$  Hz, 1H), 5.81 (dd,  $J_{\text{H-F}} = 34.3$  Hz,  $J_{\text{H-H}} = 9.1$  Hz, 1H), 4.74 (s, 2H), 4.63–4.47 (m, 2H), 4.32–4.18 (m, 4H), 3.05–2.87 (m, 2H), 2.49–2.39 (m, 2H), 2.22 (s, 3H), 1.86–1.57 (m, 2H).  $^{13}\text{C}$  NMR (75 MHz,  $\text{DMSO}-d_6$ ):  $\delta$  171.0, 165.4, 151.3 (d,  $J_{\text{C-F}} = 297$  Hz), 146.0, 142.8, 140.9, 135.14, 135.10, 131.0, 129.0, 128.8, 128.7, 128.6, 128.3, 127.5, 127.0, 125.9, 121.0, 120.5 (d,  $J_{\text{C-F}} = 3.7$  Hz), 116.6, 116.5, 64.3, 64.0, 57.6, 55.1, 43.6 (d,  $J_{\text{C-F}} = 1.6$  Hz), 36.6, 35.0, 30.9, 20.6. mp 193–195 °C. LC–MS (ESI,  $m/z$ ):  $[\text{M} + \text{H}]^+$  calcd for  $\text{C}_{37}\text{H}_{37}\text{FN}_2\text{O}_6\text{S}$ , 657.25; found, 657.4. Purity: 97%.  $[\alpha]_{\text{D}}^{22} 8^\circ$  (c 0.5,  $\text{CHCl}_3/\text{MeOH}$  1:1).

**N-((S)-1-(((S,E)-1-(Benzylsulfonyl)-1-fluoro-5-phenylpent-1-en-3-yl)amino)-1-oxo-3-(p-tolyl)propan-2-yl)-3,5-difluorobenzamide (3f)**. Synthesized by following procedure D with 0.12 g of compound 35, 0.036 g 3,5-difluorobenzoic acid, 0.073 g TBTU, and 0.12 mL DIEA. Column chromatography: petroleum ether/EtOAc 3:1 to pure EtOAc. Yield: 0.12 g (81%), colorless solid.  $^1\text{H}$  NMR (300 MHz,  $\text{DMSO}-d_6$ ):  $\delta$  8.82 (d,  $J = 8.1$  Hz, 1H), 8.32 (d,  $J = 8.0$  Hz, 1H), 7.61–7.40 (m, 3H), 7.40–7.23 (m, 8H), 7.23–7.10 (m, 5H), 7.05 (d,  $J = 7.9$

H<sub>2</sub>, 2H), 5.79 (dd,  $J_{\text{H-F}} = 33.9$  Hz,  $J_{\text{H-H}} = 9.3$  Hz, 1H), 4.75 (s, 2H), 4.65–4.48 (m, 2H), 3.02 (dd,  $J = 13.5, 5.1$  Hz, 1H), 2.92 (dd,  $J = 13.6, 10.0$  Hz, 1H), 2.48–2.39 (m, 1H), 2.22 (s, 3H), 1.83–1.56 (m, 2H). <sup>13</sup>C NMR (75 MHz, DMSO-*d*<sub>6</sub>):  $\delta$  170.5, 163.86, 163.7 (t,  $J_{\text{C-F}} = 2.6$  Hz), 162.1 (dd,  $J_{\text{C-F}} = 251, 12$  Hz), 151.3 (d,  $J_{\text{C-F}} = 298$  Hz), 140.9, 137.4 (t,  $J_{\text{C-F}} = 8.4$  Hz), 135.3, 134.8, 131.0, 129.0, 128.7, 128.6, 128.3, 127.5, 126.0, 120.4 (d,  $J_{\text{C-F}} = 4.0$  Hz), 110.8 (dd,  $J_{\text{C-F}} = 26, 8.4$  Hz), 106.9 (t,  $J_{\text{C-F}} = 25$  Hz), 57.6, 55.3, 43.7 (d,  $J_{\text{C-F}} = 1.5$  Hz), 36.6, 35.0, 30.9, 20.6. mp 196–198 °C (decomposition). LC–MS (ESI, *m/z*): [M + H]<sup>+</sup> calcd for C<sub>35</sub>H<sub>33</sub>F<sub>3</sub>N<sub>2</sub>O<sub>4</sub>S, 635.22; found, 635.3. Purity: 95%. [ $\alpha$ ]<sub>D</sub><sup>25</sup> 9° (c 0.5, MeOH/CHCl<sub>3</sub> 1:1).

**Phenyl (*S,E*)-1-Fluoro-3-((*S*)-2-(isonicotinamido)-3-(*m*-tolyl)propanamido)-5-phenylpent-1-ene-1-sulfonate (3g).** Synthesized by following procedure D with 0.11 g of compound 32, 0.026 g isonicotinic acid, 0.067 g TBTU, and 0.11 mL DIEA. Column chromatography: petroleum ether/EtOAc 1:3. Yield: 0.086 g (69%), colorless solid. <sup>1</sup>H NMR (300 MHz, CDCl<sub>3</sub>):  $\delta$  8.68 (d,  $J = 4.7$  Hz, 2H), 7.56 (d,  $J = 5.7$  Hz, 2H), 7.40 (d,  $J = 7.6$  Hz, 1H), 7.37–7.28 (m, 5H), 7.25–7.11 (m, 4H), 7.04 (d,  $J = 7.6$  Hz, 1H), 6.99–6.90 (m, 3H), 6.84 (d,  $J = 7.5$  Hz, 1H), 6.24 (d,  $J = 7.8$  Hz, 1H), 5.57 (dd,  $J_{\text{H-F}} = 32.5$  Hz,  $J_{\text{H-H}} = 9.1$  Hz, 1H), 4.78–4.58 (m, 2H), 4.36 (s, 2H), 3.15 (dd,  $J = 13.4, 6.2$  Hz, 1H), 2.93 (dd,  $J = 13.4, 8.5$  Hz, 1H), 2.43–2.26 (m, 2H), 2.24 (s, 3H), 1.74–1.48 (m, 2H). <sup>13</sup>C NMR (75 MHz, CDCl<sub>3</sub>):  $\delta$  170.2, 165.2, 152.5 (d,  $J_{\text{C-F}} = 301$  Hz), 150.3, 141.2, 140.1, 138.8, 136.0, 131.0, 130.0, 129.5, 129.2, 129.0, 128.7, 128.4, 128.3, 126.7, 126.5, 126.5, 121.2, 119.4 (d,  $J_{\text{C-F}} = 4.1$  Hz), 58.7, 55.5, 44.8 (d,  $J_{\text{C-F}} = 2.3$  Hz), 38.7, 35.6, 35.7, 31.6, 21.4. mp 81–82 °C. LC–MS (ESI, *m/z*): [M + H]<sup>+</sup> calcd for C<sub>34</sub>H<sub>34</sub>FN<sub>3</sub>O<sub>4</sub>S, 600.24; found, 600.4. Purity: 95%. [ $\alpha$ ]<sub>D</sub><sup>25</sup> 7° (c 0.5, MeOH).

***N*-((*S*)-1-(((*S,E*)-1-(Benzylsulfonyl)-1-fluoro-5-phenylpent-1-en-3-yl)amino)-1-oxo-3-(*m*-tolyl)propan-2-yl)-2,3-dihydrobenzo[b][1,4]-dioxine-6-carboxamide (3h).** Synthesized by following procedure D with 0.11 g of compound 32, 0.037 g 1,4-benzodioxane-6-carboxylic acid, 0.067 g TBTU and 0.11 mL DIEA. Column chromatography: petroleum ether/EtOAc 2:1 to 0:1. Yield: 0.094 g (69%), colorless solid. <sup>1</sup>H NMR (300 MHz, DMSO-*d*<sub>6</sub>):  $\delta$  8.43 (d,  $J = 8.1$  Hz, 1H), 8.25 (d,  $J = 8.0$  Hz, 1H), 7.46–7.23 (m, 9H), 7.23–7.03 (m, 6H), 6.97 (d,  $J = 7.2$  Hz, 1H), 6.90 (d,  $J = 8.3$  Hz, 1H), 5.83 (dd,  $J_{\text{H-F}} = 34.2$  Hz,  $J_{\text{H-H}} = 9.0$  Hz, 1H), 4.74 (s, 2H), 4.64–4.49 (m, 2H), 4.39–4.17 (m, 4H), 3.08–2.86 (m, 2H), 2.49–2.38 (m, 2H), 2.23 (s, 3H), 1.87–1.55 (m, 2H). <sup>13</sup>C NMR (75 MHz, DMSO-*d*<sub>6</sub>):  $\delta$  171.0, 165.5, 151.3 (d,  $J_{\text{C-F}} = 298$  Hz), 146.1, 142.8, 140.9, 138.2, 137.0, 131.0, 129.8, 128.7, 128.6, 128.3, 127.9, 127.5, 127.1, 126.9, 126.2, 125.9, 120.9, 120.5 (d,  $J_{\text{C-F}} = 4.2$  Hz), 116.6, 116.5, 64.3, 64.0, 57.6, 55.0, 43.6 (d,  $J_{\text{C-F}} = 0.9$  Hz), 36.9, 35.1, 30.9, 21.0. mp 188–190 °C. LC–MS (ESI, *m/z*): [M + H]<sup>+</sup> calcd for C<sub>37</sub>H<sub>37</sub>FN<sub>2</sub>O<sub>6</sub>S, 657.25; found, 657.4. Purity >99%. [ $\alpha$ ]<sub>D</sub><sup>25</sup> 11° (c 0.5, CHCl<sub>3</sub>).

***N*-((*S*)-1-(((*S,E*)-1-(Benzylsulfonyl)-1-fluoro-5-phenylpent-1-en-3-yl)amino)-1-oxo-3-(*m*-tolyl)propan-2-yl)-3,5-difluorobenzamide (3i).** Synthesized by following procedure D with 0.12 g of compound 32, 0.036 g 3,5-difluorobenzoic acid, 0.073 g TBTU, and 0.12 mL DIEA. Column chromatography: petroleum ether/EtOAc 2:1. Yield: 0.11 g (77%), colorless solid. <sup>1</sup>H NMR (300 MHz, DMSO-*d*<sub>6</sub>):  $\delta$  8.83 (d,  $J = 8.1$  Hz, 1H), 8.33 (d,  $J = 7.8$  Hz, 1H), 7.61–7.02 (m, 17H), 6.98 (d,  $J = 7.1$  Hz, 1H), 5.81 (dd,  $J_{\text{H-F}} = 34.1$  Hz,  $J_{\text{H-H}} = 9.0$  Hz, 1H), 4.74 (s, 2H), 4.67–4.46 (m, 2H), 3.04 (dd,  $J = 13.5, 4.7$  Hz, 1H), 2.93 (dd,  $J = 13.5, 4.7$  Hz, 1H), 2.48–2.39 (m, 2H), 2.23 (s, 3H), 1.83–1.59 (m, 2H). <sup>13</sup>C NMR (75 MHz, DMSO-*d*<sub>6</sub>):  $\delta$  170.5, 163.8 (t,  $J_{\text{C-F}} = 2.7$  Hz), 162.1 (dd,  $J_{\text{C-F}} = 247$  Hz, 13 Hz), 151.3 (d,  $J_{\text{C-F}} = 298$  Hz), 140.9, 137.9, 137.5 (t,  $J_{\text{C-F}} = 8.5$  Hz), 137.1, 131.0, 129.8, 128.8, 128.6, 128.3, 128.0, 127.5, 127.0, 126.2, 126.0, 120.42 (d,  $J_{\text{C-F}} = 3.5$  Hz), 110.8 (dd,  $J_{\text{C-F}} = 25$  Hz, 8.6 Hz), 106.8 (t,  $J_{\text{C-F}} = 26$  Hz), 57.6, 55.2, 43.7 (d,  $J_{\text{C-F}} = 2.0$  Hz), 36.9, 35.0, 30.9, 21.0. mp 176–178 °C. LC–MS (ESI, *m/z*): [M + H]<sup>+</sup> calcd for C<sub>35</sub>H<sub>33</sub>F<sub>3</sub>N<sub>2</sub>O<sub>4</sub>S, 635.22; found, 635.3. Purity >99%. [ $\alpha$ ]<sub>D</sub><sup>25</sup> 6° (c 0.5, CHCl<sub>3</sub>).

***N*-((*S*)-1-(((*S,E*)-1-Fluoro-5-phenyl-1-(phenylsulfonyl)pent-1-en-3-yl)amino)-1-oxo-3-phenylpropan-2-yl)isonicotinamide (4a).**<sup>17</sup> Synthesized by following procedure E with 0.14 g of compound 13, 0.107 g compound X, 0.13 g TBTU, 0.062 g HOBt, and 0.21 mL DIEA. Column chromatography: DCM/MeOH 19:1. Yield: 0.17 g (75%),

colorless solid. <sup>1</sup>H NMR (300 MHz, CDCl<sub>3</sub>):  $\delta$  8.71 (br, 2H), 7.95 (d,  $J = 7.5$  Hz, 2H), 7.76–7.54 (m, 5H), 7.50 (d,  $J = 7.4$  Hz, 1H), 7.40–7.08 (m, 8H), 6.99 (d,  $J = 6.4$  Hz, 2H), 6.40 (d,  $J = 7.7$  Hz, 1H), 6.03 (dd,  $J_{\text{H-F}} = 31.9$  Hz,  $J_{\text{H-H}} = 8.8$  Hz, 1H), 4.87–4.60 (m, 2H), 3.21 (dd,  $J = 13.5, 6.3$  Hz, 1H), 3.08 (dd,  $J = 13.5, 8.2$  Hz, 1H), 2.49 (t,  $J = 7.4$  Hz, 2H), 1.96–1.68 (m, 2H). <sup>13</sup>C NMR (75 MHz, CDCl<sub>3</sub>):  $\delta$  170.3, 164.9, 155.1 (d,  $J_{\text{C-F}} = 301$  Hz), 149.4, 142.1, 140.2, 137.1, 136.2, 134.9, 129.7, 129.4, 129.1, 128.8, 128.7, 128.3, 127.7, 126.50, 121.7, 117.0 (d,  $J_{\text{C-F}} = 5.3$  Hz), 55.6, 45.1, 38.8, 35.7 (d,  $J_{\text{C-F}} = 1.9$  Hz), 31.8. mp 184–187 °C. LC–MS (ESI, *m/z*): [M + H]<sup>+</sup> calcd for C<sub>32</sub>H<sub>30</sub>FN<sub>3</sub>O<sub>4</sub>S, 572.20; found, 572.4. Purity: 95%. [ $\alpha$ ]<sub>D</sub><sup>25</sup> 11° (c 0.5, CHCl<sub>3</sub>).

***N*-((*S*)-1-(((*S,E*)-1-Fluoro-5-phenyl-1-(phenylsulfonyl)pent-1-en-3-yl)amino)-1-oxo-3-phenylpropan-2-yl)-2,3-dihydrobenzo[b][1,4]-dioxine-6-carboxamide (4b).** Synthesized by following procedure D with 0.100 g of compound 27, 0.036 g 1,4-benzodioxane-6-carboxylic acid, 0.064 g TBTU, and 0.104 mL DIEA. Column chromatography: petroleum ether/EtOAc 1:1. Yield: 0.084 g (67%), colorless solid. <sup>1</sup>H NMR (300 MHz, DMSO-*d*<sub>6</sub>):  $\delta$  8.43 (d,  $J = 8.0$  Hz, 1H), 8.35 (d,  $J = 7.8$  Hz, 1H), 7.94 (dt,  $J = 7.3, 1.7$  Hz, 2H), 7.85 (tt,  $J = 7.3, 1.2$  Hz, 1H), 7.73 (tt,  $J = 6.7, 1.1$  Hz, 2H), 7.43–7.06 (m, 12H), 6.89 (d,  $J = 8.3$  Hz, 1H), 6.30 (dd,  $J_{\text{H-F}} = 34.0$  Hz,  $J_{\text{H-H}} = 8.9$  Hz, 1H), 4.68–4.47 (m, 2H), 4.33–4.18 (m, 4H), 3.10–2.90 (m, 2H), 2.59–2.50 (m, 2H), 1.96–1.73 (m, 2H). <sup>13</sup>C NMR (75 MHz, DMSO-*d*<sub>6</sub>):  $\delta$  171.0, 165.4, 153.0 (d,  $J_{\text{C-F}} = 296$  Hz), 146.1, 142.8, 140.8, 138.2, 125.9, 126.6, 135.2, 130.1, 129.1, 128.27, 128.26, 128.1, 128.0, 127.8, 126.3, 125.9, 120.9, 119.2 (d,  $J_{\text{C-F}} = 4.8$  Hz), 116.6, 116.5, 64.3, 64.0, 54.9, 43.8 (d,  $J_{\text{C-F}} = 1.6$  Hz), 36.9, 35.0 (d,  $J_{\text{C-F}} = 2.3$  Hz), 31.0. mp 187–189 °C. LC–MS (ESI, *m/z*): [M + H]<sup>+</sup> calcd for C<sub>35</sub>H<sub>33</sub>FN<sub>2</sub>O<sub>6</sub>S, 629.2; found, 629.3. Purity >99%. [ $\alpha$ ]<sub>D</sub><sup>25</sup> 3° (c 0.5, CHCl<sub>3</sub>).

**3,5-Difluoro-*N*-((*S*)-1-(((*S,E*)-1-fluoro-5-phenyl-1-(phenylsulfonyl)pent-1-en-3-yl)amino)-1-oxo-3-phenylpropan-2-yl)benzamide (4c).** Synthesized by following procedure D with 0.124 g of compound 27, 0.039 g 3,5-difluorobenzoic acid, 0.079 g TBTU, and 0.125 mL DIEA. Column chromatography: petroleum ether/EtOAc 2:1. Yield: 0.12 g (81%), colorless solid. <sup>1</sup>H NMR (300 MHz, CDCl<sub>3</sub>):  $\delta$  7.99–7.90 (m, 2H), 7.73–7.63 (m, 2H), 7.57 (t,  $J = 7.6$  Hz, 2H), 7.37–7.09 (m, 12H), 7.00–6.91 (m, 2H), 6.87 (tt,  $J = 8.5, 2.3$  Hz, 1H), 6.37 (d,  $J = 7.7$  Hz, 1H), 5.96 (dd,  $J_{\text{H-F}} = 31.8$  Hz,  $J_{\text{H-H}} = 8.9$  Hz, 1H), 4.82–4.61 (m, 2H), 3.14 (dd,  $J = 13.5, 6.4$  Hz, 1H), 3.03 (dd,  $J = 13.5, 8.2$  Hz, 1H), 2.45 (t,  $J = 7.7$  Hz, 2H), 1.88–1.72 (m, 2H). <sup>13</sup>C NMR (75 MHz, CDCl<sub>3</sub>):  $\delta$  170.6, 165.0 (t,  $J_{\text{C-F}} = 2.8$  Hz), 163.0 (dd,  $J_{\text{C-F}} = 251, 12$  Hz), 155.2 (d,  $J_{\text{C-F}} = 301$  Hz), 140.2, 137.1, 136.8 (t,  $J_{\text{C-F}} = 8.3$  Hz), 136.2, 134.8, 129.7, 129.4, 129.1, 128.8, 128.7, 128.3, 127.6, 126.5, 116.9 (d,  $J_{\text{C-F}} = 5.1$  Hz), 110.5 (dd,  $J_{\text{C-F}} = 27, 8.7$  Hz), 107.4 (t,  $J_{\text{C-F}} = 25$  Hz), 55.7, 45.1 (d,  $J_{\text{C-F}} = 1.5$  Hz), 38.7, 35.7, 31.8. mp 90–92 °C. LC–MS (ESI, *m/z*): [M + H]<sup>+</sup> calcd for C<sub>33</sub>H<sub>29</sub>F<sub>3</sub>N<sub>2</sub>O<sub>4</sub>S, 607.2; found, 607.3. Purity: 95%. [ $\alpha$ ]<sub>D</sub><sup>25</sup> 5° (c 0.5, MeOH).

***N*-((*S*)-1-(((*S,E*)-1-Fluoro-5-phenyl-1-(phenylsulfonyl)pent-1-en-3-yl)amino)-1-oxo-3-(*p*-tolyl)propan-2-yl)isonicotinamide (4d).** Synthesized by following procedure D with 0.10 g of compound 33, 0.024 g isonicotinic acid, 0.063 g TBTU, and 0.10 mL DIEA. Column chromatography: pure EtOAc. Yield: 0.094 g (83%), colorless solid. <sup>1</sup>H NMR (300 MHz, CDCl<sub>3</sub>):  $\delta$  8.69 (d,  $J = 3.8$  Hz, 2H), 7.95 (d,  $J = 7.7$  Hz, 2H), 7.70 (t,  $J = 7.3$  Hz, 1H), 7.65–7.46 (m, 4H), 7.30–7.23 (m, 1H), 7.23–7.01 (m, 7H), 6.96 (d,  $J = 6.8$  Hz, 2H), 6.32 (d,  $J = 7.8$  Hz, 1H), 6.01 (dd,  $J_{\text{H-F}} = 31.9$  Hz,  $J_{\text{H-H}} = 8.8$  Hz, 1H), 4.84–4.60 (m, 2H), 3.15 (dd,  $J = 13.6, 5.7$  Hz, 1H), 3.01 (dd,  $J = 13.4, 8.2$  Hz, 1H), 2.46 (t,  $J = 7.6$  Hz, 2H), 2.32 (s, 3H), 1.90–1.73 (m, 2H). <sup>13</sup>C NMR (75 MHz, CDCl<sub>3</sub>):  $\delta$  170.3, 165.4, 155.12 (d,  $J_{\text{C-F}} = 301$  Hz), 150.7, 140.8, 140.1, 137.4, 137.1, 134.8, 132.9, 129.8, 129.7, 129.3, 128.8, 128.7, 128.3, 126.5, 121.0, 116.9 (d,  $J_{\text{C-F}} = 4.8$  Hz), 55.4, 45.0 (d,  $J_{\text{C-F}} = 1.7$  Hz), 38.4, 35.8, 31.8, 21.2. mp 84–86 °C. LC–MS (ESI, *m/z*): [M + H]<sup>+</sup> calcd for C<sub>33</sub>H<sub>32</sub>FN<sub>3</sub>O<sub>4</sub>S, 586.22; found, 586.4. Purity: 96%. [ $\alpha$ ]<sub>D</sub><sup>25</sup> 12° (c 0.5, MeOH).

***N*-((*S*)-1-(((*S,E*)-1-Fluoro-5-phenyl-1-(phenylsulfonyl)pent-1-en-3-yl)amino)-1-oxo-3-(*p*-tolyl)propan-2-yl)-2,3-dihydrobenzo[b][1,4]-dioxine-6-carboxamide (4e).** Synthesized by following procedure D with 0.065 g of compound 33, 0.023 g 1,4-benzodioxane-6-carboxylic acid, 0.041 g TBTU, and 0.066 mL DIEA. Column chromatography: petroleum ether/EtOAc 2:1 to 1:1. Yield: 0.057 g (70%), colorless



solid.  $^1\text{H}$  NMR (300 MHz,  $\text{CDCl}_3$ ):  $\delta$  8.00–7.90 (m, 2H), 7.75–7.65 (m, 1H), 7.64–7.53 (m, 2H), 7.26 (s, 1H), 7.23–7.03 (m, 8H), 6.93 (dd,  $J = 7.8, 1.5$  Hz, 2H), 6.85 (d,  $J = 8.4$  Hz, 1H), 6.79 (d,  $J = 7.7$  Hz, 1H), 6.70 (d,  $J = 7.9$  Hz, 1H), 6.02 (dd,  $J_{\text{H-F}} = 32.0$  Hz,  $J_{\text{H-H}} = 8.7$  Hz, 1H), 4.83 (q,  $J = 7.5$  Hz, 1H), 4.68 (quint,  $J = 7.7$  Hz, 1H), 4.34–4.21 (m, 4H), 3.13 (dd,  $J = 13.6, 6.3$  Hz, 1H), 3.02 (dd,  $J = 13.6, 7.8$  Hz, 1H), 2.54–2.38 (m, 2H), 2.31 (s, 3H), 1.87–1.69 (m, 2H).  $^{13}\text{C}$  NMR (75 MHz,  $\text{CDCl}_3$ ):  $\delta$  170.8, 166.8, 154.8 (d,  $J_{\text{C-F}} = 300$  Hz), 147.0, 143.6, 140.3, 137.3, 137.0, 134.7, 133.3, 129.7, 129.6, 129.3, 128.8, 128.6, 128.4, 126.9, 126.3, 120.6, 117.62 (d,  $J_{\text{C-F}} = 5.1$  Hz), 117.5, 116.8, 64.7, 64.3, 55.1, 44.9 (d,  $J_{\text{C-F}} = 1.7$  Hz), 38.3, 35.7, 31.8, 21.2. mp 95–97 °C. LC–MS (ESI,  $m/z$ ):  $[\text{M} + \text{H}]^+$  calcd for  $\text{C}_{36}\text{H}_{35}\text{FN}_2\text{O}_6\text{S}$ , 643.23; found, 643.3. Purity: 96%.  $[\alpha]_{\text{D}}^{22} 13^\circ$  (c 1,  $\text{CHCl}_3$ ).

**3,5-Difluoro-N-((S)-1-(((S,E)-1-fluoro-5-phenyl-1-(phenylsulfonyl)pent-1-en-3-yl)amino)-1-oxo-3-(p-tolyl)propan-2-yl)benzamide (4f).** Synthesized by following procedure D with 0.065 g of compound 33, 0.020 g 3,5-difluorobenzoic acid, 0.041 g TBTU, and 0.066 mL DIEA. Column chromatography: petroleum ether/EtOAc 3:1. Yield: 0.059 g (73%), colorless solid.  $^1\text{H}$  NMR (300 MHz,  $\text{CDCl}_3$ ):  $\delta$  8.00–7.91 (m, 2H), 7.74–7.63 (m, 1H), 7.62–7.53 (m, 2H), 7.31 (d,  $J = 7.6$  Hz, 1H), 7.25–7.09 (m, 7H), 7.05 (d,  $J = 8.0$  Hz, 2H), 6.97–6.82 (m, 3H), 6.39 (d,  $J = 7.7$  Hz, 1H), 5.98 (dd,  $J_{\text{H-F}} = 31.9$  Hz,  $J_{\text{H-H}} = 8.8$  Hz, 1H), 4.83–4.60 (m, 2H), 3.11 (dd,  $J = 13.5, 6.3$  Hz, 1H), 2.99 (dd,  $J = 13.5, 8.2$  Hz, 1H), 2.52–2.40 (m, 2H), 2.31 (s, 3H), 1.90–1.74 (m, 2H).  $^{13}\text{C}$  NMR (75 MHz,  $\text{CDCl}_3$ ):  $\delta$  170.7, 164.95 (t,  $J_{\text{C-F}} = 2.9$  Hz), 163.02 (dd,  $J_{\text{C-F}} = 251, 12$  Hz), 155.12 (d,  $J_{\text{C-F}} = 301$  Hz), 140.2, 137.3, 137.2, 136.9 (t,  $J_{\text{C-F}} = 8.3$  Hz), 134.8, 133.0, 129.8, 129.7, 129.3, 128.8, 128.7, 128.3, 126.5, 117.05 (d,  $J_{\text{C-F}} = 4.8$  Hz), 110.50 (dd,  $J_{\text{C-F}} = 27, 9.4$  Hz), 107.37 (t,  $J_{\text{C-F}} = 25$  Hz), 55.6, 45.1 (d,  $J_{\text{C-F}} = 1.6$  Hz), 38.3, 35.7 (d,  $J_{\text{C-F}} = 1.5$  Hz), 31.8, 21.2. mp 174–176 °C. LC–MS (ESI,  $m/z$ ):  $[\text{M} + \text{H}]^+$  calcd for  $\text{C}_{34}\text{H}_{31}\text{F}_3\text{N}_3\text{O}_4\text{S}$ , 621.21; found, 621.3. Purity: 95%.  $[\alpha]_{\text{D}}^{22} 9^\circ$  (c 0.5, MeOH).

**N-((S)-1-(((S,E)-1-Fluoro-5-phenyl-1-(phenylsulfonyl)pent-1-en-3-yl)amino)-1-oxo-3-(m-tolyl)propan-2-yl)isonicotinamide (4g).** Synthesized by following procedure D with 0.10 g of compound 30, 0.024 g isonicotinic acid, 0.063 g TBTU, and 0.10 mL DIEA. Column chromatography: pure EtOAc. Yield: 0.071 g (63%), colorless solid.  $^1\text{H}$  NMR (300 MHz,  $\text{CDCl}_3$ ):  $\delta$  8.69 (d,  $J = 5.2$  Hz, 2H), 7.94 (d,  $J = 7.5$  Hz, 2H), 7.74–7.65 (m, 1H), 7.63–7.48 (m, 4H), 7.34–7.11 (m, 6H), 7.11–6.88 (m, 5H), 6.31 (d,  $J = 7.8$  Hz, 1H), 6.01 (dd,  $J_{\text{H-F}} = 31.9$  Hz,  $J_{\text{H-H}} = 8.8$  Hz, 1H), 4.84–4.59 (m, 2H), 3.16 (dd,  $J = 13.5, 6.2$  Hz, 1H), 3.00 (dd,  $J = 13.5, 8.4$  Hz, 1H), 2.45 (t,  $J = 7.5$  Hz, 2H), 2.29 (s, 3H), 1.89–1.73 (m, 2H).  $^{13}\text{C}$  NMR (75 MHz,  $\text{CDCl}_3$ ):  $\delta$  170.3, 165.4, 155.10 (d,  $J_{\text{C-F}} = 301$  Hz), 150.6, 140.9, 140.1, 138.8, 137.0, 136.0, 134.7, 130.1, 129.7, 129.0, 128.8, 128.7, 128.4, 128.3, 126.5, 126.4, 121.1, 116.9 (d,  $J_{\text{C-F}} = 5.2$  Hz), 55.4, 45.1 (d,  $J_{\text{C-F}} = 1.9$  Hz), 38.7, 35.8 (d,  $J_{\text{C-F}} = 1.4$  Hz), 31.8, 21.5. mp 182–184 °C. LC–MS (ESI,  $m/z$ ):  $[\text{M} + \text{H}]^+$  calcd for  $\text{C}_{33}\text{H}_{32}\text{FN}_3\text{O}_4\text{S}$ , 586.22; found, 586.4. Purity: 95%.  $[\alpha]_{\text{D}}^{22} 3^\circ$  (c 0.5,  $\text{CHCl}_3$ ).

**N-((S)-1-(((S,E)-1-Fluoro-5-phenyl-1-(phenylsulfonyl)pent-1-en-3-yl)amino)-1-oxo-3-(m-tolyl)propan-2-yl)-2,3-dihydrobenzob[1,4]dioxine-6-carboxamide (4h).** Synthesized by following procedure D with 0.10 g of compound 30, 0.035 g 1,4-benzodioxane-6-carboxylic acid, 0.063 g TBTU, and 0.10 mL DIEA. Column chromatography: petroleum ether/EtOAc 1:1. Yield: 0.10 g (84%), colorless solid.  $^1\text{H}$  NMR (300 MHz,  $\text{DMSO}-d_6$ ):  $\delta$  8.44 (d,  $J = 8.1$  Hz, 1H), 8.38 (d,  $J = 7.8$  Hz, 1H), 7.94 (dt,  $J = 7.3, 1.5$  Hz, 2H), 7.89–7.80 (m, 1H), 7.80–7.68 (m, 2H), 7.42–7.30 (m, 2H), 7.29–7.02 (m, 8H), 6.98 (d,  $J = 6.9$  Hz, 1H), 6.90 (d,  $J = 8.3$  Hz, 1H), 6.31 (dd,  $J_{\text{H-F}} = 34.0$  Hz,  $J_{\text{H-H}} = 8.9$  Hz, 1H), 4.65–4.46 (m, 2H), 4.27 (d,  $J = 5.4$  Hz, 4H), 3.08–2.84 (m, 2H), 2.61–2.50 (m, 2H), 2.25 (s, 3H), 1.96–1.72 (m, 2H).  $^{13}\text{C}$  NMR (75 MHz,  $\text{DMSO}-d_6$ ):  $\delta$  171.1, 165.5, 152.9 (d,  $J_{\text{C-F}} = 295$  Hz), 146.1, 142.8, 140.8, 138.1, 137.0, 136.6, 135.2, 130.1, 129.8, 128.3, 128.3, 128.2, 127.9, 127.0, 126.9, 126.2, 125.9, 121.0, 119.3 (d,  $J_{\text{C-F}} = 4.3$  Hz), 116.6, 116.5, 64.3, 64.0, 55.0, 43.8 (d,  $J_{\text{C-F}} = 1.5$  Hz), 36.8, 35.4, 31.0, 21.0. mp 186–188 °C. LC–MS (ESI,  $m/z$ ):  $[\text{M} + \text{H}]^+$  calcd for  $\text{C}_{36}\text{H}_{35}\text{FN}_2\text{O}_6\text{S}$ , 643.23; found, 643.3. Purity: >99%.  $[\alpha]_{\text{D}}^{22} 11^\circ$  (c 1,  $\text{CHCl}_3$ ).

**3,5-Difluoro-N-((S)-1-(((S,E)-1-fluoro-5-phenyl-1-(phenylsulfonyl)pent-1-en-3-yl)amino)-1-oxo-3-(m-tolyl)propan-2-**

**yl)benzamide (4i).** Synthesized by following procedure D with 0.10 g of compound 30, 0.031 g 3,5-difluorobenzoic acid, 0.063 g TBTU, and 0.10 mL DIEA. Column chromatography: petroleum ether/EtOAc 2:1. Yield: 0.075 g (62%), colorless solid.  $^1\text{H}$  NMR (300 MHz,  $\text{CDCl}_3$ ):  $\delta$  7.95 (d,  $J = 7.5$  Hz, 2H), 7.72–7.64 (m, 1H), 7.57 (t,  $J = 7.6$  Hz, 2H), 7.29–7.23 (m, 1H), 7.25–6.81 (m, 13H), 6.38 (d,  $J = 7.7$  Hz, 1H), 6.01 (dd,  $J_{\text{H-F}} = 31.8$  Hz,  $J_{\text{H-H}} = 8.8$  Hz, 1H), 4.81–4.60 (m, 2H), 3.12 (dd,  $J = 13.5, 6.5$  Hz, 1H), 2.98 (dd,  $J = 13.5, 8.1$  Hz, 1H), 2.45 (t,  $J = 7.7$  Hz, 2H), 2.28 (s, 3H), 1.88–1.74 (m, 2H).  $^{13}\text{C}$  NMR (75 MHz,  $\text{CDCl}_3$ ):  $\delta$  170.6, 165.02 (t,  $J_{\text{C-F}} = 2.4$  Hz), 162.99 (dd,  $J_{\text{C-F}} = 251, 12$  Hz), 155.14 (d,  $J_{\text{C-F}} = 301$  Hz), 140.2, 138.8, 137.1, 136.8 (t,  $J_{\text{C-F}} = 8.4$  Hz), 136.2, 134.8, 130.1, 129.7, 129.0, 128.8, 128.7, 128.4, 128.3, 126.5, 117.0 (d,  $J_{\text{C-F}} = 4.9$  Hz), 110.5 (dd,  $J_{\text{C-F}} = 26, 8.7$  Hz), 107.4 (t,  $J_{\text{C-F}} = 25$  Hz), 55.6, 45.2 (d,  $J_{\text{C-F}} = 1.6$  Hz), 38.5, 35.7, 31.8, 21.4. mp 176–178 °C. LC–MS (ESI,  $m/z$ ):  $[\text{M} + \text{H}]^+$  calcd for  $\text{C}_{34}\text{H}_{31}\text{F}_3\text{N}_3\text{O}_4\text{S}$ , 621.21; found, 621.3. Purity >99%.  $[\alpha]_{\text{D}}^{22} 5^\circ$  (c 0.5, MeOH/ $\text{CHCl}_3$  1:1).

**N-((S)-1-(((S,E)-1-Fluoro-5-(methylthio)-1-(phenylsulfonyl)pent-1-en-3-yl)amino)-1-oxo-3-phenylpropan-2-yl)-4-methylpiperazine-1-carboxamide (4j).** Synthesized by following procedure E with 0.11 g of compound 16, 0.089 g compound IX, 0.088 g TBTU, 0.042 g HOBt, and 0.14 mL DIEA. Column chromatography: DCM/MeOH 19:1. Yield: 0.11 g (73%), colorless solid. (300 MHz,  $\text{CD}_2\text{Cl}_2$ ):  $\delta$  7.85 (dd,  $J = 7.3, 1.7$  Hz, 2H), 7.71–7.59 (m, 1H), 7.59–7.47 (m, 2H), 7.25–7.13 (m, 3H), 7.12–7.01 (m, 3H), 5.99 (dd,  $J_{\text{H-F}} = 32.4$  Hz,  $J_{\text{H-H}} = 8.8$  Hz, 1H), 5.06 (d,  $J = 7.7$  Hz, 1H), 4.76–4.59 (m, 1H), 4.41 (q,  $J = 7.2$  Hz, 1H), 3.21 (q,  $J = 4.5$  Hz, 4H), 3.02–2.79 (m, 2H), 2.31–2.25 (m, 2H), 2.22 (t,  $J = 5.1$  Hz, 4H), 2.16 (s, 3H), 1.90 (s, 3H), 1.82–1.60 (m, 2H). (75 MHz,  $\text{CD}_2\text{Cl}_2$ ):  $\delta$  172.3, 157.5, 155.0 (d,  $J_{\text{C-F}} = 298$  Hz), 137.6, 137.2, 135.2, 130.1, 129.9, 129.1, 127.4, 118.2 (d,  $J_{\text{C-F}} = 4.9$  Hz), 56.3, 55.1, 54.0, 46.4, 44.7 (d,  $J_{\text{C-F}} = 1.8$  Hz), 44.3, 39.0, 33.8, 30.4, 15.7. mp 110–112 °C. HR–MS (ESI,  $m/z$ ):  $[\text{M} + \text{Na}]^+$  calcd for  $\text{C}_{27}\text{H}_{35}\text{FN}_4\text{O}_4\text{S}_2$ , 585.1981; found, 585.1973.  $[\alpha]_{\text{D}}^{22} 12^\circ$  (c 1,  $\text{CHCl}_3$ ).

**N-((S)-1-(((S,E)-1-Fluoro-5-(methylthio)-1-(phenylsulfonyl)pent-1-en-3-yl)amino)-1-oxo-3-phenylpropan-2-yl)isonicotinamide (4k).** Synthesized by following procedure E with 0.11 g of compound 16, 0.074 g compound X, 0.088 g TBTU, 0.042 g HOBt, and 0.14 mL DIEA. Column chromatography: DCM/MeOH 95:5. Yield: 0.098 g (66%), colorless solid. (300 MHz,  $\text{CD}_2\text{Cl}_2$ ):  $\delta$  8.70 (d,  $J = 4.5$  Hz, 2H), 7.94 (d,  $J = 7.5$  Hz, 2H), 7.76–7.53 (m, 5H), 7.44–7.15 (m, 9H), 7.07 (d,  $J = 7.3$  Hz, 1H), 6.26 (d,  $J = 7.8$  Hz, 1H), 6.04 (dd,  $J_{\text{H-F}} = 32.2$  Hz,  $J_{\text{H-H}} = 8.8$  Hz, 1H), 4.92–4.55 (m, 2H), 3.23–3.00 (m, 2H), 2.44–2.24 (m, 2H), 2.05–1.91 (m, 3H), 1.88–1.74 (m, 2H). (75 MHz,  $\text{CD}_2\text{Cl}_2$ ):  $\delta$  170.0, 165.2, 151.4, 150.6, 140.7, 139.4, 137.0, 136.2, 134.8, 129.6, 129.3, 128.9, 128.6, 127.3, 120.8, 55.1, 45.3, 38.3, 29.8, 15.2. mp 64–66 °C. HR–MS (ESI,  $m/z$ ):  $[\text{M} + \text{Na}]^+$  calcd for  $\text{C}_{27}\text{H}_{28}\text{FN}_4\text{O}_4\text{S}_2$ , 564.1403; found, 564.1411.  $[\alpha]_{\text{D}}^{22} 21^\circ$  (c 1,  $\text{CHCl}_3$ ).

**N-((S)-1-(((R,E)-1-(Benzylthio)-4-fluoro-4-(phenylsulfonyl)but-3-en-2-yl)amino)-1-oxo-3-phenylpropan-2-yl)-4-methylpiperazine-1-carboxamide (4l).** Synthesized by following procedure E with 0.11 g of compound 17, 0.077 g compound IX, 0.076 g TBTU, 0.036 g HOBt, and 0.13 mL DIEA. Column chromatography: DCM/MeOH 9:1. Yield: 0.093 g (63%). (300 MHz,  $\text{CDCl}_3$ ):  $\delta$  8.02–7.91 (m, 2H), 7.79–7.67 (m, 1H), 7.67–7.54 (m, 2H), 7.43–7.09 (m, 10H), 6.81 (dd,  $J = 47.2, 7.8$  Hz, 1H), 6.16 (dd,  $J = 43.5, 31.8, 8.6$  Hz, 1H), 5.15 (dd,  $J = 14.7, 7.4$  Hz, 1H), 4.93–4.75 (m, 1H), 4.52 (m, 1H), 3.64 (s, 2H), 3.54–3.30 (m, 4H), 3.18–2.99 (m, 2H), 2.67–2.47 (m, 2H), 2.50–2.38 (m, 4H), 2.36 (s, 3H). (75 MHz,  $\text{CDCl}_3$ ):  $\delta$  171.7, 156.9, 137.4, 137.4, 137.0, 136.93, 136.90, 136.87, 134.8, 129.7, 129.5, 129.4, 129.0, 128.9, 128.85, 128.76, 127.5, 127.3, 127.2, 116.6, 116.57, 116.5, 77.2, 55.9, 55.88, 54.4, 54.4, 45.9, 45.8, 44.5, 44.3, 43.55, 38.8, 38.6, 36.5, 35.1, 35.0. mp 84–86 °C. HR–MS (ESI,  $m/z$ ):  $[\text{M} + \text{Na}]^+$  calcd for  $\text{C}_{32}\text{H}_{37}\text{FN}_4\text{O}_4\text{S}_2$ , 647.2138; found, 647.2152.  $[\alpha]_{\text{D}}^{22} -13^\circ$  (c 1,  $\text{CHCl}_3$ ).

**Synthesis of the Metabolites. tert-Butyl 4-(((S)-1-(((S,E)-1-Fluoro-5-phenyl-1-(phenylsulfonyl)pent-1-en-3-yl)amino)-1-oxo-3-phenylpropan-2-yl)carbamoyl)piperazine-1-carboxylate (36).** Compound XIII (0.31 g) was dissolved in DCM and cooled to 0 °C. 0.11 g HOBt, 0.26 g TBTU, and 0.42 mL DIEA were added and the mixture was stirred for 30 min. 0.24 g of compound 13 was added and the mixture was stirred for an additional 24 h at rt. The reaction was stopped with 7 equiv of water and the mixture was washed with a saturated solution of

NaHCO<sub>3</sub> and brine, dried with Na<sub>2</sub>SO<sub>4</sub>, and the solvent was removed under reduced pressure. The crude product was purified by column chromatography (cyclohexane/EtOAc 1:1), resulting in a colorless oil (0.21 g, 45%). <sup>1</sup>H NMR (300 MHz, CDCl<sub>3</sub>): δ 7.97–7.88 (m, 2H), 7.74–7.65 (m, 1H), 7.63–7.53 (m, 2H, *H*-27), 7.35–7.11 (m, 8H), 7.02 (ddd, *J* = 7.8, 3.2, 1.5 Hz, 2H), 6.54 (d, *J* = 41.8 Hz, 1H), 5.99 (dd, *J* = 32.0, 8.7 Hz, 1H), 5.11 (d, *J* = 27.5 Hz, 1H), 4.71–4.56 (m, 1H), 4.47 (d, *J*<sub>C-F</sub> = 10.3 Hz), 3.45–3.17 (m, 8H), 3.14–2.91 (m, 2H), 2.56–2.36 (m, 2H), 1.95–1.62 (m, 2H), 1.46 (s, 9H). <sup>13</sup>C NMR (75 MHz, CDCl<sub>3</sub>): δ 171.6, 157.0, 154.7, 140.4, 137.1 (d, *J* = 7.3 Hz), 136.8, 134.8, 129.7, 129.4, 128.9, 128.8, 128.7, 128.4, 127.3 (d, *J* = 5.1 Hz), 126.4, 117.4, 80.4, 56.1, 45.1, 43.7, 38.5, 35.8, 31.8, 28.5.

(*S*)-4-((1-Ethoxy-1-oxo-3-phenylpropan-2-yl)carbamoyl)-1-methylpiperazine 1-oxide (**28**). Compound **IX** (1.3 g) was dissolved in DCM and cooled to 0 °C. 0.7 g of 3-chloroperbenzoic acid was added and the mixture was stirred for 16 h. Triphenylphosphine was added to stop the reaction. The solvent was removed under reduced pressure, giving the crude product as a colorless oil (0.82 g, 63%). <sup>1</sup>H NMR (300 MHz, methanol-*d*<sub>4</sub>): δ 7.35–7.11 (m, 5H), 4.87 (t, *J* = 2.0 Hz, 4H), 4.49 (td, *J* = 5.9, 2.9 Hz, 1H), 4.22–4.03 (m, 2H), 3.47–3.40 (m, 1H), 3.23–2.87 (m, 4H), 2.39 (d, *J* = 2.9 Hz, 3H), 2.04–1.89 (m, 2H), 1.26–1.10 (m, 3H). <sup>13</sup>C NMR (75 MHz, methanol-*d*<sub>4</sub>): δ 174.4, 159.3, 138.8, 130.2, 129.4, 127.8, 62.2, 57.0, 55.2, 45.6, 44.1, 38.5, 14.4.

(*S*)-4-((1-Carboxy-2-phenylethyl)carbamoyl)-1-methylpiperazine 1-oxide (**38**). Compound **37** (0.65 g) was dissolved in THF and cooled to 0 °C, and 0.33 g of LiOH in water was added dropwise. The mixture was stirred for 3 h at room temperature. The product was isolated from the aqueous phase giving a colorless solid (0.31 g, 53%). <sup>1</sup>H NMR (300 MHz, DMSO-*d*<sub>6</sub>): δ 11.49 (s, 1H), 7.39–6.82 (m, 5H), 4.15–3.96 (m, 1H), 3.96–3.67 (m, 1H), 3.16–2.68 (m, 8H), 2.50 (s, 2H), 2.33 (s, 3H). <sup>13</sup>C NMR (75 MHz, DMSO-*d*<sub>6</sub>): δ 173.9, 157.1, 138.6, 129.3, 128.2, 126.4, 55.8, 51.9, 42.0, 40.8, 36.4.

*Ethyl Isonicotinate* (**39**). Isonicotinic acid (2.46 g) was dissolved in 40 mL ethanol and 1 mL of concentrated H<sub>2</sub>SO<sub>4</sub> was added dropwise. The mixture was refluxed for 24 h and the solvent was removed under reduced pressure. The residue was extracted with DCM and the combined extracts were washed with a saturated solution of NaHCO<sub>3</sub>, resulting in a colorless oil (2.2 g, 73%). <sup>1</sup>H NMR (300 MHz, DMSO-*d*<sub>6</sub>): δ 8.83–8.73 (m, 2H), 7.88–7.73 (m, 2H), 4.34 (q, *J* = 7.1 Hz, 2H), 1.32 (t, *J* = 7.1 Hz, 3H). <sup>13</sup>C NMR (75 MHz, DMSO-*d*<sub>6</sub>): δ 164.8, 150.8, 137.2, 122.6, 61.7, 14.1.

4-(Ethoxycarbonyl)pyridine 1-Oxide (**40**). Compound **39** (1.51 g) was dissolved in DCM and cooled to 0 °C. 1.73 g of 3-chloroperbenzoic acid was added and the mixture was stirred for 16 h. Triphenylphosphine was added to stop the reaction. The solvent was removed under reduced pressure, giving the crude product that was further purified by column chromatography (cyclohexane/EtOAc 1:6), resulting in a colorless oil (0.24 g, 29%). <sup>1</sup>H NMR (300 MHz, DMSO-*d*<sub>6</sub>): δ 8.43–8.19 (m, 2H), 7.97–7.77 (m, 2H), 4.31 (q, *J* = 7.1 Hz, 2H), 1.31 (t, *J* = 7.1 Hz, 3H). <sup>13</sup>C NMR (75 MHz, DMSO-*d*<sub>6</sub>): δ 163.7, 139.9, 126.85, 125.7, 61.9, 14.5.

4-Carboxypyridine 1-Oxide (**41**). Compound **40** (0.20 g) was dissolved in THF and cooled to 0 °C. 0.20 g of LiOH was dissolved in water and added dropwise to the mixture, then stirred for 3 h at rt. The product was isolated from the aqueous phase giving a colorless solid (0.17 g, 100%). <sup>1</sup>H NMR (300 MHz, DMSO-*d*<sub>6</sub>): δ 8.31 (d, *J* = 6.2 Hz, 2H), 7.82 (d, *J* = 6.2 Hz, 2H). <sup>13</sup>C NMR (75 MHz, DMSO-*d*<sub>6</sub>): δ 165.00, 139.8, 127.5, 127.1.

4-(((*S*)-1-(((*S*),*E*)-1-Fluoro-5-phenyl-1-(phenylsulfonyl)pent-1-en-3-yl)amino)-1-oxo-3-phenylpropan-2-yl)carbamoyl)piperazine 1-ium Chloride (**1a**). A 4 M solution of HCl in dioxane (3 mL) was added to 0.208 g of compound **36**. The mixture was stirred for 12 h and the solvent was removed under reduced pressure. The residue was washed three times with diethyl ether in an ultrasonic bath and then lyophilized, resulting in a colorless solid (0.177 g, 93%). <sup>1</sup>H NMR (300 MHz, DMSO-*d*<sub>6</sub>): δ 8.53 (s, 2H), 8.10–7.97 (m, 2H), 7.98–7.66 (m, 3H), 7.40–6.89 (m, 11H), 6.51 (dd, *J* = 32.7, 9.8 Hz, 1H), 4.58–4.40 (m, 1H), 4.33–3.93 (m, 1H), 3.61–3.44 (m, 8H), 3.09–2.83 (m, 4H), 2.34–1.78 (m, 2H). <sup>13</sup>C NMR (75 MHz, DMSO-*d*<sub>6</sub>): δ 163.2, 157.2, 139.3, 136.6, 135.8, 132.6, 130.2, 129.1, 128.1, 126.1, 119.7, 117.8,

115.1, 57.2, 52.4, 46.0, 42.4, 42.4, 36.5, 35.2, 35.0, 33.3. mp 93–94 °C. LC–MS (ESI, *m/z*): [M + H]<sup>+</sup> calcd for C<sub>31</sub>H<sub>35</sub>FN<sub>4</sub>O<sub>4</sub>S, 579.24; found, 579.3. Purity: 98%. [α]<sub>D</sub><sup>25</sup> 10° (c 0.5, MeOH).

4-(((*S*)-1-(((*S*),*E*)-1-Fluoro-5-phenyl-1-(phenylsulfonyl)pent-1-en-3-yl)amino)-1-oxo-3-phenylpropan-2-yl)carbamoyl)-1-methylpiperazine 1-oxide (**1b**). Compound **38** (0.20 g) was dissolved in a 1:1 mixture of DCM/DMF and cooled to 0 °C. 0.05 g HOBt, 0.11 g TBTU, and 0.20 mL DIEA were added, and the mixture was stirred for 30 min until all components dissolved. 0.10 g of compound **13** were added, and the mixture was stirred for an additional 48 h at room temperature. The reaction was stopped by adding 7 equiv of water and the residue was extracted with EtOAc and washed with water (2×), NaHCO<sub>3</sub> (2×), 1 M HCl (2×), and brine (1×). The solvent was removed under reduced pressure and the crude product was purified by preparative HPLC and eluted with 70% water and 30% ACN, resulting in a colorless oil (0.04 g, 23%). <sup>1</sup>H NMR (300 MHz, DMSO-*d*<sub>6</sub>): δ 10.13 (s, 1H), 8.43–7.45 (m, 10H), 7.33–7.03 (m, 5H), 6.33–6.26 (m, 1H), 5.81 (dd, *J* = 22.1, 10.2 Hz, 1H), 5.50–5.28 (m, 1H), 4.48 (q, *J* = 8.0 Hz, 1H), 4.36–4.20 (m, 2H), 3.71–3.12 (m, 8H), 2.50 (quint, *J* = 1.9 Hz, 3H), 2.06 (d, *J* = 43.8 Hz, 2H), 2.04–1.64 (m, 2H). <sup>13</sup>C NMR (300 MHz, DMSO-*d*<sub>6</sub>): δ 172.0, 157.3, 142.4, 139.6, 136.9, 134.0, 129.8, 129.0, 128.9, 128.6, 128.2, 127.7, 126.0, 105.6, 60.2, 57.2, 50.4, 42.5, 36.9, 30.4. LC–MS (ESI, *m/z*): [M + H]<sup>+</sup> calcd for C<sub>33</sub>H<sub>37</sub>FN<sub>4</sub>O<sub>5</sub>S, 609.25; found, 609.4. Purity: 99%. [α]<sub>D</sub><sup>25</sup> 4° (c 0.5, MeOH).

4-(((*S*)-1-Oxo-1-(((*S*),*E*)-1-(phenoxysulfonyl)-5-phenylpent-1-en-3-yl)amino)-3-(*p*-tolyl)propan-2-yl)carbamoyl)pyridine 1-Oxide (**2l**). Compound **41** (0.038 g) was dissolved in DCM and cooled to 0 °C. 0.036 g HOBt, 0.087 g TBTU, and 0.19 mL DIEA were added and the mixture was stirred for 30 min. Then, 0.14 g of compound **34**-(**H**) was added and the mixture was stirred for an additional 24 h at room temperature. The reaction was stopped by adding 7 equiv of water and the residue was extracted with DCM and washed with water (2×), NaHCO<sub>3</sub> (2×), 1 M HCl (2×), and brine (1×). The solvent was removed under reduced pressure and the product was further purified by column chromatography (EtOAc/MeOH 9:1), resulting in a colorless solid (0.021 g, 13%). <sup>1</sup>H NMR (300 MHz, DMSO-*d*<sub>6</sub>): δ 9.11–8.90 (m, 1H), 8.51–8.39 (m, 1H), 8.36–8.20 (m, 2H), 7.91–7.78 (m, 2H), 7.52–7.38 (m, 2H), 7.37–7.29 (m, 2H), 7.27–7.18 (m, 6H), 7.15–7.00 (m, 4H), 6.68 (dt, *J* = 15.4, 4.0 Hz, 1H), 6.35 (dd, *J* = 15.4, 3.0 Hz, 1H), 4.72 (q, *J* = 10.1, 9.0 Hz, 1H), 4.41 (s, 1H), 3.13–2.92 (m, 2H), 2.66–2.46 (m, 2H), 2.22 (s, 3H), 1.27–1.09 (m, 2H). <sup>13</sup>C NMR (75 MHz, DMSO-*d*<sub>6</sub>): δ 171.4, 163.6, 149.6, 141.4, 139.3, 136.0, 135.0, 130.4, 129.5, 129.3, 128.8 (d, *J* = 3.6 Hz), 127.9, 126.3, 125.5, 123.6, 123.0, 55.9, 49.4, 39.9 (m), 34.5, 31.6, 21.1. mp 112–114 °C. LC–MS (ESI, *m/z*): [M + H]<sup>+</sup> calcd for C<sub>33</sub>H<sub>33</sub>N<sub>3</sub>O<sub>6</sub>S, 600.21; found, 600.3. Purity: 97%. [α]<sub>D</sub><sup>25</sup> 6° (c 0.5, MeOH).

**Enzyme Assays. Fluorometric Assays.** Rhodensain was expressed as published previously.<sup>34</sup> The increase of fluorescence upon cleavage of the fluorogenic substrate Cbz-Phe-Arg-AMC (Bachem) by rhodensain, CatB, or CatL was monitored using a TECAN Infinite F200 Pro fluorimeter (δ excitation: 365 nm, δ emission: 460 nm). The enzymes were diluted from a stock solution (rhodensain: 4 mg/mL in 10 mM sodium citrate buffer, pH 5.5; CatB (human liver, Calbiochem): 0.532 mg/mL; CatL (human liver, Calbiochem): 0.266 mg/mL) with enzyme buffer (rhodensain: 50 mM sodium acetate pH 5.5, 5 mM EDTA, 200 mM NaCl and 2 mM DTT; CatB/CatL: 50 mM Tris–HCl, 5 mM EDTA, 200 mM NaCl, 2 mM DTT, pH 6.5) and were incubated for 1 h at rt. Assays were performed in black, flat-bottom 96-well microtiter plates (Greiner bio-one) with a total volume of 200 μL at 37 °C. Inhibitors and the substrate were prepared as stock solutions in DMSO. Dilution series of inhibitors in DMSO with a minimum of seven different concentrations were prepared in duplicate at least. 180 μL assay buffer (rhodensain: 50 mM sodium acetate pH 5.5, 5 mM EDTA, 200 mM NaCl, and 0.005% Brij35; CatB/CatL: 50 mM Tris–HCl, 5 mM EDTA, 200 mM NaCl, 0.005% Brij35, pH 6.5) was added to the 96-well plates, then 5 μL of the respective enzyme in enzyme buffer, followed by 10 μL DMSO with or without inhibitor and finally 5 μL substrate (final substrate concentrations for rhodensain 10 μM, for CatB 100 μM, and for CatL 6.5 μM). Fluorescence emission was monitored directly after addition of the substrate. The presented data



are mean values of three independent measurements. Standard deviations are less than 10% unless otherwise depicted.

Screening of activity against the catalytically active subunits of the proteasome (commercially obtained from Enzo) and Dengue virus NS2/NS3 protease was performed with an inhibitor concentration of 11  $\mu\text{M}$  in DMSO.<sup>68</sup> Human 20S proteasome (from human erythrocytes, 0.5 mg/mL) was diluted with enzyme buffer (for trypsin-like activity: 50 mM Tris-HCl, 50 mM NaCl, 0.5 mM EDTA, pH 7.4; for  $\alpha$ -chymotrypsin-/caspase-like activity: 50 mM Tris-HCl, 25 mM KCl, 10 mM NaCl, 1 mM MgCl<sub>2</sub>, 0.03% SDS, pH 7.5). Trypsin-like activity was measured with the fluorogenic substrate boc-Leu-Arg-Arg-AMC (Bachem),  $\alpha$ -chymotrypsin-like activity with Succ-Leu-Leu-Val-Tyr-AMC (Bachem), and caspase-like activity with Cbz-Leu-Leu-Glu-AMC (Bachem). Measurements were conducted in black, flat-bottom 96-well microtiter plates (Greiner bio-one) by successive addition of 180  $\mu\text{L}$  enzyme buffer, 5  $\mu\text{L}$  proteasome in enzyme buffer, 10  $\mu\text{L}$  inhibitor (11  $\mu\text{M}$  in DMSO) or 10  $\mu\text{L}$  pure DMSO, and 5  $\mu\text{L}$  of the respective substrate (final substrate concentrations for trypsin-like activity 85  $\mu\text{M}$ ,  $\alpha$ -chymotrypsin-like activity 70  $\mu\text{M}$ , and caspase-like activity 80  $\mu\text{M}$ ). Fluorescence emission was monitored directly after addition of the substrate. Dengue virus NS2B/NS3 protease was diluted from a stock solution (1 mg/mL) with enzyme buffer (50 mM Tris-HCl, 1 mM Chaps, 20% glycerol).<sup>68</sup> Screening was performed with the substrate boc-Gly-Arg-Arg-AMC (Bachem) in black, flat-bottom 96-well microtiter plates (Greiner bio-one) by successive addition of 180  $\mu\text{L}$  enzyme buffer, 5  $\mu\text{L}$  Dengue protease in enzyme buffer, 10  $\mu\text{L}$  inhibitor (11  $\mu\text{M}$  in DMSO) or 10  $\mu\text{L}$  pure DMSO, and 5  $\mu\text{L}$  of the substrate (final substrate concentration 100  $\mu\text{M}$ ). Fluorescence emission was monitored directly after addition of the substrate.

The presented inhibition data for all enzymes are mean values of three independent measurements. Standard deviations are less than 10% unless otherwise depicted.

**Calculations.** The GraFit program (version 5.0.13, 2006, Erithacus Software Ltd., UK) was used for data analysis and non-linear regression.

For inhibitors showing time-independent inhibition (2a-(Z), 2k, 2j, 3a-3i, and 4a-4l), the residual enzyme activity was plotted against the inhibitor concentration. IC<sub>50</sub> values were obtained by non-linear regression using the equation

$$v_i = \frac{v_0}{1 + \left(\frac{[I]}{IC_{50}}\right)^S}$$

with  $v_0$  = enzyme activity in the absence of inhibitor,  $v_i$  = enzyme activity in the presence of inhibitor,  $[I]$  = inhibitor concentration, and  $S$  = slope factor.

$K_i$  values were obtained by correcting the IC<sub>50</sub> values to zero substrate concentration using the Cheng-Prusoff relationship<sup>32</sup>

$$K_i = \frac{IC_{50}}{1 + \frac{[S]}{K_M}}$$

Rhodesain:  $[S] = 10 \mu\text{M}$ ,  $K_M = 0.8265 \mu\text{M}$ , CatL:  $[S] = 6.25 \mu\text{M}$ ,  $K_M = 6.5 \mu\text{M}$ , CatB:  $[S] = 100 \mu\text{M}$ , and  $K_M = 150 \mu\text{M}$ .

Calculation for the inhibitors with slow, tight-binding properties (2a-2i) is presented in the Results and Discussion section.

**Dilution Assays.** Rhodesain (5  $\mu\text{L}$  from 4 mg/mL stock solution) in enzyme buffer (85  $\mu\text{L}$ ) was incubated for 30 min with inhibitors (10  $\mu\text{L}$  in DMSO) at concentrations corresponding to 10-fold the IC<sub>50</sub> value obtained from fluorometric enzyme assay to ensure complete inhibition. These mixtures (2  $\mu\text{L}$ ) were diluted 100-fold in assay buffer (198  $\mu\text{L}$ ) containing 5  $\mu\text{L}$  substrate (400  $\mu\text{M}$ ) to give a final substrate concentration of 10  $\mu\text{M}$ . Recovery of enzyme activity was measured immediately using a fluorescence readout. Rhodesain with DMSO and no inhibitor added was used as a reference while the irreversible inhibitor K11777 was used as an irreversible control.

**Dialysis Experiments.** Dialysis experiments for rhodesain were performed in a custom-built dialysis chamber, allowing the parallel examination of five samples.<sup>26</sup> A 3.5 kDa MW cut-off dialysis tubing (Carl Roth, Zellultrans MWCO 3.5 kDa) was cut into half and placed in

the instrument, separating a continuous flow of buffer from five cavities at the top of the instrument, where the samples (800  $\mu\text{L}$ ) were added. Therefore, 20  $\mu\text{L}$  rhodesain in enzyme buffer was added to 740  $\mu\text{L}$  assay buffer and 40  $\mu\text{L}$  DMSO with or without inhibitor. Inhibitor concentrations of 10-fold the IC<sub>50</sub> value were chosen in order to guarantee complete inhibition. After incubation for 30 min, the mixtures were transferred to the cavities in the instrument and dialyzed against a continuous flow of assay buffer containing 5% DMSO (300 mL/h). Samples (97.5  $\mu\text{L}$ ) were taken at different time points (10, 30, 60, and 120 min) and 2.5  $\mu\text{L}$  of a substrate solution was added to give a final substrate concentration of 10  $\mu\text{M}$ . Enzyme activity was determined by directly measuring the fluorescence emission. The results are given in fractional activity of uninhibited rhodesain used in the same experiment as positive control.

**Docking Procedures.** *Procedure for Non-covalent Docking with FlexX/LeadIT (vs. 2.1.3).*<sup>11</sup> Non-covalent docking experiments were performed using the crystal structure of rhodesain with covalently bound inhibitor K11777 (pdb entry 2p7u).<sup>60</sup> The binding site was defined as a 6.5 Å shell around K11777. Water molecules present in the crystal structure were omitted except HOH-512, which mediates hydrogen bonding between the inhibitor and the peptide backbone. Generation of 3D-coordinates and energy minimization of the ligands were accomplished with the Molecular Operating Environment (MOE2014.09) using the MMFF94x force field.<sup>26</sup> Docking calculations were executed with LeadIT version 2.1.3.<sup>27</sup> The results presented in Table 1 are those with the best HYDE score<sup>69,70</sup> selected from the 10 highest-priced solutions according to FlexX score (Table 7.1).

*Procedure for Covalent Docking with DOCKTITE.*<sup>60</sup> Covalent docking was performed with the DOCKTITE software implementation (version 1.2) for Molecular Operating Environment (MOE, 2014.09; Chemical Computing Group ULC, 1010 Sherbooke St. West, Suite #910, Montreal, QC, Canada, H3A 2R7, 2021)<sup>11,27</sup> using the crystal structure of rhodesain with covalently bound inhibitor K11777 (pdb entry 2p7u).<sup>60</sup> Energy minimization of the ligands was performed with MOE using the MMFF94x force field.<sup>71</sup> The different warheads were implemented into the DOCKTITE warhead filter file as described in the DOCKTITE manual. The standard DOCKTITE protocol was followed as described. The main pharmacophore docking step was performed without pharmacophore restriction for the nucleophilic sulfur of Cys25. The Amber12:EHT force field<sup>72</sup> was used for the pharmacophore docking step. Docking solutions were rescored with the MOE implemented scoring functions Affinity dG and additionally with the external empirical scoring function DSX.<sup>73</sup> The results shown in Table S1 are those with the best DSX scores.

**Mass Spectrometry (MS).** *ESI MS Analysis.* Lyophilized rhodesain was reconstituted at 4 mg/mL in 50 mM NaOAc, 200 mM NaCl, and 5 mM EDTA (pH 5.5). Prior to MS analysis, rhodesain was purified by weak anion exchange (WAX) chromatography using an ÅKTA protein purification system (GE Healthcare) equipped with a ProPac WAX-10G 4 × 50 mm guard and a ProPac WAX-10 4 × 250 mm analytical column (Thermo Fisher Scientific). 100  $\mu\text{L}$  of rhodesain stock solution (4 mg/mL) was diluted in 20 mM imidazole, 1 mM DTT in water (pH 6.0) to a final volume of 1 mL, and separated running a gradient from 0 to 40% B in 40 min. Mobile phase A was 20 mM imidazole, 1 mM DTT in water (pH 6) and Solvent B 1 M NaCl, 20 mM imidazole, and 1 mM DTT in water (pH 6). Collected fractions were tested for activity.

For mass spectrometric analysis, the WAX fraction containing active rhodesain was further diluted in 50 mM NaOAc, 200 mM NaCl, 5 mM EDTA, and 5 mM DTT (pH 5.5) and incubated for 1 h at rt. After the addition of the inhibitors at a final concentration of 10  $\mu\text{M}$ , samples were analyzed by LC-MS using a nanoAcquity UPLC system (Waters Corporation) coupled to a nano-ESI-Q-TOF mass spectrometer (Synapt G2-S HDMS, Waters Corporation). Rhodesain without compound served as control. Protein-drug complexes were loaded onto a 200  $\mu\text{m}$  × 5 cm PepSwift Monolithic PS-DVB column from Dionex (Thermo Scientific) using direct injection mode. For LC separation, two mobile phases were used. Mobile phase A contained 0.1% formic acid (FA) and 3% DMSO in ultrapure water, whereas mobile phase B consisted of 0.1% FA and 3% DMSO in ACN. A gradient of 10–90% mobile phase B was run over 7 min at a flow rate of

2000 nL/min. Column temperature was set to 45 °C. After separation, the column was rinsed with 90% of mobile phase B and re-equilibrated under initial conditions. All MS analyses were conducted in positive-mode ESI.

**MALDI-TOF MS Analysis.** For this analysis, a recombinant rhodesain mutant expressed in *Pichia pastoris* was used as described in the enzyme assay section. The lyophilized protein was reconstituted in buffer A (pH 5.5, 50 mM NaOAc, 200 mM NaCl, 5 mM EDTA) at a concentration of 4 mg/mL (= 174  $\mu$ M). This stock solution was diluted into buffer B (pH 5.5, 50 mM NaOAc, 200 mM NaCl, 5 mM EDTA, 5 mM DTT) to a final protein concentration of 1 or 10  $\mu$ M and incubated for approximately 1 h, after which the compound of interest (4 mM stock in DMSO) was added at a final inhibitor concentration of 100  $\mu$ M. Later, the analytes were desalted using Zeba Spin Desalting Columns (7 kDa MWCO, 0.5 mL; Thermo Fisher Scientific) in accordance with the manufacturer's instructions and afterward coprecipitated with a MALDI-matrix, utilizing two separate approaches: For the first method, a thin layer of sinapinic acid (saturated ethanolic solution) was prepared on the target, onto which, after film formation, a volumetric 3:1 mixture of matrix-solution to analyte solution was applied. For the second method, using a mixture of  $\alpha$ -cyano-4-hydroxycinnamic acid and 2,5-dihydroxybenzoic acid,<sup>40,44</sup> the preparation of a basal matrix film was omitted and a volumetric 1:1 mixture of matrix-solution to analyte solution was prepared and applied to the target. After evaporation of the solvents (ca. 15 min), measurements were carried out on a rapifleX MALDI-TOF/TOF mass spectrometer (Bruker Daltonik GmbH, Bremen, Germany). The instrument is equipped with a scanning smartbeam 10 kHz Nd:YAG laser at a wavelength of 355 nm and a 10 bit 5 GHz digitizer. The acceleration voltage was set to 20 kV and the mass spectra were recorded in positive ion linear mode. Calibration was done with the Bruker protein calibration standard II in a mass range from 10 to 70 kDa. Samples were measured at a laser power of 100% (sinapinic acid) or 70% (matrix mixture), with random walk ionization across the sample spot. As control samples, rhodesain in buffer B with a DMSO concentration matching the samples, rhodesain incubated with a reportedly non-covalent inhibitor,<sup>11</sup> and a known covalent-irreversible inhibitor (KI1777)<sup>74</sup> were used. Data analysis was performed using the open-source software mMass.<sup>68</sup>

**QM/MM Computations.** MD simulations were performed with the Amber program package (version 2018) in combination with the FF14SB force field. The unknown parameters for the ligand were calculated using GAFF.<sup>75</sup> The obtained enzymatic system was balanced with sodium ions. We added an octahedral water envelope of 10 Å consisting of TIP3P water molecules (Figure S11).<sup>76</sup> All MD simulations were performed under periodic boundary conditions in three consecutive steps. In the first step, the cage of water molecules and then the whole system was minimized. In the next step, the system was heated in a controlled way from 0 to 300 K at 1 bar, using the SHAKE algorithm<sup>77</sup> employing the Langevin or Berendsen thermostat.<sup>77,78</sup> In the last step, the actual MD simulation with a duration of at least 10 ns was performed.

We used the subtractive QM/MM approach employing the electrostatic embedding scheme as implemented in the program package Gaussian (version 2016).<sup>79</sup> The QM part is specified in Figure S12. Please note that larger QM spaces did not lead to considerably changes (Table S4). For the QM part, we employed the  $\omega$ B97XD functional in combination with the 6-31+G\* basis sets.<sup>80–82</sup> The TAO-Toolkit was used.<sup>83</sup> For the intrinsic reaction coordinate (IRC) computations, the transition states were determined using the Berny-Algorithm.<sup>84</sup> All transition states were proved by frequency calculations.

The reaction paths were characterized by a two-step procedure. The covalent step of the inhibition mechanism first consists of the attack of the sulfur center of the thiolate group of Cys25 on the C<sub>2</sub> center of the alkene group. Additionally, a proton transfer from the protonated His152 moiety to the C<sub>1</sub> center occurs (Figure 1). Because it is unclear whether both steps proceed subsequently or simultaneously, we first computed two-dimensional scans selecting the distances R(S<sub>Cys</sub>–C<sub>2</sub>) and R(H<sub>His</sub>–C<sub>1</sub>) as main reaction parameters (Figure 14). By varying the main reaction parameters and optimizing all other internal

coordinates for each pair of main coordinates, a minimum energy path (MEP) from the reactant to the product is obtained, which gives the first information about the shape of the reaction path. Starting from the barriers obtained in these scans, we performed intrinsic reaction coordinate (IRC) simulations. Due to the roughness of the computed PES, often more than one transition state was found for the two-dimensional surface. In such cases, we started IRC from each TS to ensure that they lead to similar reactants and products. This was indeed the case. One example is shown in Figures S8 and S10 in which computations started from slightly different TS but yielded comparable shapes for the reaction paths. The same holds for the second step of the reaction path given in Figure 16. For this frame, we found four TS whose IRCs all lead to very similar results.

**Antitrypanosomal Activity and Cytotoxicity.** Antitrypanosomal activity of **2a**, **2d**, **2e**, **3d**, **4d**, and **4e** against the *T. brucei brucei* BS449 cell line, a descendant of the Lister 427 strain,<sup>85,86</sup> was determined using the ATPlite assay as described previously.<sup>56,57,87</sup> **2a**, **2d**, **2e**, **3d**, **4d**, and **4e** were prepared as 5 mM stock solutions in DMSO and diluted in HMI-9 medium in multiple steps (1:3, then 1:10, and subsequently in ten 1:2 dilution steps using separate microplates). In white 96-well microplates (PerkinElmer), 10  $\mu$ L of the final 101 dilutions were added to 90  $\mu$ L of a cell suspension containing 2500 cells/mL, leading to final concentrations of each tested compound from 16.67  $\mu$ M to 32.55 nM in the microplates. As a negative control, 0.3% DMSO was added to the cell suspension corresponding to the highest DMSO concentration added by compound application. Addition of 10% DMSO served as a positive control because all cells die at this concentration. The plates were prepared as triplicates and incubated for 24 and 48 h at 37 °C and 5% CO<sub>2</sub>. After the respective incubation time, 50  $\mu$ L ATPlite 1 step solution (PerkinElmer) was added to each well. The plate was shaken orbitally for 2 min and luminescence was measured at room temperature with an Infinite M200 PRO plate reader (Tecan Trading AG). The measured luminescence was plotted against the compound concentration to obtain a dose–response curve. The EC<sub>50</sub> values were determined using GraFit version 5.013 (EriThacus Software Ltd.).

Antitrypanosomal activity of the compounds **1**, **4a**, **4j**, and **4l** was determined as described previously using the Alamar Blue assay.<sup>54,55</sup> Cytotoxicities against the macrophage cell line J774.1 and HeLa cells were investigated according to previously described methods.<sup>12,88</sup>

**In Vitro Metabolism Studies.** Rat liver microsomes were purchased from Sigma-Aldrich and characterized for cytochrome P450, cytochrome B5, and the activity of CYP1A, CYP3A, CYP2C, and cytochrome *c* reductase. The assay was performed as published previously.<sup>68</sup>

First, NADPH was generated by incubating potassium phosphate buffer (395  $\mu$ L, 100 mM, pH 7.4), MgCl<sub>2</sub> (25  $\mu$ L, 80 mM), glucose-6-phosphate (25  $\mu$ L, 100 mM), NADP disodium salt (25  $\mu$ L, 20 mM), and glucose-6-dehydrogenase (25  $\mu$ L, 100 IU/mL, Sigma-Aldrich) at 37 °C for 10 min. After addition of the microsomes (25  $\mu$ L, 20 mg/mL) and incubation (10 min) at 37 °C, the inhibitors (1  $\mu$ L, 5.21 mM in acetonitrile) were added to the mixture and the incubation continued at 37 °C for 60 min. Aliquots of 50  $\mu$ L were taken at 0, 15, 30, 45, and 60 min and added to 100  $\mu$ L of ice-cold acetonitrile to stop the reaction. The samples were centrifuged at 4 °C, 10,000g for 10 min. The supernatant was analyzed by LC–MS/MS using an Agilent Poroshell 120 EC-C18 150  $\times$  2.10 mm 4  $\mu$ m column; mobile phase: compound **1** (35% acetonitrile, 55% H<sub>2</sub>O, 10% of a 0.1% solution of formic acid in water) and compound **2d**-(H) (55% acetonitrile, 35% H<sub>2</sub>O, 10% of a 0.1% solution of formic acid in water). Ion chromatograms were obtained using electronic filters for the ions of interest. Control incubations were performed with potassium phosphate buffer instead of microsomes. The LC–MS chromatograms and their corresponding mass spectra were analyzed using MestReNova (v. 12.0.4).<sup>89</sup>

**In Vivo Distribution Studies. Animals and Treatments.** 60 male and female CD1 mice of 35–45 g body weight (56–62 days of age) were purchased from Charles River Laboratories, Sulzfeld, Germany. Five mice per cage were housed in a controlled room (22 °C, 50–65% humidity; day/night cycle of 12/12 h) with free access to water and the standard laboratory diet (Altromin, Germany). After 7 days of



acclimatization, they were randomly divided into eight groups in which each group received four different testing compounds (**1**, **2d-(H)**) at a dose of 25 mg/kg by i.p. injection or oral gavage (p.o.). Compound **1** was diluted in 1% DMSO, while **2d-(H)** was diluted in 2% DMSO. The i.p. injection was given once only while the p.o. administrations were given for 4 days, twice daily (8 doses in total) at 9 and 18 o'clock. The dose of 25 mg/kg was chosen based on preliminary tests. 60 min after the administration of the testing compounds, blood was collected (about 0.2 mL) from the facial vein using a lancet (Goldenrod animal lancet). At the end of the experiment (3 h after the last drug administration), the animals were sacrificed by decapitation under isoflurane anesthesia. Trunk blood was collected, and the brain was removed and homogenized. Experiments were carried out according to the German Law for Animal Protection and were registered with Regierungspräsidium Darmstadt (FR/1021). All efforts were made to minimize animal numbers and animal suffering.

**Microdialysis Experiments.** Mice were anesthetized with isoflurane (induction dose 5%, maintenance dose 1.5% v/v in synthetic air) (Air Liquide, Düsseldorf, Germany) and placed in a stereotaxic frame (Stoelting, Chicago, IL, USA). A Y-shaped, concentric microdialysis probe with a molecular weight cutoff of 30 kDa and an exchange area of 2 mm was manufactured as described previously.<sup>90</sup> The probe was implanted in the hippocampus with the following coordinates from bregma: AP -2.0 mm; L +2.0 mm; DV -2.3 mm.<sup>91</sup> The mice were allowed to recover overnight. On the next day, the probes were perfused (rate: 2  $\mu$ L/min) with artificial cerebrospinal fluid (aCSF; 147 mM NaCl, 4 mM KCl, 1.2 mM CaCl<sub>2</sub>, and 1.2 mM MgCl<sub>2</sub>) for 4 h and dialysates were collected every 20 min. After dialysates were collected for 1 h for equilibration, the test compound was given as described above. A blood sample was collected 1 h after administration of the test compound. At the end of the experiment (3 h after the last drug administration), the animals were sacrificed by decapitation under isoflurane anesthesia. Trunk blood was collected, and the brain was removed and homogenized.

**Sample Preparation and LC-MS Analysis.** The blood was centrifuged at 4 °C, 1500g for 20 min and the plasma supernatant was extracted with acetonitrile and centrifuged again at 4 °C, 10,000g for 10 min. The supernatant was analyzed by LC-MS using an Agilent Poroshell 120 EC-C18 150  $\times$  2.10 mm 4  $\mu$ m column; mobile phase: compound **1** (35% acetonitrile, 55% H<sub>2</sub>O, 10% of a 0.1% solution of formic acid in water) and compound **2d-(H)** (55% acetonitrile, 35% H<sub>2</sub>O, 10% of a 0.1% solution of formic acid in water). Ion chromatograms were obtained using electronic filters for the ions of interest. The LC-MS chromatograms and their corresponding mass spectra were analyzed using MestReNova (v. 12.0.4).<sup>89</sup>

The brain tissue was homogenized using a mixture of acetonitrile/MilliQ-water (ratio 2:1, 2 mL per 300 mg brain) in a tissue grinder (Potter S, B. Braun, Melsungen, Germany) at 1,500 rpm and 15 strokes. Afterward, the homogenate was centrifuged at 4 °C, 10,000g for 10 min and the supernatant was lyophilized. The lyophilizate was extracted with 400  $\mu$ L acetonitrile and this extract was analyzed via LC-MS as described above. The fractions of the microdialysate were used without further processing. The AUC that was obtained from the extracted ion chromatograms was normalized to a volume of 500  $\mu$ L for the plasma samples or a weight of 450 mg for the brain homogenates. The average AUC for every sample was calculated from experiments performed in triplicate.

## ■ ASSOCIATED CONTENT

### SI Supporting Information

The Supporting Information is available free of charge at <https://pubs.acs.org/doi/10.1021/acs.jmedchem.1c01002>.

Scores for non-covalent (FlexX) and covalent docking (DOCKTITE); MALDI-TOF MS spectra of complexes of rhodesain with different inhibitors and different matrix substances; ESI MS spectra of complexes of rhodesain with inhibitors (**Z**)-**2a** and **2j**; additional data for the QM/MM computations; and ESI MS spectra of the in

vitro metabolism and in vivo distribution studies of **1** and **2d-(H)** (PDF)

HPLC traces of lead compounds and molecular formula strings (CSV)

## ■ AUTHOR INFORMATION

### Corresponding Author

Tanja Schirmeister – Institute of Pharmaceutical and Biomedical Sciences (IPBS), Johannes Gutenberg University, 55128 Mainz, Germany; Email: [schirmei@uni-mainz.de](mailto:schirmei@uni-mainz.de)

### Authors

Sascha Jung – Institute of Pharmaceutical and Biomedical Sciences (IPBS), Johannes Gutenberg University, 55128 Mainz, Germany; Present Address: Faculty of Chemistry and Chemical Biology, TU Dortmund, Otto-Hahn-Str. 6, 44227 Dortmund, Germany

Natalie Fuchs – Institute of Pharmaceutical and Biomedical Sciences (IPBS), Johannes Gutenberg University, 55128 Mainz, Germany; [orcid.org/0000-0001-6404-676X](https://orcid.org/0000-0001-6404-676X)

Patrick Johe – Institute of Pharmaceutical and Biomedical Sciences (IPBS), Johannes Gutenberg University, 55128 Mainz, Germany

Annika Wagner – Department of Chemistry, Biochemistry Section, Johannes Gutenberg University, 55128 Mainz, Germany; Present Address: Institute of Organic Chemistry & Macromolecular Chemistry (IOMC), Friedrich Schiller University, Humboldtstraße 10, 07743 Jena, Germany; Cluster of Excellence “Balance of the Microverse”, Friedrich-Schiller-University Jena, Germany.

Erika Diehl – Department of Chemistry, Biochemistry Section, Johannes Gutenberg University, 55128 Mainz, Germany

Tri Yuliani – Institute for Pharmacology and Clinical Pharmacy, Goethe University, 60439 Frankfurt, Germany; Present Address: Research Center for Chemistry, Indonesian Institute of Sciences (LIPI), Gd. 452 Kawasan PUSPIPTEK, Tangerang Selatan, Indonesia.

Collin Zimmer – Institute of Pharmaceutical and Biomedical Sciences (IPBS), Johannes Gutenberg University, 55128 Mainz, Germany

Fabian Barthels – Institute of Pharmaceutical and Biomedical Sciences (IPBS), Johannes Gutenberg University, 55128 Mainz, Germany

Robert A. Zimmermann – Institute of Pharmaceutical and Biomedical Sciences (IPBS), Johannes Gutenberg University, 55128 Mainz, Germany

Philipp Klein – Department of Chemistry, Organic Chemistry Section, Johannes Gutenberg University, 55128 Mainz, Germany

Waldemar Waigel – Department of Physical and Theoretical Chemistry, Julius-Maximilians-University, 97074 Würzburg, Germany

Jessica Meyr – Department of Physical and Theoretical Chemistry, Julius-Maximilians-University, 97074 Würzburg, Germany

Till Opatz – Department of Chemistry, Organic Chemistry Section, Johannes Gutenberg University, 55128 Mainz, Germany; [orcid.org/0000-0002-3266-4050](https://orcid.org/0000-0002-3266-4050)

Stefan Tenzer – Institute for Immunology, University Medical Center, Johannes Gutenberg University, 55131 Mainz, Germany; [orcid.org/0000-0003-3034-0017](https://orcid.org/0000-0003-3034-0017)

**Ute Distler** – Institute for Immunology, University Medical Center, Johannes Gutenberg University, 55131 Mainz, Germany; [orcid.org/0000-0002-8031-6384](https://orcid.org/0000-0002-8031-6384)

**Hans-Joachim Räder** – Max Planck Institute for Polymer Research, 55128 Mainz, Germany; [orcid.org/0000-0002-7292-4013](https://orcid.org/0000-0002-7292-4013)

**Christian Kersten** – Institute of Pharmaceutical and Biomedical Sciences (IPBS), Johannes Gutenberg University, 55128 Mainz, Germany

**Bernd Engels** – Department of Physical and Theoretical Chemistry, Julius-Maximilians-University, 97074 Würzburg, Germany; [orcid.org/0000-0003-3057-389X](https://orcid.org/0000-0003-3057-389X)

**Ute A. Hellmich** – Department of Chemistry, Biochemistry Section, Johannes Gutenberg University, 55128 Mainz, Germany; Center for Biomolecular Magnetic Resonance (BMRZ), Goethe University, 60438 Frankfurt, Germany; Present Address: Institute of Organic Chemistry & Macromolecular Chemistry (IOMC), Friedrich Schiller University, Humboldtstraße 10, 07743 Jena, Germany; Cluster of Excellence “Balance of the Microverse”, Friedrich-Schiller-University Jena, Germany.

**Jochen Klein** – Institute for Pharmacology and Clinical Pharmacy, Goethe University, 60439 Frankfurt, Germany

Complete contact information is available at:

<https://pubs.acs.org/10.1021/acs.jmedchem.1c01002>

#### Author Contributions

\*\*S.J. and N.F. contributed equally.

#### Funding

Financial support by the Rhine-Main Universities fund (RMU-Initiativfonds Forschung) is gratefully acknowledged. Funded by the Deutsche Forschungsgemeinschaft (DFG, German Research Foundation) under Germany's Excellence Strategy—EXC 2051—Project ID390713860.

#### Notes

The authors declare no competing financial interest.

#### ACKNOWLEDGMENTS

E.D. acknowledges a PhD fellowship from the Sibylle Kalkhof-Rose-Stiftung.

#### ABBREVIATIONS

AcOH, acetic acid; aCSF, artificial cerebrospinal fluid; ADME, absorption, distribution, metabolism, excretion; AMC, 7-amido-4-methylcoumaryl; aq, aqueous; Arg, arginine; Asp, aspartate; AUC, area under the curve; Bn, benzyl; boc, *tert*-butyl carbonate; CatB, cathepsin B; CatL, cathepsin L; Cbz, carbobenzyloxy; chymotrp., chymotrypsin; cpd, compound; Cys, cysteine; CYP, cytochrome P450; DCM, dichloromethane; DCTB, *trans*-2-[3-(4-*tert*-butylphenyl)-2-methyl-2-propenylidene]malononitrile; DECP, diethyl chlorophosphate; DIEA, *N,N*-diisopropylethylamine; DHBD, 2,3-dihydrobenzo-*[b]*[1,4]dioxine; DMF, dimethyl formamide; DMSO, dimethyl sulfoxide; DTT, dithiothreitol; EDC, 1-ethyl-3-(3-dimethylaminopropyl)carbodiimide; EDTA, ethylenediamine tetraacetic acid; EtOAc, ethyl acetate; ESI, electrospray ionization; Glu, glutamate; Gly, glycine; HAT, Human African Trypanosomiasis; HeLa cells, Henrietta Lacks cells; HOBt, hydroxybenzotriazole; HPhe, homophenylalanine; HPLC, high-pressure liquid chromatography; HWE, Horner–Wadsworth–Emmons; i.p., intraperitoneal; KHMDS, potassium bis(trimethylsilyl)amide; LC, liquid chromatography; Leu, leucine;

LHMDS, lithium bis(trimethylsilyl)amide; MALDI, matrix-assisted laser desorption/ionization; *m*CPBA, *meta*-chloroperbenzoic acid; Me, methyl; Met, methionine; MM, molecular mechanics; MOE, molecular operating environment; MS, mass spectrometry; MS-Cl, mesyl chloride; mp, melting point; NADPH, nicotinamide adenine dinucleotide phosphate (reduced form); *n*-BuLi, *n*-butyllithium; n.d., not determined; NHS, *N*-hydroxysuccinimide; NMR, nuclear magnetic resonance; NTD, neglected tropical disease; PDB, Protein Database; Ph, phenyl; Phe, phenylalanine; Pip, piperazine; ppm, parts per million; Pyr, pyridine; QM, quantum mechanics; RMSD, root-mean-square deviation; rt, room temperature; SAR, structure–activity relationship; SPR, surface plasmon resonance; Succ, *N*-succinyl; *T. b. gambiense*, *Trypanosoma brucei gambiense*; *T. b. rhodesiense*, *Trypanosoma brucei rhodesiense*; TBTU, 2-(1H-benzotriazole-1-yl)-1,1,3,3-tetramethyluronium tetrafluoroborate; TEA, triethyl amine; TFA, trifluoroacetic acid; THF, tetrahydrofuran; TLC, thin layer chromatography; TOF, time of flight; Tris, tris(hydroxymethyl)aminomethane; Trp, tryptophan; Tyr, tyrosine; UV, ultraviolet; val, valine; VS, vinyl sulfone; X-ray, energetic high-frequency electromagnetic radiation

#### REFERENCES

- (1) Malvy, D.; Chappuis, F. Sleeping Sickness. *Clin. Microbiol. Infect.* **2011**, *17*, 986–995.
- (2) Brun, R.; Blum, J.; Chappuis, F.; Burri, C. Human African Trypanosomiasis. *Lancet* **2010**, *375*, 148–159.
- (3) Priotto, G.; Kasparian, S.; Mutombo, W.; Nguouama, D.; Ghorashian, S.; Arnold, U.; Ghabri, S.; Baudin, E.; Buard, V.; Kazadi-Kyanza, S.; Ilunga, M.; Mutangala, W.; Pohlig, G.; Schmid, C.; Karunakara, U.; Torrele, E.; Kande, V. Nifurtimox-Eflornithine Combination Therapy for Second-Stage African Trypanosoma Brucei Gambiense Trypanosomiasis: A Multicentre, Randomised, Phase III, Non-Inferiority Trial. *Lancet* **2009**, *374*, 56–64.
- (4) Mesu, V. K. B. K.; Kalonji, W. M.; Bardonneau, C.; Mordt, O. V.; Blesson, S.; Simon, F.; Delhomme, S.; Bernhard, S.; Kuziena, W.; Lubaki, J.-P. F.; Vuvu, S. L.; Ngima, P. N.; Mbembo, H. M.; Ilunga, M.; Bonama, A. K.; Heradi, J. A.; Solomo, J. L. L.; Mandula, G.; Badibabi, L. K.; Dama, F. R.; Lukula, P. K.; Tete, D. N.; Lumbala, C.; Scherrer, B.; Strub-Wourgaft, N.; Tarral, A. Oral Fexinidazole for Late-Stage African Trypanosoma Brucei Gambiense Trypanosomiasis: A Pivotal Multicentre, Randomised, Non-Inferiority Trial. *Lancet* **2018**, *391*, 144–154.
- (5) Fairlamb, A. H. Chemotherapy of Human African Trypanosomiasis: Current and Future Prospects. *Trends Parasitol.* **2003**, *19*, 488–494.
- (6) Steverding, D.; Sexton, D. W.; Wang, X.; Gehrke, S. S.; Wagner, G. K.; Caffrey, C. R. Trypanosoma Brucei: Chemical Evidence That Cathepsin L Is Essential for Survival and a Relevant Drug Target. *Int. J. Parasitol.* **2012**, *42*, 481–488.
- (7) Nikolskaia, O. v.; de A Lima, A. P. C.; Kim, Y. v.; Lonsdale-Eccles, J. D.; Fukuma, T.; Scharfstein, J.; Grab, D. J. Blood-Brain Barrier Traversal by African Trypanosomes Requires Calcium Signaling Induced by Parasite Cysteine Protease. *J. Clin. Invest.* **2006**, *116*, 2739–2747.
- (8) Scory, S.; Caffrey, C. R.; Stierhof, Y.-D.; Ruppel, A.; Steverding, D. Trypanosoma Brucei: Killing of Bloodstream Formsin Vitroandin Vivo by the Cysteine Proteinase Inhibitor Z-Phe-Ala-CHN2. *Exp. Parasitol.* **1999**, *91*, 327–333.
- (9) Kerr, I. D.; Wu, P.; Marion-Tsukamaki, R.; Mackey, Z. B.; Brinen, L. S. Crystal Structures of TbCatB and Rhodesain, Potential Chemotherapeutic Targets and Major Cysteine Proteases of Trypanosoma Brucei. *PLoS Neglected Trop. Dis.* **2010**, *4*, No. e701.
- (10) Johé, P.; Jaenicke, E.; Neuweiler, H.; Schirmeister, T.; Kersten, C.; Hellmich, U. A. Structure, Interdomain Dynamics and PH-Dependent Autoactivation of pro-Rhodesain, the Main Lysosomal



Cysteine Protease from African Trypanosomes. *J. Biol. Chem.* **2021**, *296*, 100565.

(11) Kerr, I. D.; Lee, J. H.; Farady, C. J.; Marion, R.; Rickert, M.; Sajid, M.; Pandey, K. C.; Caffrey, C. R.; Legac, J.; Hansell, E.; Mckerrow, J. H.; Craik, C. S.; Rosenthal, P. J.; Brinen, L. S. Vinyl Sulfones as Antiparasitic Agents and a Structural Basis for Drug Design. *J. Biol. Chem.* **2009**, *284*, 25697–25703.

(12) Schirmeister, T.; Kesselring, J.; Jung, S.; Schneider, T. H.; Weickert, A.; Becker, J.; Lee, W.; Bamberger, D.; Wich, P. R.; Distler, U.; Tenzer, S.; Johé, P.; Hellmich, U. A.; Engels, B. Quantum Chemical-Based Protocol for the Rational Design of Covalent Inhibitors. *J. Am. Chem. Soc.* **2016**, *138*, 8332–8335.

(13) Singh, J.; Petter, R. C.; Baillie, T. A.; Whitty, A. The Resurgence of Covalent Drugs. *Nat. Rev. Drug Discovery* **2011**, *10*, 307–317.

(14) Bauer, R. A. Covalent Inhibitors in Drug Discovery: From Accidental Discoveries to Avoided Liabilities and Designed Therapies. *Drug Discovery Today* **2015**, *20*, 1061–1073.

(15) Kalgutkar, A. S.; Dalvie, D. K. Drug Discovery for a New Generation of Covalent Drugs. *Expert Opin. Drug Discovery* **2012**, *7*, 561–581.

(16) Lammert, C.; Einarsson, S.; Saha, C.; Niklasson, A.; Björnsson, E.; Chalasani, N. Relationship between Daily Dose of Oral Medications and Idiosyncratic Drug-Induced Liver Injury: Search for Signals. *Hepatology* **2008**, *47*, 2003–2009.

(17) Lee, C.-U.; Grossmann, T. N. Reversible Covalent Inhibition of a Protein Target. *Angew. Chem., Int. Ed.* **2012**, *51*, 8699–8700.

(18) Copeland, R. A.; Pompliano, D. L.; Meek, T. D. Drug-Target Residence Time and Its Implications for Lead Optimization. *Nat. Rev. Drug Discovery* **2006**, *5*, 730–739.

(19) Bradshaw, J. M.; McFarland, J. M.; Paavilainen, V. O.; Bisconte, A.; Tam, D.; Phan, V. T.; Romanov, S.; Finkle, D.; Shu, J.; Patel, V.; Ton, T.; Li, X.; Loughhead, D. G.; Nunn, P. A.; Karr, D. E.; Gerritsen, M. E.; Funk, J. O.; Owens, T. D.; Verner, E.; Brameld, K. A.; Hill, R. J.; Goldstein, D. M.; Taunton, J. Prolonged and Tunable Residence Time Using Reversible Covalent Kinase Inhibitors. *Nat. Chem. Biol.* **2015**, *11*, 525–531.

(20) Johe, P.; Jung, S.; Endres, E.; Kersten, C.; Zimmer, C.; Ye, W.; Sönnichsen, C.; Hellmich, U. A.; Sotriffer, C.; Schirmeister, T.; Neuweiler, H. Warhead Reactivity Limits the Speed of Inhibition of the Cysteine Protease Rhodospain. *ACS Chem. Biol.* **2021**, *16*, 661–670.

(21) Schechter, I.; Berger, A. On the Size of the Active Site in Proteases. I. Papain. *Biochem. Biophys. Res. Commun.* **1967**, *27*, 157–162.

(22) Jaishankar, P.; Hansell, E.; Zhao, D.-M.; Doyle, P. S.; McKerrow, J. H.; Renslo, A. R. Potency and Selectivity of P2/P3-Modified Inhibitors of Cysteine Proteases from Trypanosomes. *Bioorg. Med. Chem. Lett.* **2008**, *18*, 624–628.

(23) Schirmeister, T.; Schmitz, J.; Jung, S.; Schmenger, T.; Krauth-Siegel, R. L.; Gütschow, M. Evaluation of Dipeptide Nitriles as Inhibitors of Rhodospain, a Major Cysteine Protease of Trypanosoma Brucei. *Bioorg. Med. Chem. Lett.* **2017**, *27*, 45–50.

(24) Yang, P.-Y.; Wang, M.; Li, L.; Wu, H.; He, C. Y.; Yao, S. Q. Design, Synthesis and Biological Evaluation of Potent Azadipeptide Nitrile Inhibitors and Activity-Based Probes as Promising Anti-Trypanosoma Brucei Agents. *Chem.—Eur. J.* **2012**, *18*, 6528–6541.

(25) Caffrey, C. R.; Hansell, E.; Lucas, K. D.; Brinen, L. S.; Alvarez Hernandez, A.; Cheng, J.; Gwaltney, S. L.; Roush, W. R.; Stierhof, Y.-D.; Bogoy, M.; Steverding, D.; McKerrow, J. H. Active Site Mapping, Biochemical Properties and Subcellular Localization of Rhodospain, the Major Cysteine Protease of Trypanosoma Brucei Rhodospain. *Mol. Biochem. Parasitol.* **2001**, *118*, 61–73.

(26) LeadIT/FlexX; BioSolveIT GmbH: St. Augustin, Germany 2012.

(27) Scholz, C.; Knorr, S.; Hamacher, K.; Schmidt, B. DOCKTITE-A Highly Versatile Step-by-Step Workflow for Covalent Docking and Virtual Screening in the Molecular Operating Environment. *J. Chem. Inf. Model.* **2015**, *55*, 398–406.

(28) Ng, S. L.; Yang, P.-Y.; Chen, K. Y.-T.; Srinivasan, R.; Yao, S. Q. “Click” Synthesis of Small-Molecule Inhibitors Targeting Caspases. *Org. Biomol. Chem.* **2008**, *6*, 844–847.

(29) Sun, A. C.; McClain, E. J.; Beatty, J. W.; Stephenson, C. R. J. Visible Light-Mediated Decarboxylative Alkylation of Pharmaceutically Relevant Heterocycles. *Org. Lett.* **2018**, *20*, 3487–3490.

(30) Ehmke, V.; Winkler, E.; Banner, D. W.; Haap, W.; Schweizer, W. B.; Rottmann, M.; Kaiser, M.; Freymond, C.; Schirmeister, T.; Diederich, F. Optimization of Triazine Nitriles as Rhodospain Inhibitors: Structure-Activity Relationships, Bioisosteric Imidazopyridine Nitriles, and X-Ray Crystal Structure Analysis with Human Cathepsin L. *ChemMedChem* **2013**, *8*, 967–975.

(31) DIXON, M. The Determination of Enzyme Inhibitor Constants. *Biochem. J.* **1953**, *55*, 170–171.

(32) Yung-Chi, C.; Prusoff, W. H. Relationship between the Inhibition Constant (KI) and the Concentration of Inhibitor Which Causes 50 per Cent Inhibition (I50) of an Enzymatic Reaction. *Biochem. Pharmacol.* **1973**, *22*, 3099–3108.

(33) Purich, D. L. *Enzyme Kinetics, Catalysis and Control, A Reference of Theory and Best-Practice Methods*; Elsevier, 2010.

(34) Ludewig, S.; Kossner, M.; Schiller, M.; Baumann, K.; Schirmeister, T. Enzyme Kinetics and Hit Validation in Fluorimetric Protease Assays. *Curr. Top. Med. Chem.* **2010**, *10*, 368–382.

(35) Berman, H. M.; Westbrook, J.; Feng, Z.; Gilliland, G.; Bhat, T. N.; Weissig, H.; Shindyalov, I. N.; Bourne, P. E. The Protein Data Bank. *Nucleic Acids Res.* **2000**, *28*, 235–242.

(36) Hardegger, L. A.; Kuhn, B.; Spinnler, B.; Anselm, L.; Ecabert, R.; Stihle, M.; Gsell, B.; Thoma, R.; Diez, J.; Benz, J.; Plancher, J. M.; Hartmann, G.; Banner, D. W.; Haap, W.; Diederich, F. Systematic Investigation of Halogen Bonding in Protein-Ligand Interactions. *Angew. Chem., Int. Ed.* **2011**, *50*, 314–318.

(37) Mirković, B.; Renko, M.; Turk, S.; Sosič, I.; Jevnikar, Z.; Obermajer, N.; Turk, D.; Gobec, S.; Kos, J. Novel Mechanism of Cathepsin B Inhibition by Antibiotic Nitroxoline and Related Compounds. *ChemMedChem* **2011**, *6*, 1351–1356.

(38) Illy, C.; Quraishi, O.; Wang, J.; Purisima, E.; Vernet, T.; Mort, J. S. Role of the Occluding Loop in Cathepsin B Activity. *J. Biol. Chem.* **1997**, *272*, 1197–1202.

(39) Zehl, M.; Allmaier, G. n. Investigation of Sample Preparation and Instrumental Parameters in the Matrix-Assisted Laser Desorption/Ionization Time-of-Flight Mass Spectrometry of Noncovalent Peptide/Peptide Complexes. *Rapid Commun. Mass Spectrom.* **2003**, *17*, 1931–1940.

(40) Salih, B.; Zenobi, R. MALDI Mass Spectrometry of Dye - Peptide and Dye - Protein Complexes. *Anal. Chem.* **1998**, *70*, 1536–1543.

(41) Woods, A. S.; Huestis, M. A. A Study of Peptide-Peptide Interaction by Matrix-Assisted Laser Desorption/Ionization. *J. Am. Soc. Mass Spectrom.* **2001**, *12*, 88–96.

(42) Heck, A. J. R.; van den Heuvel, R. H. H. Investigation of Intact Protein Complexes by Mass Spectrometry. *Mass Spectrom. Rev.* **2004**, *23*, 368–389.

(43) Laugesen, S.; Roepstorff, P. Combination of Two Matrices Results in Improved Performance of MALDI MS for Peptide Mass Mapping and Protein Analysis. *J. Am. Soc. Mass Spectrom.* **2003**, *14*, 992–1002.

(44) Klein, P.; Johe, P.; Wagner, A.; Jung, S.; Kühlbörn, J.; Barthels, F.; Tenzer, S.; Distler, U.; Waigel, W.; Engels, B.; Hellmich, U. A.; Opatz, T.; Schirmeister, T. New Cysteine Protease Inhibitors: Electrophilic (Het)Arenes and Unexpected Prodrug Identification for the Trypanosoma Protease Rhodospain. *Molecules* **2020**, *25*, 1451.

(45) Whittall, R. M.; Li, L. High-Resolution Matrix-Assisted Laser Desorption/Ionization in a Linear Time-of-Flight Mass Spectrometer. *Anal. Chem.* **1995**, *67*, 1950–1954.

(46) Bahr, U.; Stahl-Zeng, J.; Gleitsmann, E.; Karas, M. Delayed Extraction Time-of-Flight MALDI Mass Spectrometry of Proteins above 25 000 Da. *J. Mass Spectrom.* **1997**, *32*, 1111–1116.

(47) Kollmeier, A. S.; de la Torre, X.; Müller, C.; Botrè, F.; Parr, M. K. In-Depth Gas Chromatography/Tandem Mass Spectrometry Fragmentation Analysis of Formestane and Evaluation of Mass Spectral Discrimination of Isomeric 3-Keto-4-Ene Hydroxy Steroids. *Rapid Commun. Mass Spectrom.* **2020**, *34*, No. e8937.



- (48) Mladenovic, M.; Ansorg, K.; Fink, R. F.; Thiel, W.; Schirmeister, T.; Engels, B. Atomistic Insights into the Inhibition of Cysteine Proteases: First QM/MM Calculations Clarifying the Stereoselectivity of Epoxide-Based Inhibitors. *J. Phys. Chem. B* **2008**, *112*, 11798–11808.
- (49) Mladenovic, M.; Junold, K.; Fink, R. F.; Thiel, W.; Schirmeister, T.; Engels, B. Atomistic Insights into the Inhibition of Cysteine Proteases: First QM/MM Calculations Clarifying the Regiospecificity and the Inhibition Potency of Epoxide- and Aziridine-Based Inhibitors. *J. Phys. Chem. B* **2008**, *112*, 5458–5469.
- (50) Vicik, R.; Busemann, M.; Gelhaus, C.; Stiefl, N.; Scheiber, J.; Schmitz, W.; Schulz, F.; Mladenovic, M.; Engels, B.; Leippe, M.; Baumann, K.; Schirmeister, T. Aziridine-Based Inhibitors of Cathepsin L: Synthesis, Inhibition Activity, and Docking Studies. *ChemMedChem* **2006**, *1*, 1126–1141.
- (51) Müller, K.; Faeh, C.; Diederich, F. Fluorine in Pharmaceuticals: Looking beyond Intuition. *Science* **2007**, *317*, 1881–1886.
- (52) Tosstorff, A.; Cole, J. C.; Taylor, R.; Harris, S. F.; Kuhn, B. Identification of Noncompetitive Protein-Ligand Interactions for Structural Optimization. *J. Chem. Inf. Model.* **2020**, *60*, 6595–6611.
- (53) Maeda, S.; Harabuchi, Y.; Ono, Y.; Taketsugu, T.; Morokuma, K. Intrinsic Reaction Coordinate: Calculation, Bifurcation, and Automated Search. *Int. J. Quantum Chem.* **2015**, *115*, 258–269.
- (54) Vicik, R.; Hoerr, V.; Glaser, M.; Schultheis, M.; Hansell, E.; McKerrow, J. H.; Holzgrabe, U.; Caffrey, C. R.; Ponte-Sucré, A.; Moll, H.; Stich, A.; Schirmeister, T. Aziridine-2,3-Dicarboxylate Inhibitors Targeting the Major Cysteine Protease of *Trypanosoma Brucei* as Lead Trypanocidal Agents. *Bioorg. Med. Chem. Lett.* **2006**, *16*, 2753–2757.
- (55) Ettari, R.; Pinto, A.; Previti, S.; Tamborini, L.; Angelo, I. C.; la Pietra, V.; Marinelli, L.; Novellino, E.; Schirmeister, T.; Zappalà, M.; Grasso, S.; de Micheli, C.; Conti, P. Development of Novel Dipeptide-like Rhodesain Inhibitors Containing the 3-Bromoisoxazoline Warhead in a Constrained Conformation. *Bioorg. Med. Chem.* **2015**, *23*, 7053–7060.
- (56) Wagner, A.; Le, T. A.; Brennich, M.; Klein, P.; Bader, N.; Diehl, E.; Paszek, D.; Weickhmann, A. K.; Dirdjaja, N.; Krauth-Siegel, R. L.; Engels, B.; Opatz, T.; Schindelin, H.; Hellmich, U. A. Inhibitor-Induced Dimerization of an Essential Oxidoreductase from African Trypanosomes. *Angew. Chem., Int. Ed.* **2019**, *58*, 3640–3644.
- (57) Previti, S.; Ettari, R.; Cosconati, S.; Amendola, G.; Chouchene, K.; Wagner, A.; Hellmich, U. A.; Ulrich, K.; Krauth-Siegel, R. L.; Wich, P. R.; Schmid, I.; Schirmeister, T.; Gut, J.; Rosenthal, P. J.; Grasso, S.; Zappalà, M. Development of Novel Peptide-Based Michael Acceptors Targeting Rhodesain and Falcipain-2 for the Treatment of Neglected Tropical Diseases (NTDs). *J. Med. Chem.* **2017**, *60*, 6911–6923.
- (58) Mellott, D. M.; Tseng, C.-T.; Drelich, A.; Fajtová, P.; Chenna, B. C.; Kostomiris, D. H.; Hsu, J.; Zhu, J.; Taylor, Z. W.; Kocurek, K. I.; Tat, V.; Katzfuss, A.; Li, L.; Giardini, M. A.; Skinner, D.; Hirata, K.; Yoon, M. C.; Beck, S.; Carlin, A. F.; Clark, A. E.; Beretta, L.; Maneval, D.; Hook, V.; Frueh, F.; Hurst, B. L.; Wang, H.; Raushel, F. M.; O'Donoghue, A. J.; de Siqueira-Neto, J. L.; Meek, T. D.; McKerrow, J. H. A Clinical-Stage Cysteine Protease Inhibitor Blocks SARS-CoV-2 Infection of Human and Monkey Cells. *ACS Chem. Biol.* **2021**, *16*, 642–650.
- (59) Jacobsen, W.; Christians, U.; Benet, L. Z. In Vitro Evaluation of the Disposition of a Novel Cysteine Protease Inhibitor. *Drug Metab. Dispos.* **2000**, *28*, 1343–1351.
- (60) *Molecular Operating Environment (MOE)* | MOEsaic/PSILO; Chemical Computing Group Inc.: Montreal, QC, Canada, 2014.
- (61) Lei, X.; Jalla, A.; Abou Shama, M.; Stafford, J.; Cao, B. Chromatography-Free and Eco-Friendly Synthesis of Aryl Tosylates and Mesylates. *Synthesis* **2015**, *47*, 2578–2585.
- (62) Stokes, B. J.; Liu, S.; Driver, T. G. Rh<sub>2</sub>(II)-Catalyzed Nitro-Group Migration Reactions: Selective Synthesis of 3-Nitroindoles from  $\beta$ -Nitro Styryl Azides. *J. Am. Chem. Soc.* **2011**, *133*, 4702–4705.
- (63) Scheidt, K. A.; Roush, W. R.; McKerrow, J. H.; Selzer, P. M.; Hansell, E.; Rosenthal, P. J. Structure-Based Design, Synthesis and Evaluation of Conformationally Constrained Cysteine Protease Inhibitors. *Bioorg. Med. Chem.* **1998**, *6*, 2477–2494.
- (64) Ivkovic, J.; Lembacher-Fadum, C.; Breinbauer, R. A Rapid and Efficient One-Pot Method for the Reduction of N-Protected  $\alpha$ -Amino Acids to Chiral  $\alpha$ -Amino Aldehydes Using CDI/DIBAL-H. *Org. Biomol. Chem.* **2015**, *13*, 10456–10460.
- (65) White, J. D.; Xu, Q.; Lee, C.-S.; Valeriote, F. A. Total Synthesis and Biological Evaluation of (+)-Kalkitoxin, a Cytotoxic Metabolite of the Cyanobacterium *Lyngbya Majuscula*. *Org. Biomol. Chem.* **2004**, *2*, 2092–2102.
- (66) Weissenborn, M. J.; Wehner, J. W.; Gray, C. J.; Šardžik, R.; Eyers, C. E.; Lindhorst, T. K.; Flitsch, S. L. Formation of Carbohydrate-Functionalised Polystyrene and Glass Slides and Their Analysis by MALDI-TOF MS. *Beilstein J. Org. Chem.* **2012**, *8*, 753–762.
- (67) Andrei, D.; Wnuk, S. F. Synthesis of the Multisubstituted Halogenated Olefins via Cross-Coupling of Dihaloalkenes with Alkylzinc Bromides. *J. Org. Chem.* **2006**, *71*, 405–408.
- (68) Millies, B.; von Hammerstein, F.; Gellert, A.; Hammerschmidt, S.; Barthels, F.; Göppel, U.; Immerheiser, M.; Elgner, F.; Jung, N.; Basic, M.; Kersten, C.; Kiefer, W.; Bodem, J.; Hildt, E.; Windbergs, M.; Hellmich, U. A.; Schirmeister, T. Proline-Based Allosteric Inhibitors of Zika and Dengue Virus NS2B/NS3 Proteases. *J. Med. Chem.* **2019**, *62*, 11359–11382.
- (69) Schneider, N.; Lange, G.; Hindle, S.; Klein, R.; Rarey, M. A Consistent Description of HYdrogen Bond and DEhydration Energies in Protein-Ligand Complexes: Methods behind the HYDE Scoring Function. *J. Comput.-Aided Mol. Des.* **2013**, *27*, 15–29.
- (70) Reulecke, I.; Lange, G.; Albrecht, J.; Klein, R.; Rarey, M. Towards an Integrated Description of Hydrogen Bonding and Dehydration: Decreasing False Positives in Virtual Screening with the HYDE Scoring Function. *ChemMedChem* **2008**, *3*, 885–897.
- (71) Halgren, T. A. Merck Molecular Force Field. I. Basis, Form, Scope, Parameterization, and Performance of MMFF94. *J. Comput. Chem.* **1996**, *17*, 490–519.
- (72) Maier, J. A.; Martinez, C.; Kasavajhala, K.; Wickstrom, L.; Hauser, K. E.; Simmerling, C. Ff14SB: Improving the Accuracy of Protein Side Chain and Backbone Parameters from Ff99SB. *J. Chem. Theory Comput.* **2015**, *11*, 3696–3713.
- (73) Neudert, G.; Klebe, G. DSX: A Knowledge-Based Scoring Function for the Assessment of Protein-Ligand Complexes. *J. Chem. Inf. Model.* **2011**, *51*, 2731–2745.
- (74) Marinas, M.; Sa, E.; Rojas, M. M.; Moalem, M.; Urbano, F. J.; Guillou, C.; Rallo, L. A Nuclear Magnetic Resonance (<sup>1</sup>H and <sup>13</sup>C) and Isotope Ratio Mass Spectrometry ( $\delta^{13}\text{C}$ ,  $\delta^2\text{H}$  and  $\delta^{18}\text{O}$ ) Study of Andalusian Olive Oils. *Rapid Commun. Mass Spectrom.* **2010**, *24*, 1457–1466.
- (75) Wang, J.; Wolf, R. M.; Caldwell, J. W.; Kollman, P. A.; Case, D. A. Development and Testing of a General Amber Force Field. *J. Comput. Chem.* **2004**, *25*, 1157–1174.
- (76) Jorgensen, W. L.; Chandrasekhar, J.; Madura, J. D.; Impey, R. W.; Klein, M. L. Comparison of Simple Potential Functions for Simulating Liquid Water. *J. Chem. Phys.* **1983**, *79*, 926–935.
- (77) Ryckaert, J.-P.; Ciccotti, G.; Berendsen, H. J. C. Numerical Integration of the Cartesian Equations of Motion of a System with Constraints: Molecular Dynamics of n-Alkanes. *J. Comput. Phys.* **1977**, *23*, 327–341.
- (78) Berendsen, H. J. C.; Postma, J. P. M.; van Gunsteren, W. F.; Dinola, A.; Haak, J. R. Molecular Dynamics with Coupling to an External Bath. *J. Chem. Phys.* **1984**, *81*, 3684–3690.
- (79) Frisch, M. J.; Trucks, G. W.; Schlegel, H. B.; Scuseria, G. E.; Robb, M. A.; Cheeseman, J. R.; Scalmani, G.; Barone, V.; Petersson, G. A.; Nakatsuji, H.; Li, X.; Caricato, M.; Marenich, A. V.; Bloino, J.; Janesko, B. G.; Gomperts, R.; Mennucci, B.; Hratchian, H. P.; Ortiz, J. V.; Izmaylov, A. F.; Sonnenberg, J. L.; Ding, F.; Lipparini, F.; Egidi, F.; Goings, J.; Peng, B.; Petrone, A.; Henderson, T.; Ranasinghe, D.; Zakrzewski, V. G.; Gao, J.; Rega, N.; Zheng, G.; Liang, W.; Hada, M.; Ehara, M.; Fukuda, R.; Hasegawa, J.; Ishida, M.; Nakajima, T.; Honda, Y.; Kitao, O.; Nakai, H.; Vreven, T.; Throssell, K.; Montgomery, J. A., Jr.; Peralta, J. E.; Ogliaro, F.; Bearpark, M. J.; Heyd, J. J.; Brothers, E. N.; Kudin, K. N.; Staroverov, V. N.; Keith, T. A.; Kobayashi, R.; Normand, J.; Raghavachari, K.; Rendell, A. P.; Burant, J. C.; Iyengar, S. S.; Tomasi, J.; Cossi, M.; Millam, J. M.; Klene, M.; Adamo, C.; Cammi, R.; Ochterski, J. W.; Martin, R. L.; Morokuma, K.; Farkas, O.; Foresman, J.

B.; Fox, D. J. *Gaussian 16*, Rev. C.01; Gaussian Inc., Wallingford, CT, 2016.

(80) Hariharan, P. C.; Pople, J. A. The Influence of Polarization Functions on Molecular Orbital Hydrogenation Energies. *Theor. Chim. Acta* **1973**, *28*, 213–222.

(81) Chai, J.-D.; Head-Gordon, M. Long-Range Corrected Hybrid Density Functionals with Damped Atom-Atom Dispersion Corrections. *Phys. Chem. Chem. Phys.* **2008**, *10*, 6615–6620.

(82) Ditchfield, R.; Hehre, W. J.; Pople, J. A. Self-Consistent Molecular-Orbital Methods. IX. An Extended Gaussian-Type Basis for Molecular-Orbital Studies of Organic Molecules. *J. Chem. Phys.* **1971**, *54*, 724.

(83) Tao, P.; Schlegel, H. B. A Toolkit to Assist ONIOM Calculations. *J. Comput. Chem.* **2010**, *31*, 2363–2369.

(84) Li, X.; Frisch, M. J. Energy-Represented Direct Inversion in the Iterative Subspace within a Hybrid Geometry Optimization Method. *J. Chem. Theory Comput.* **2006**, *2*, 835–839.

(85) Biebinger, S.; Elizabeth Wirtz, L.; Lorenz, P.; Christine Clayton, C. Vectors for Inducible Expression of Toxic Gene Products in Bloodstream and Procyclic Trypanosoma Brucei. *Mol. Biochem. Parasitol.* **1997**, *85*, 99–112.

(86) Cunningham, M. P.; Vickerman, K. Antigenic Analysis in the Trypanosoma Brucei Group, Using the Agglutination Reaction. *Trans. R. Soc. Trop. Med. Hyg.* **1962**, *56*, 48–59.

(87) Klein, P.; Barthels, F.; Johe, P.; Wagner, A.; Tenzer, S.; Distler, U.; Le, T. A.; Schmid, P.; Engel, V.; Engels, B.; Hellmich, U. A.; Opatz, T.; Schirmeister, T. Naphthoquinones as Covalent Reversible Inhibitors of Cysteine Proteases—Studies on Inhibition Mechanism and Kinetics. *Molecules* **2020**, *25*, 2064.

(88) Barthels, F.; Marincola, G.; Marciniak, T.; Konhäuser, M.; Hammerschmidt, S.; Bierlmeier, J.; Distler, U.; Wich, P. R.; Tenzer, S.; Schwarzer, D.; Ziebuhr, W.; Schirmeister, T. Asymmetric Disulfanylbenzamides as Irreversible and Selective Inhibitors of Staphylococcus Aureus Sortase A. *ChemMedChem* **2020**, *15* (10), 839–850.

(89) Mnova 12.0.4—Mestrelab. [https://mestrelab.com/download\\_file/mnova-12-0-4/](https://mestrelab.com/download_file/mnova-12-0-4/) (accessed May 3, 2021).

(90) Lietsche, J.; Gorka, J.; Hardt, S.; Karas, M.; Klein, J. Custom-Made Microdialysis Probe Design. *J. Visualized Exp.* **2015**, *2015*, 53048.

(91) Buttner-Ennever, J. *The Rat Brain in Stereotaxic Coordinates*, 3; Paxinos, G.; Watson, C.; Academic Press: San Diego, 1996; *Journal of Anatomy* **1997**, Vol. *191* (2), pp 315–317.